

Supporting Information for

The SARS-COV-2 Spike Protein Binds Sialic Acids and Enables Rapid Detection in a Lateral Flow Point of Care Diagnostic Device

Alexander N. Baker,^{a,‡} Sarah-Jane Richards,^{a,‡} Collette S. Guy,^{a,b} Thomas R. Congdon,^a
Muhammad Hasan,^a Alexander J. Zwetsloot,^c Angelo Gallo,^a Józef R. Lewandowski,^a Phillip
J. Stansfeld^{a,b} Anne Straube,^c Marc Walker,^f Simona Chessa,^c Giulia Pergolizzi,^c Simone
Dedola,^c Robert A. Field^{c,d} and Matthew I. Gibson^{a,e*}

a) Department of Chemistry, University of Warwick, UK, CV4 7AL

b) School of Life Sciences, University of Warwick, UK, CV4 7AL

c) Icen Diagnostics Ltd, Norwich Research Park, Norwich, NR4 7GJ

d) Department of Chemistry and Manchester Institute of Biotechnology, University of
Manchester, Manchester, UK, M1 7DN

e) Warwick Medical School, University of Warwick, UK, CV4 7AL

f) Department of Physics, University of Warwick, UK, CV4 7AL

Corresponding Author Email, m.i.gibson@warwick.ac.uk

Contents

Contents	3
Physical and Analytical Methods.....	7
NMR Spectroscopy	7
Mass Spectrometry.....	7
FT-IR Spectroscopy	7
Size Exclusion Chromatography.....	7
X-ray Photoelectron Spectroscopy (XPS)	8
Dynamic Light Scattering	8
UV-vis Spectroscopy	9
Transmission Electron Microscopy	9
Biolayer Interferometry (BLI)	9
Modelling.....	9
¹ H STD NMR Experiments	10
Protein Thermal Shift Assay.....	10
Materials	11
Synthetic Methods	14
Synthesis of 2-(dodecylthiocarbonylthio)-2-methyl propionic acid (DMP).....	14
Synthesis of Pentafluorophenyl-2-dodecylthiocarbonylthio)-2-methylpropanoate (PFP-DMP)	15
Representative polymerization of 2-hydroxyethyl acrylamide.....	16

Representative DP40 Poly(N-hydroxyethyl acrylamide) glycan functionalisation using 2-amino-2-deoxy-N-acetyl-D-neuraminic acid.....	17
2-chloro-1,3-dimethylimidazolinium hexafluorophosphate	18
2-azido-1,3-dimethylimidazolinium hexafluorophosphate (ADMP).....	19
1-Azido-1-deoxy-D-glucose	19
1-Amino-1-deoxy-D-glucose.....	20
O -(N-acetyl- α -neuraminosyl)-(2 \rightarrow 3)- O - β -D-galactopyranosyl-(1 \rightarrow 4)-1-azido-1-deoxy-glucose. [2,3SL-N ₃]	22
O -(N-acetyl- α -neuraminosyl)-(2 \rightarrow 6)- O - β -D-galactopyranosyl-(1 \rightarrow 4)-1-azido-1-deoxy-glucose. [2,6 SL-N ₃]	26
O -(N-acetyl- α -neuraminosyl)-(2 \rightarrow 6)- O - β -D-galactopyranosyl-(1 \rightarrow 4)-1-amino-1-deoxy-glucose. [2,6SL-NH ₂].....	26
N-Acetyl Neuraminic Acid derivative synthesis	29
2-azido-5-(acetamido)-3,5-dideoxy-D-glycero- α -D-galacto-non-2-ulopyranosonate (6). α 2-azido-2-deoxy-N-acetyl-D-neuraminic acid.	33
α 2-Amino-2-deoxy-N-acetyl-D-neuraminic acid (7).	35
Citrate-stabilised 16nm Gold Nanoparticle Synthesis ⁶	38
Citrate-stabilised 35 nm Gold Nanoparticle Synthesis	38
Gold Nanoparticle Polymer Coating Functionalisation – 16 nm.....	39
Gold Nanoparticle Polymer Coating Functionalisation – 35, 55 and 70 nm.....	39
BSA blocking of Nanoparticle surface	39
Expression and purification of SARS-COV-2 Spike (S1) in HEK293 Cells	40

Recombinant Expression and Purification of SARS-COV-2,S1 (first 300 amino acids) for Thermal Shift Assay	42
Synthesis of Low Concentration SARS-COV-2,S1-coated Polystyrene Nanoparticle Virus Mimics	43
Synthesis of High Concentration SARS-COV-2,S1-coated Polystyrene Nanoparticle Virus Mimics	43
Lateral Flow Strip Production, Running and Analysis Protocols	44
Protocol for manufacturing lateral flow strips	44
Protocol for test line addition to the lateral flow strips.....	44
Protocol for running lateral flow test without target analyte in buffer	44
Protocol for running lateral flow test with polystyrene nanoparticle virus mimic analyte in buffer.....	45
Standard protocol for lateral flow strip analysis	45
Lateral flow signal to noise analysis.....	46
Lateral flow signal intensity analysis.....	47
Silver Staining Procedure	47
Lateral flow assay buffer - 10× HEPES buffer (10% PVP ₄₀₀) in 100 mL H ₂ O.....	47
Lateral Flow Complete Device Production, Running and Analysis Protocols.....	48
Protocol for manufacturing lateral flow complete devices	48
Protocol for Conjugate Pad Production	49
10× Conjugate Pad Buffer	49
Protocol for running lateral flow test without target analyte in buffer	50

Lateral flow signal to noise analysis.....	51
Lateral flow signal intensity analysis.....	51
Additional Data and Figures	52
Sequence Alignment comparison for coronaviruses.....	52
Glycan Synthesis additional data.....	53
Polymer Characterization.....	55
Nanoparticle Characterization	58
Lateral Flow Strips and Plotted Data.....	64
Lateral Flow Strips – Blocking Experiments.....	81
Lateral Flow Cassettes and Strips, and Plotted Data	83
Cassettes from Pseudotyped Lentivirus Experiments.....	94
Lateral Flow Influenza Controls	95
Analyzed XPS (x-ray Photoelectron Spectroscopy) data	96
¹ H STD NMR Spectra.....	125
Spike (S1) Protein Thermal Shift Binding Analysis.....	126
References.....	127

Physical and Analytical Methods

NMR Spectroscopy

^1H -NMR, ^{13}C -NMR and ^{19}F -NMR spectra were recorded at 300 MHz, 400 MHz or 500 MHz on a Bruker DPX-300, DPX-400 or DPX-500 spectrometer respectively, with chloroform-*d* (CDCl_3) or deuterium oxide (D_2O) as the solvent. Chemical shifts of protons are reported as δ in parts per million (ppm) and are relative to either CDCl_3 (7.26) or D_2O (4.79).

Mass Spectrometry

Low resolution mass spectra (LRMS) were recorded on a Bruker Esquire 2000 spectrometer using electrospray ionisation (ESI). M/z values are reported in Daltons.

FT-IR Spectroscopy

Fourier Transform-Infrared (FT-IR) spectroscopy measurements were carried out using an Agilent Cary 630 FT-IR spectrometer, in the range of 650 to 4000 cm^{-1} .

Size Exclusion Chromatography

Size exclusion chromatography (SEC) analysis was performed on an Agilent Infinity II MDS instrument equipped with differential refractive index (DRI), viscometry (VS), dual angle light scatter (LS) and variable wavelength UV detectors. The system was equipped with 2 x PLgel Mixed D columns (300 x 7.5 mm) and a PLgel 5 μm guard column. The mobile phase used was DMF (HPLC grade) containing 5 mM NH_4BF_4 at 50 $^\circ\text{C}$ at flow rate of 1.0 $\text{mL}\cdot\text{min}^{-1}$. Poly(methyl methacrylate) (PMMA) standards (Agilent EasyVials) were used for calibration between 955,000 – 550 $\text{g}\cdot\text{mol}^{-1}$. Analyte samples were filtered through a nylon membrane with 0.22 μm pore size before injection. Number average molecular weights (M_n), weight average molecular weights (M_w) and dispersities ($D_M = M_w/M_n$) were determined by conventional calibration and universal calibration using Agilent GPC/SEC software.

X-ray Photoelectron Spectroscopy (XPS)

The samples were attached to electrically-conductive carbon tape, mounted on to a sample bar and loaded in to a Kratos Axis Ultra DLD spectrometer which possesses a base pressure below 1×10^{-10} mbar. XPS measurements were performed in the main analysis chamber, with the sample being illuminated using a monochromated Al K α x-ray source. The measurements were conducted at room temperature and at a take-off angle of 90° with respect to the surface parallel. The core level spectra were recorded using a pass energy of 20 eV (resolution approx. 0.4 eV), from an analysis area of 300 μm x 700 μm . The spectrometer work function and binding energy scale of the spectrometer were calibrated using the Fermi edge and 3d_{5/2} peak recorded from a polycrystalline Ag sample prior to the commencement of the experiments. In order to prevent surface charging the surface was flooded with a beam of low energy electrons throughout the experiment and this necessitated recalibration of the binding energy scale. To achieve this, the C-C/C-H component of the C 1s spectrum was referenced to 285.0 eV. The data were analysed in the CasaXPS package, using Shirley backgrounds and mixed Gaussian-Lorentzian (Voigt) lineshapes. For compositional analysis, the analyser transmission function has been determined using clean metallic foils to determine the detection efficiency across the full binding energy range.

Dynamic Light Scattering

Hydrodynamic diameters (D_h) and size distributions of particles were determined by dynamic light scattering (DLS) using a Malvern Zetasizer Nano ZS with a 4 mW He-Ne 633 nm laser module operating at 25 °C. Measurements were carried out at an angle of 173° (back scattering), and results were analysed using Malvern DTS 7.03 software. All determinations were repeated 5 times with at least 10 measurements recorded for each run. D_h values were calculated using the Stokes-Einstein equation where particles are assumed to be spherical.

UV-vis Spectroscopy

Absorbance measurements were recorded on an Agilent Cary 60 UV-Vis Spectrophotometer and on a BioTek Epoch microplate reader.

Transmission Electron Microscopy

Dry-state stained TEM imaging was performed on a JEOL JEM-2100Plus microscope operating at an acceleration voltage of 200 kV. All dry-state samples were diluted with deionized water and then deposited onto formvar-coated copper grids.

Biolayer Interferometry (BLI)

Biolayer Interferometry was carried out on ForteBio Octet Red96 (Forte Bio, USA). Assays were performed in black 96 well plates. Assays were carried out at 30 °C and agitated at 1,000 rpm. Amine reactive (ARG2) biosensor tips (Forte Bio, USA) were hydrated in milliQ H₂O water for at least 10 mins prior to use. A stable baseline was established in milliQ water for 1 minute. The biosensors were first activated using EDC/NHS for 10 minutes and functionalized by loading with 50 µg.mL⁻¹ protein in pH 6 Acetate buffer for 10 mins followed by 5 minutes quenching with 1 M ethanolamine and 1 minute equilibration step in 10 mM HEPES with 0.15 M NaCl, 0.1 mM CaCl₂ and 0.01 mM MnCl₂ to remove any unbound protein and to establish a stable baseline. Following protein immobilization, the binding association with glycan-functionalized AuNPs was carried out in 10 mM HEPES with 0.15 M NaCl, 0.1 mM CaCl₂ and 0.01 mM MnCl₂, for 30 minutes followed by dissociation in 10 mM HEPES with 0.15 M NaCl, 0.1 mM CaCl₂ and 0.1 mM MnCl₂ for 10 minutes.

Modelling

Models of the S1 domain were constructed based principally on the Cryo-EM structure of SARS-COV-2 (PDB entry 6VSB), with missing loops and the α_{2,3}' sialyllactose modeled in

from the Cryo-EM structure of MERS (PDB entry 6Q04), using a combination of Swiss-model, Pymol and energy minimisation using Gromacs.

¹H STD NMR Experiments

All the STD NMR spectra were acquired on a Bruker Avance 700.24 MHz at 298 K. The STD NMR experiments were performed in Potassium Phosphate 50mM and 10% D₂O buffer, pH 7.4. For the complexes SARS-COV-2 Spike protein (S1), the protein concentration was ~ 50 μM while each ligand concentration was 5 mM. The on- and off-resonance spectra were acquired using a train of 50 ms Gaussian selective saturation pulses (4μW) using a total of 3s of saturation time, and a relaxation delay (D1) of 3.5s. The water signal was suppressed using the excitation sculpting technique (*stdiffesgp.3*) while the residual protein resonances were filtered using a T_{1ρ}-filter of 50 ms. All the spectra were acquired with a spectral width of 15 kHz (20 ppm) and 32K data points using 128 scans. The on-resonance spectra were acquired by saturating at 0.91 ppm while the off-resonance spectra were acquired by saturating at 40 ppm.

Protein Thermal Shift Assay

The thermal shift reaction was performed with a BioRad CFX96 real-time PCR machine. The sample was heated from 25 °C to 95 °C and the fluorescence intensity change monitored using the Protein Thermal Shift™ Dye kit (Thermo Fisher Scientific, Cat # 4461146). Analysis for binding induced shifts in thermal transition was performed in PBS buffer with Precision Melt Analysis Software provided by the manufacturer (BioRad) and a protein concentration of 0.2 mg/mL. The data was collected over 5 runs for each sugar and sugar concentration.

Materials

All chemicals were used as supplied unless otherwise stated. *N*-Hydroxyethyl acrylamide (97 %), 4,4'-azobis(4-cyanovaleric acid) (98 %), mesitylene (reagent grade), triethylamine (> 99%), sodium citrate tribasic dihydrate (> 99 %), gold(III) chloride trihydrate (99.9%), ammonium carbonate (reagent grade), potassium phosphate tri-basic (\geq 98%, reagent grade), potassium hexafluorophosphate (99.5%), deuterium oxide (D₂O, 99.9%), deuterated chloroform (CDCl₃, 99.8%), diethyl ether (\geq 99.8%, ACS reagent grade), sodium azide (\geq 99.5%, reagent plus grade), hydrazine hydrate (50-60%), methanol (\geq 99.8%, ACS reagent grade), Amberlite® IR120 (H⁺ form), toluene (\geq 99.7%,), Tween-20 (molecular biology grade), HEPES, PVP40 (poly(vinyl pyrrolidone)₄₀₀ (Average Mw ~40,000)), sucrose (Bioultra grade), carbon disulphide (\geq 99.8%), acetone (\geq 99%), 1-dodecane thiol (\geq 98%), pentafluorophenol (\geq 99%, reagent plus), micro particles based on polystyrene (100nm) and a silver staining kit (Silver Enhancer Kit), Dowex 50WX8 hydrogen Form 100-200 mesh, acetic anhydride, *N*-acetyl neuraminic acid and acetyl chloride were purchased from Sigma-Aldrich. 2,3'-sialyllactose, 2,6'-sialyllactose and galactosamine HCl were purchased from Carbosynth. Palladium hydroxide (20% on carbon), anhydrous trehalose were purchased from Alfa Aesar. 2-chloro-1,3-dimethylimidazolium chloride (90%), DMF (>99%), 2-bromo-2-methyl propionic acid (98%) were purchased from Acros Organics. HPLC grade acetonitrile (\geq 99.8%), glucose (lab-reagent grade), hexane fraction from petrol (lab reagent grade), DCM (99% lab reagent grade), sodium hydrogen carbonate (\geq 99%), ethyl acetate (\geq 99.7%, analytical reagent grade), sodium chloride (\geq 99.5%), calcium chloride, 40-60 petroleum ether (lab reagent grade), hydrochloric acid (~37%, analytical grade), glacial acetic acid (analytical grade), magnesium sulphate (reagent grade) were purchased from Thermo Fisher Scientific.

Nitrocellulose Immunopore RP 90-150 s/4cm 25mm was purchased from GE Healthcare. Lateral flow backing cards 60mm by 301.58mm (KN-PS1060.45 with KN211 adhesive) and lateral flow cassettes (KN-CT105) were purchased from Kenosha Tapes. Cellulose fibre wick material 20 cm by 30 cm by 0.825 mm (290 gsm and 180 mL/min) (Surewick CFSP223000) was purchased from EMD Millipore. Glass fibre conjugate pads (GFCP103000) 10 mm by 300 mm was purchased from Merck. Thick Chromatography Paper (for sample pads), Grade 237, Ahlstrom 20 cm by 20 cm were purchased from VWR International.

Soybean agglutinin, Ricinus Communis Agglutinin I (RCA₁₂₀), Ulex Europaeus Agglutinin I and wheat germ agglutinin were purchased from Vector Laboratories. 2,3'-sialyllactose-BSA (3 atom spacer, NGP0702), 2,6'-sialyllactose-BSA (3 atom spacer, NGP0706), Galα1-3Galβ1-4GlcNAc-BSA (3 atom spacer, NGP0330) and N-acetylneuraminic acid-BSA (6 atom spacer, NGP6111) were purchased from Dextra Laboratories. Figures S39, 40, 41 and 42. and Tables S2, 3, 4, 5, 6, 7, 13, 14 and 15. used SARS-COV-2 spike glycoprotein (S1), Sheep Fc-Tag (HEK293) from The Native Antigen Company; SARS-COV-1 spike glycoprotein (S1), His-Tag (HEK293) was also purchased from here. Commercial spike protein was used for the BLI studies (Figure 3 main paper. Commercial and expressed (details are included below) in-house spike protein was used for lateral flow analyses.

Clear and black half area 96-well plates were purchased from Greiner Bio-one. Streptavidin (SA) biosensors were purchased from Forte Bio.

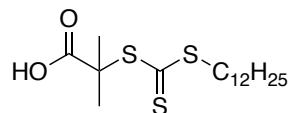
Spike (SARS-COV2) pseudotyped lentivirus (*Luc* Reporter) (Catalogue number: 79942, Lot number: 200730) was purchased from amsbio.

Biological reagents are listed as used in *Expression and Purification of SARS-COV-2 Spike (S1) in HEK293 Cells* and *Recombinant Expression and Purification of SARS-COV-2 (first 300 amino acids) for Thermal Shift Assay*.

Distilled water used for buffers was MilliQ grade 18.2 m Ω resistance.

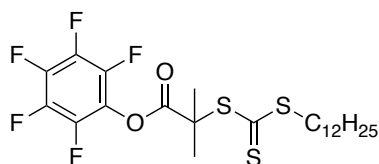
Synthetic Methods

Synthesis of 2-(dodecylthiocarbanothionylthio)-2-methyl propionic acid (DMP)



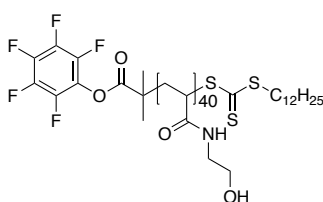
This was synthesised, according to a previously published procedure.¹ 2.00 g (9.88 mmol) of 1-dodecane thiol was added dropwise to stirring 2.10 g (9.89 mmol) of K₃PO₄ in 30 mL of acetone at RTP, the mixture was left to stir for 25 minutes to form a white suspension. 2.05 g (26.93 mmol) of carbon disulphide was then added and left for 10 minutes, a yellow solution formed. 1.5 g (8.98 mmol) of 2-bromo-2-methyl-propionic acid was then added and the solution left to stir for 16 hours. The solvent was removed under vacuum. The crude product was dissolved in 100 mL of 1M HCl and extracted with DCM (2×100 mL). The organic layer was washed with 200 mL water and 200 mL brine. The organic layer was dried with MgSO₄ and filtered under gravity. The solvent was then removed from the filtrate under vacuum. The crude product was purified using a silica column (40-60 PET:DCM:glacial acetic acid 75:24:1) and recrystallised in n-hexane to give a yellow solid (58%). δ_{H} (300 MHz, CDCl₃) 3.28 (2H, t, *J* 7.5, SCH₂CH₂), 1.80 - 1.45 (8H, m, C(CH₃)₂ and SCH₂CH₂), 1.45 - 1.2 (18H, m, (CH₂)₉CH₃), 0.87 (3H, t, *J* 6.0, CH₃). δ_{C} (400 MHz, CDCl₃) 221.00 (1C, SC(S)S), 178.26 (1C, C(O)), 55.66 (1C, C(CH₃)₂), 37.66 (1C, SCH₂), 32.06 - 27.96 (9C, SCH₂(CH₂)₉), 25.38 (2C, C(CH₃)₂), 22.84 (1C, CH₂CH₃), 14.27 (1C, CH₂CH₃). *m/z* calculated as 364.16; found for ESI [M+H]⁺ 365.3 and [M+Na]⁺ 387.3. FTIR (cm⁻¹) – 2955.8, 2916.6 & 2849.5 (methyl and methylene), 1701.5 (ester C=O), 1459.3, 1436.9 & 1412.7 (methyl and methylene), 1280.3 (C(CH₃)₂), 1064.2 (S-C(S)-S).

Synthesis of Pentafluorophenyl-2-dodecylthiocarbonothioylthio)-2-methylpropanoate (PFP-DMP)



This was synthesised, according to a previously published procedure.¹ 4.06 g (11.13 mmol) of DMP, 3.65 g (19.04 mmol) of EDC and 2.30 g (18.82 mmol) of DMAP were dissolved in 160 mL DCM and degassed for 30 minutes. 7.28 g (39.55 mmol) of pentafluorophenol was added in 20 mL of DCM and the mixture stirred for 18 hours at RTP. The organic layer was washed with 3 M HCl (200mL), 1 M NaHCO₃ (200 mL) and 0.5 M NaCl (200 mL). The organic layer was dried with MgSO₄ and filtered under gravity. The solvent was then removed from the filtrate under vacuum. The crude product was recrystallised in ethyl acetate (or hexane) overnight at -8°C and dried to give yellow crystals (90.9%). δ_{H} (300 MHz, CDCl₃) 3.31 (2H, t, J 7.5, SCH₂CH₂), 1.86 (6H, s, C(CH₃)₂), 1.69 (2H, qn, J 7.5, SCH₂), 1.48 - 1.16 (18H, m, CH₂CH₂CH₂CH₂CH₂CH₂CH₂CH₂CH₂CH₂CH₃), 0.94 - 0.82 (3H, m, CH₃). δ_{C} (300 MHz, CDCl₃) 220.06 (1C, SC(S)S), 169.71 (1C, C(O)), 143.13 (2C, meta C), 139.79 (1C, ipso C), 139.61 (1C, para C), 136.30 (2C, Ortho C), 55.50 (1C, C(CH₃)₂), 37.26 (1C, SCH₂), 32.03 - 22.81 (10C, SCH₂(CH₂)₁₀), 25.37 (2C, C(CH₃)₂), 14.11 (1C, CH₂CH₃). δ_{F} (300 MHz, CDCl₃) -151.44 - -151.61 (2F, m, OCC₂H₂C₂H₂CH), -148.50 (1F, t, J 21.5, OCC₂H₂C₂H₂CH), -162.23 - -162.47 (2F, m, OCC₂H₂C₂H₂CH). m/z calculated as 530.14; found for ESI [M+Na]⁺ 553.3 and [M+CH₃CN+Na]⁺ 593.5. FTIR (cm⁻¹) – 2955.8, 2916.6 & 2849.5 (methyl and methylene), 1701.5 (ester C=O), 1518.9 (aromatic C=C or C-F), 1459.3, 1436.9 & 1412.7 (methyl and methylene), 1280.3 (C(CH₃)₂), 1067.9 (S-C(S)-S).

Representative polymerization of 2-hydroxyethyl acrylamide



PHEA40 as representative example. 2.0 g (17.37 mmol) of 2-hydroxyethyl acrylamide, 0.043 g (0.15 mmol) of ACVA and 0.368 g (0.69 mmol) of PFP-DMP was added to 16 mL 1:1 toluene:methanol and degassed with nitrogen for 30 minutes. The reaction vessel was stirred and heated to 70 °C for 2 hours. The solvent was removed under vacuum. The crude product was dissolved in the minimum amount of methanol. Diethyl ether cooled in liquid nitrogen was added to the methanol to form a precipitate. The mixture was centrifuged for 2 minutes at 13 krpm and the liquid decanted off. The solid was dissolved in methanol and removed under vacuum to give a yellow crystalline solid.

PHEA40 - δ_H (300 MHz, D₂O) 8.35 - 7.95 (21H, m, NH), 3.97-3.56 (78H, m, NHCH₂), 3.56 - 3.03 (80H, m, CH₂OH & SCH₂), 2.41-1.90 (41H, m, CH₂CHC(O) & C(CH₃)₂), 1.90 - 0.99 (108H, m, CH₂CHC(O) & CH₂CH₂CH₂CH₂CH₂CH₂CH₂CH₂CH₂CH₂CH₂CH₃), 0.83 - 0.72 (5H, m, CH₂CH₃) δ_F (300 MHz, D₂O) - 152.0- -164.3 (5F, m, C₆F₅). FTIR (cm⁻¹) – 3263.3 (OH, broad), 3088.1 & 2924.1 (C(O)NH and NH), 1638.2 & 1541.3 (C(O)NH) Yield - 73%

PHEA50 - δ_H (300 MHz, D₂O) 8.31 - 7.97 (23H, m, NH), 3.99-3.55 (86H, m, NHCH₂), 3.55 - 3.09 (100H, m, CH₂OH & SCH₂), 2.49 - 1.90 (46H, m, CH₂CHC(O) & C(CH₃)₂), 1.90 - 0.98 (110H, m, CH₂CHC(O) & CH₂CH₂CH₂CH₂CH₂CH₂CH₂CH₂CH₂CH₂CH₂CH₃), 0.84 - 0.72 (5H, m, CH₂CH₃)

PHEA58 - δ_H (300 MHz, D₂O) 8.36 - 7.98 (29H, m, NH), 4.00 - 3.55 (H, 108H, m, NHCH₂), 3.55 - 3.15 (127H, m, CH₂OH & SCH₂), 2.36 - 1.88 (56H, m, CH₂CHC(O) & C(CH₃)₂), 1.87

- 1.09 (128H, m, $CH_2CHC(O)$ & $CH_2CH_2CH_2CH_2CH_2CH_2CH_2CH_2CH_2CH_2CH_3$), 0.83 - 0.72 (5H, m, CH_2CH_3)

PHEA72 - δ_H (300 MHz, D_2O) 8.30 - 7.96 (34H, m, NH), 3.96 - 3.52 (126H, m, $NHCH_2$), 3.52 - 3.07 (155H, m, CH_2OH & SCH_2), 2.36 - 1.88 (70H, m, $CH_2CHC(O)$ & $C(CH_3)_2$), 1.88 - 1.03 (148H, m, $CH_2CHC(O)$ & $CH_2CH_2CH_2CH_2CH_2CH_2CH_2CH_2CH_2CH_2CH_3$), 0.82 - 0.70 (5H, m, CH_2CH_3)

Representative DP40 Poly(N-hydroxyethyl acrylamide) glycan functionalisation using 2-amino-2-deoxy-N-acetyl-D-neuraminic acid

0.2 g (0.039 mmol) of poly(2-hydroxyethyl acrylamide)₄₀ and 0.078 mmol of glycan were added to 20 mL of DMF containing 0.05 M TEA. The reaction was stirred at 50 °C for 16 hours. Solvent was removed under vacuum. The crude product was dissolved in the minimum amount of methanol. Diethyl ether cooled in liquid nitrogen was added to the methanol to form a precipitate. The mixture was centrifuged for 2 minutes at 13krpm and the liquid decanted off. The solid was dissolved in methanol and solvent removed under vacuum to give an orange/brown crystalline solid. Loss of fluorine signal in the ^{19}F NMR was used to indicate the reaction had gone to completion. δ_H (300 MHz, D_2O) 8.21 - 7.99 (25H, m, NH), 4.10 - 3.57 (~90H, m, $NHCH_2$ & glycan protons), 3.57 - 2.99 (~82H, m, CH_2OH & SCH_2 & glycan protons), 2.40 - 1.87 (50H, m, $CH_2CHC(O)$, $C(CH_3)_2$ & glycan protons), 1.87 - 0.99 (110H, m, $CH_2CHC(O)$ & $CH_2CH_2CH_2CH_2CH_2CH_2CH_2CH_2CH_2CH_3$ & glycan protons), 0.86 - 0.74 (5H, m, CH_2CH_3).

NB: This approach was used for other sugars also.

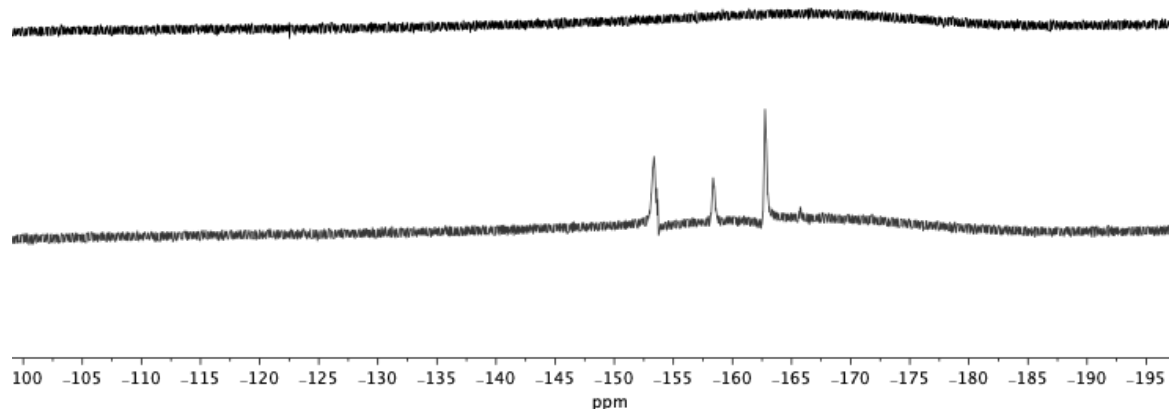
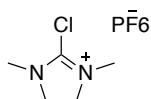


Figure S1. ^{19}F NMR After (top) and before (bottom) reaction with α 2-amino-2-deoxy-*N*-acetyl-D-neuraminic acid functionalization.

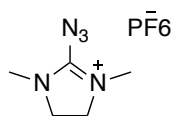
2-chloro-1,3-dimethylimidazolinium hexafluorophosphate



Synthesis was carried out following the procedure of Lim et al.² In a 100 mL round bottom flask equipped with a rubber septum, 2-chloro-1,3-dimethylimidazolinium chloride **1** (5 g, 29.6 mmol, 1.0 equiv) is dissolved in anhydrous acetonitrile (15 mL) and stirred under an N_2 atmosphere. KPF_6 (5.40 g, 29.6 mmol, 1 equiv) is added by temporary removal of the septum. After 2 h the mixture is filtered off using a sintered funnel packed with dry Celite[®] (2 g). The filtered cake is washed with acetonitrile and the filtrate is concentrated in vacuo. The resultant solid is dissolved in a small amount of acetonitrile and diethyl ether is added until a precipitate is formed. Stir for 3-5 min. The precipitate is collected by suction filtration, washed with diethyl ether and dry under vacuum to afford product as an off-white solid (7.5 g, 90%).

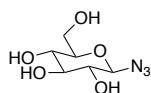
δ_{H} (400 MHz, CD_3CN) 3.13 (6H, s), 3.93 (4H, s); δ_{C} (400 MHz, CD_3CN) 35.1, 50.7.

2-azido-1,3-dimethylimidazolinium hexafluorophosphate (ADMP)



Synthesis was carried out following the procedure of Lim et al.² 2-chloro-1,3-dimethylimidazolinium hexafluorophosphate (7 g, 25.1 mmol, 1.0 equiv) was dissolved in anhydrous acetonitrile (25 mL) and stirred at 0 °C under N₂ atmosphere. NaN₃ (2.45 g, 27.7 mmol, 1.5 equiv) was added. The reaction mixture was stirred for 6 h, then filtered off using a sintered funnel packed with dry Celite[®] (2 g). The resultant solid was dissolved in a small amount of acetonitrile and diethyl ether was added until a precipitate was formed. The precipitate was collected by suction filtration, washed with diethyl ether and dried under vacuum for 12 h to afford the crude product which recrystallised from toluene:acetone (1:1) to give the product as a white solid. (6.5 g, 90%). δ_{H} (400 MHz, CD₃CN) 3.05 (6H, s), 3.78 (4H, s); δ_{C} (400 MHz, CD₃CN) 33.8, 49.8.

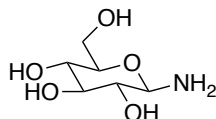
1-Azido-1-deoxy-D-glucose



Synthesis was carried out following the procedure of Lim et al.² Glucose (100 mg, 0.555 mmol) was dissolved in 4:1 D₂O/MeCN (2 mL) under nitrogen and cooled to 0 °C. Triethylamine (387 μ L, 2.78 mmol) was then added and mixture stirred at 0 °C for 10 mins. 2-azido-1,3-dimethylimidazolinium hexafluorophosphate (475 mg, 1.66 mmol) was then added and the reaction stirred at 0 °C for 3 hours, and then left at 4 °C for a further 16 hours. The reaction mixture was then diluted with water (15 mL) and washed with DCM (3 x 20 mL). The aqueous phase was then passed through a column of Amberlite[®] IR120 (H⁺, previously treated with 1M

NaOH solution), and lyophilised to give a white solid (279 mg) which was used directly in the next reaction.

1-Amino-1-deoxy-D-glucose



1-Azido-1-deoxy-D-glucose (0.555 mmol) (from above) was dissolved in methanol (5 mL) under nitrogen. Pd(OH)₂/C (20 wt %, 39 mg, 0.055 mmol) and hydrazine hydrate (50 %, 89 μL, 1.39 mmol) were then added and the reaction heated to reflux for 16 hours. The reaction mixture was then cooled, filtered (to remove Pd/C) and concentrated *in vacuo* (to remove hydrazine) to give the product as a white solid (257 mg). This reagent was used directly, as unreacted azide would not take part in the reaction with pentafluorophenyl leaving group on the polymer. Reduction was confirmed by TLC and ninhydrin staining. ¹H and ¹³C NMR confirmed multiple anomeric peaks supported by HSQC) including starting material. Product was a mixture of anomers.

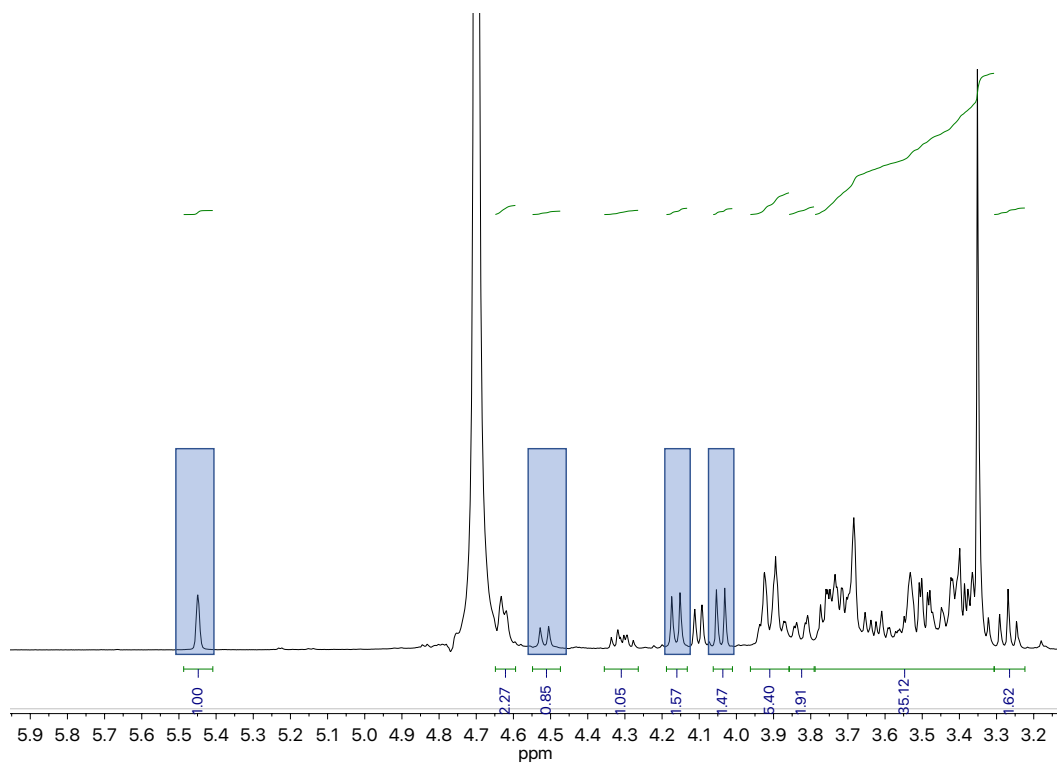


Figure S2. ^1H NMR spectra of GlcNH_2 . Highlighted areas are the anomeric protons.

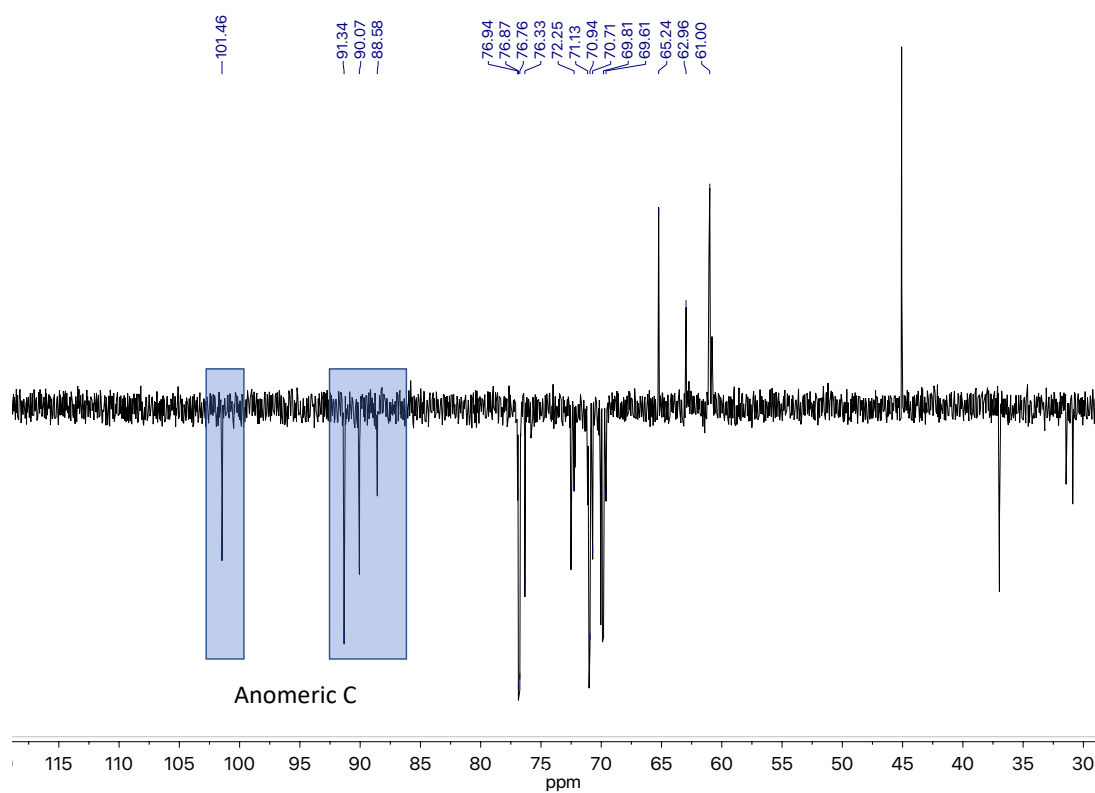
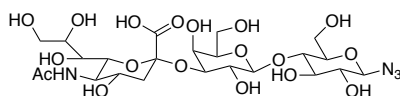


Figure S3. ^{13}C NMR spectra of GlcNH_2 . Highlighted areas are the anomeric carbons.

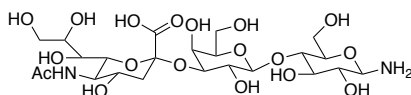
***O*-(*N*-acetyl- α -neuraminosyl)-(2 \rightarrow 3)-*O*- β -D-galactopyranosyl-(1 \rightarrow 4)-1-azido-1-deoxy-glucose. [2,3SL-N₃]**



O-(*N*-acetyl- α -neuraminosyl)-(2 \rightarrow 3)-*O*- β -D-galactopyranosyl-(1 \rightarrow 4)-glucose (50 mg, 0.076 mmol) was dissolved in 4:1 D₂O/MeCN (1 mL) under nitrogen and cooled to 0 °C. Triethylamine (53 μ L, 0.381 mmol) was then added and mixture stirred at 0 °C for 10 mins. 2-azido-1,3-dimethylimidazolium hexafluorophosphate (65 mg, 0.229 mmol) was then added and the reaction stirred at 0 °C for 3 hours, and then left at 4 °C for a further 16 hours. The reaction mixture was then diluted with water (15 mL) and washed with DCM (3 x 20 mL). The aqueous phase was then passed through a column of Amberlite[®] IR120 (H⁺, previously treated with 1M NaOH solution), and lyophilised to give a white solid (95 mg) which was used directly in the next reaction.

m/z (ES⁻) 657.1 [M-H]⁻

***O*-(*N*-acetyl- α -neuraminosyl)-(2 \rightarrow 3)-*O*- β -D-galactopyranosyl-(1 \rightarrow 4)-1-amino-1-deoxy-glucose. [2,3SL-NH₂]**



Crude *O*-(*N*-acetyl- α -neuraminosyl)-(2 \rightarrow 3)-*O*- β -D-galactopyranosyl-(1 \rightarrow 4)-1-azido-1-deoxy-glucose (0.076 mmol) was dissolved in methanol (5 mL) under nitrogen. Pd(OH)₂/C (20 wt %, 5.4 mg, 0.0076 mmol) and hydrazine hydrate (50 %, 12.2 μ L, 0.191 mmol) were then added and the reaction heated to reflux for 16 hours. The reaction mixture was then cooled, filtered (to remove Pd/C) and concentrated *in vacuo* (to remove hydrazine) to give the product as a white solid (51 mg). Product was a 2:1 mix of α : β anomers at the Glc anomeric centre.

δ_{H} (500 MHz, D₂O) 5.37 (0.65H, d, J 1.5, Glc α anomeric CH), 4.54 (1H d, J 8.0, Gal anomeric CH), 4.44 (0.35H, d, J 7.5, Glc β anomeric CH), 4.04 (1H, dd, J 10.0, 3.0), 3.98 – 4.02 (1H, m), 3.43 – 3.92 (18H, m), 2.68 (1H, dd, J 12.5, 4.5, Neu5Ac H^{3a}), 1.95 (3H, s, CH₃), 1.76 – 1.68 (1H, m, Neu5Ac H^{3b}). δ_{C} (126 MHz, D₂O) 175.0, 173.9 (CO), 102.6, 101.8, 101.4 (anomeric CH's), 99.8 (anomeric C), 77.7, 75.5, 75.1, 74.1, 72.8, 71.8, 71.4, 70.0, 69.1, 68.4, 68.1, 67.4 (CH's), 65.1, 62.5, 61.1 (CH₂O), 51.7 (CH₂N), 39.7 (CCH₂C), 22.0 (CH₃).

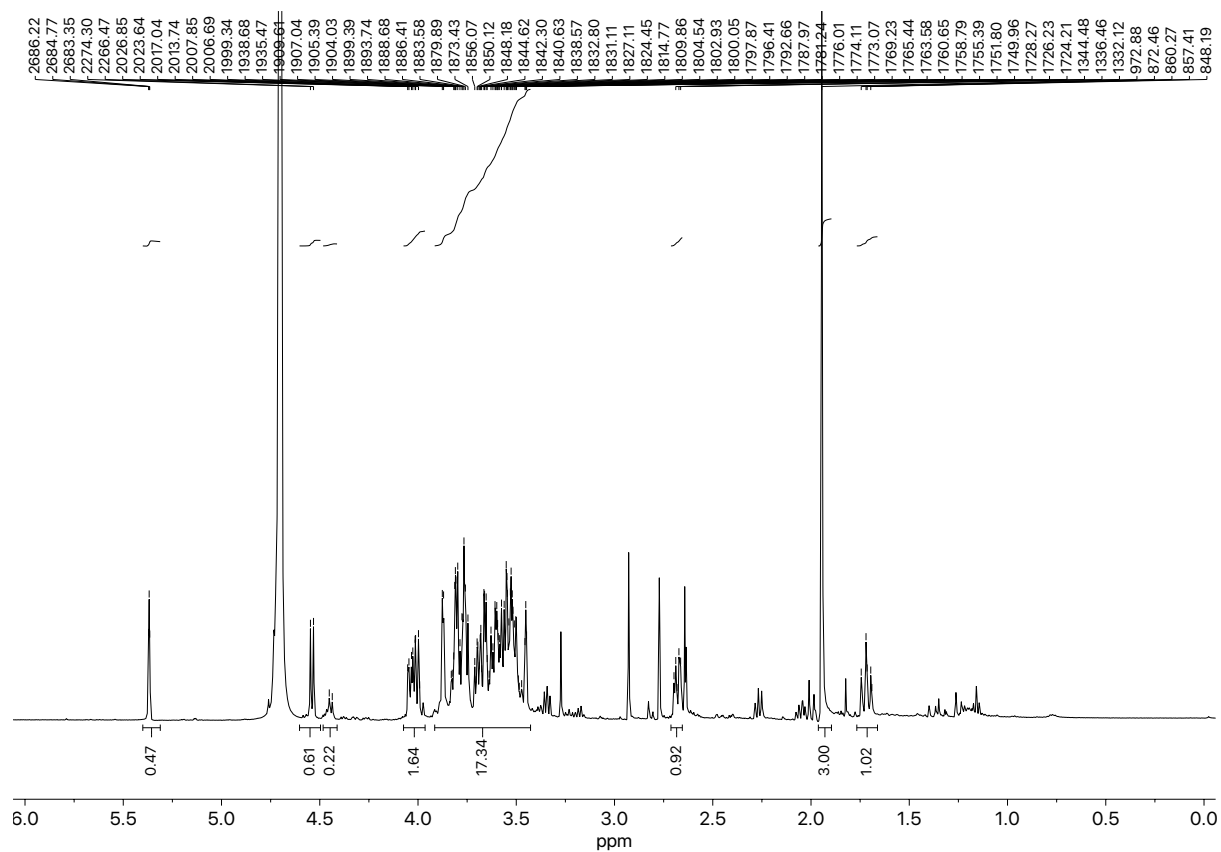


Figure S4. ^1H NMR spectrum of *O*-(*N*-acetyl- α -neuraminosyl)-(2 \rightarrow 3)-*O*- β -D-galactopyranosyl-(1 \rightarrow 4)-1-amino-1-deoxy-glucose.

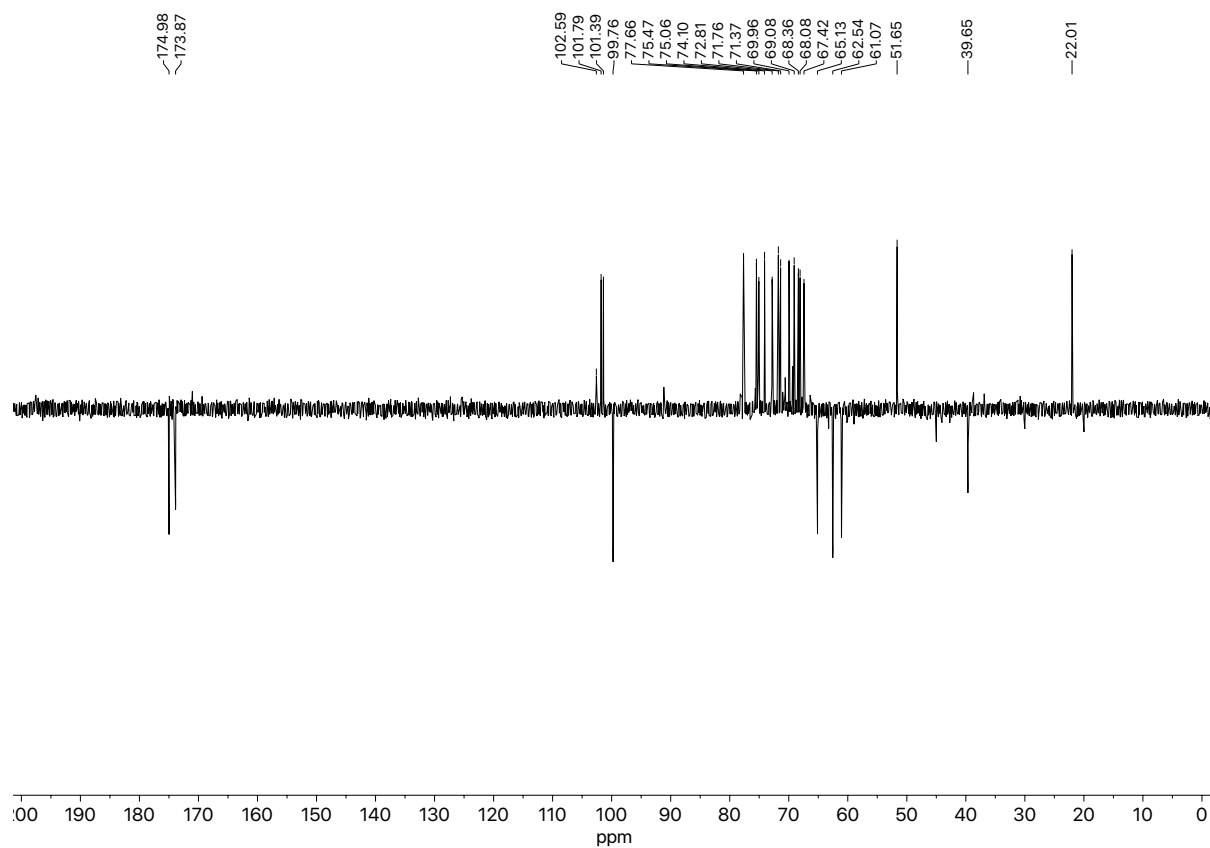
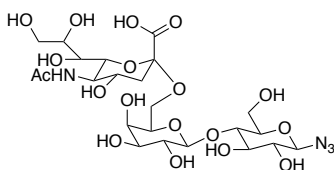


Figure S5. ^{13}C NMR spectrum of *O*-(*N*-acetyl- α -neuraminosyl)-(2 \rightarrow 3)-*O*- β -D-galactopyranosyl-(1 \rightarrow 4)-1-amino-1-deoxy-glucose.

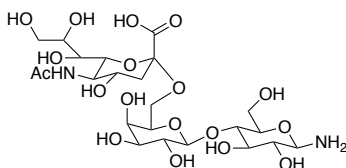
O-(*N*-acetyl- α -neuraminosyl)-(2 \rightarrow 6)-*O*- β -D-galactopyranosyl-(1 \rightarrow 4)-1-azido-1-deoxy-glucose. [2,6 SL-N₃]



O-(*N*-acetyl- α -neuraminosyl)-(2 \rightarrow 6)-*O*- β -D-galactopyranosyl-(1 \rightarrow 4)-glucose (50 mg, 0.076 mmol) was dissolved in 4:1 D₂O/MeCN (1 mL) under nitrogen and cooled to 0 °C. Triethylamine (53 μ L, 0.381 mmol) was then added and mixture stirred at 0 °C for 10 mins. 2-azido-1,3-dimethylimidazolium hexafluorophosphate (65 mg, 0.229 mmol) was then added and the reaction stirred at 0 °C for 3 hours, and then left at 4 °C for a further 16 hours. The reaction mixture was then diluted with water (15 mL) and washed with DCM (3 x 20 mL). The aqueous phase was then passed through a column of Amberlite[®] IR120 (H⁺, previously treated with 1M NaOH solution), and lyophilised to give a white solid (86 mg) which was used directly in the next reaction.

m/z (ES⁻) 657.1 [M-H]⁻

O-(*N*-acetyl- α -neuraminosyl)-(2 \rightarrow 6)-*O*- β -D-galactopyranosyl-(1 \rightarrow 4)-1-amino-1-deoxy-glucose. [2,6SL-NH₂]



Crude *O*-(*N*-acetyl- α -neuraminosyl)-(2 \rightarrow 6)-*O*- β -D-galactopyranosyl-(1 \rightarrow 4)-1-azido-1-deoxy-glucose (0.076 mmol) was dissolved in methanol (5 mL) under nitrogen. Pd(OH)₂/C (20 wt %, 5.4 mg, 0.0076 mmol) and hydrazine hydrate (50 %, 12.2 μ L, 0.191 mmol) were then added and the reaction heated to reflux for 16 hours. The reaction mixture was then cooled,

filtered (to remove Pd/C) and concentrated *in vacuo* (to remove hydrazine) to give the product as a white solid (48 mg). Product was a 2.35:1 mix of α : β anomers at the Glc anomeric centre.

δ_{H} (500 MHz, D₂O) 5.37 (0.58H (relative to Glc β anomeric), s, Glc α anomeric CH), 4.44 (1H, d, J 8.0, Gal anomeric CH), 4.33 (0.42H (relative to Glc α anomeric), d, J 7.5, Glc β anomeric CH), 4.02 (1H, d, J 8.0), 3.93 – 3.37 (19H, m), 2.66 – 2.60 (1H, m, Neu5Ac H^{3a}), 1.94 (3H, s, CH₃), 1.67 – 1.56 (1H, m, Neu5Ac H^{3b}). δ_{C} (126 MHz, D₂O) 175.0, 173.5 (CO), 101.9, 101.3, 100.5 (anomeric CH's), 98.5 (anomeric C), 77.1, 76.2, 73.9, 73.6, 73.5, 71.7, 71.6, 71.3, 70.5, 69.7, 68.4, 68.2 (CH's), 65.0, 63.5, 62.6 (CH₂O), 51.8 (CH₂N), 39.5 (CCH₂C), 22.0 (CH₃).

¹³C spectra were assigned using HSQC and HMBC.

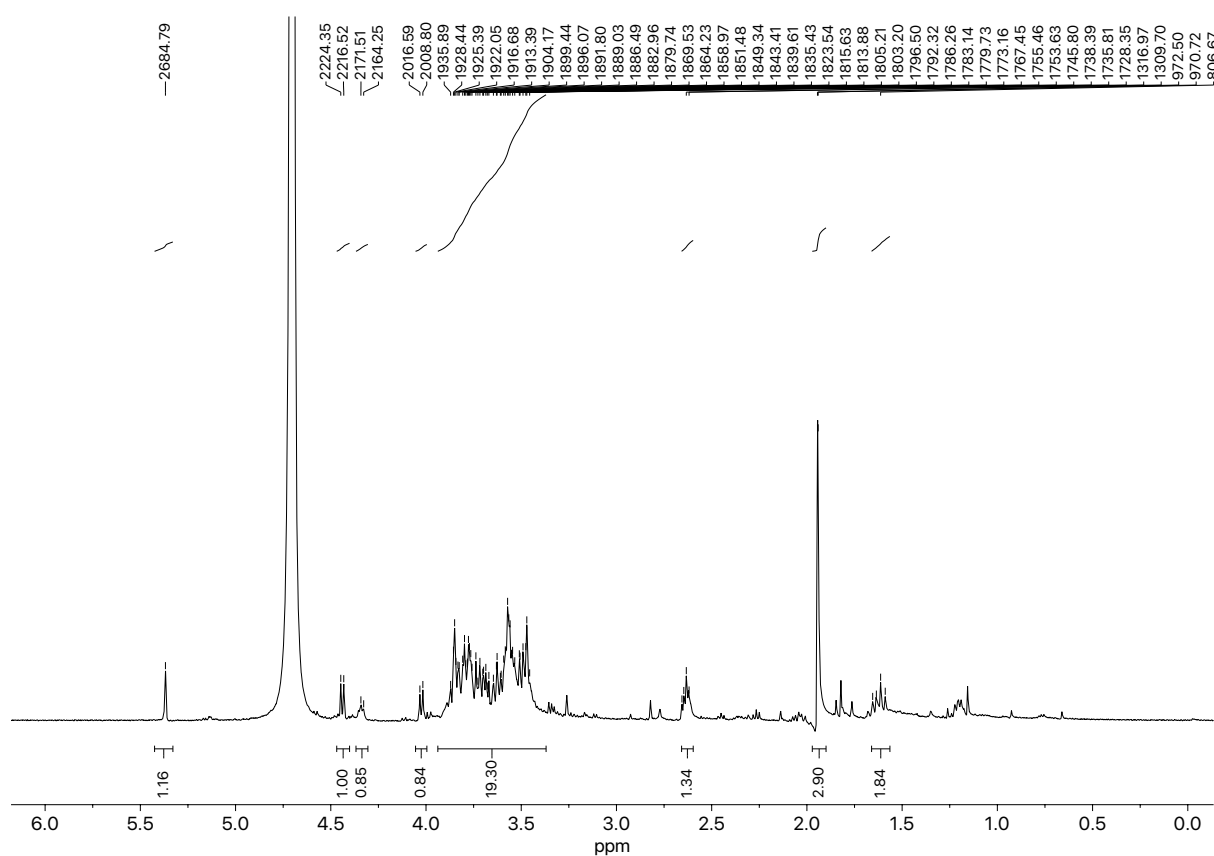


Figure S6. ¹H NMR spectrum of *O*-(*N*-acetyl- α -neuraminosyl)-(2 \rightarrow 6)-*O*- β -D-galactopyranosyl-(1 \rightarrow 4)-1-amino-1-deoxy-glucose.

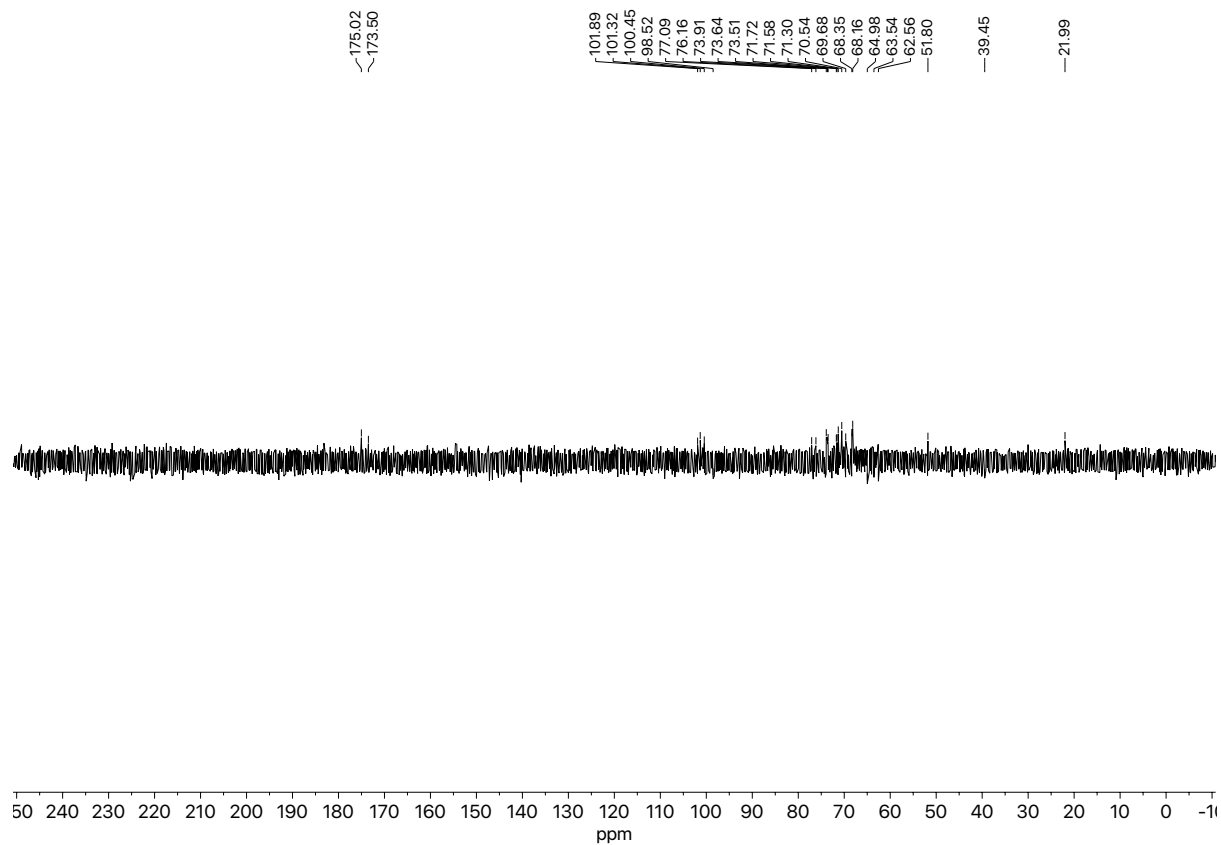


Figure S7. ^{13}C NMR spectrum of *O*-(*N*-acetyl- α -neuraminosyl)-(2 \rightarrow 6)-*O*- β -D-galactopyranosyl-(1 \rightarrow 4)-1-amino-1-deoxy-glucose.

N-Acetyl Neuraminic Acid derivative synthesis

The overall procedure is shown in Figure S8. based upon established procedures, which are indicated.

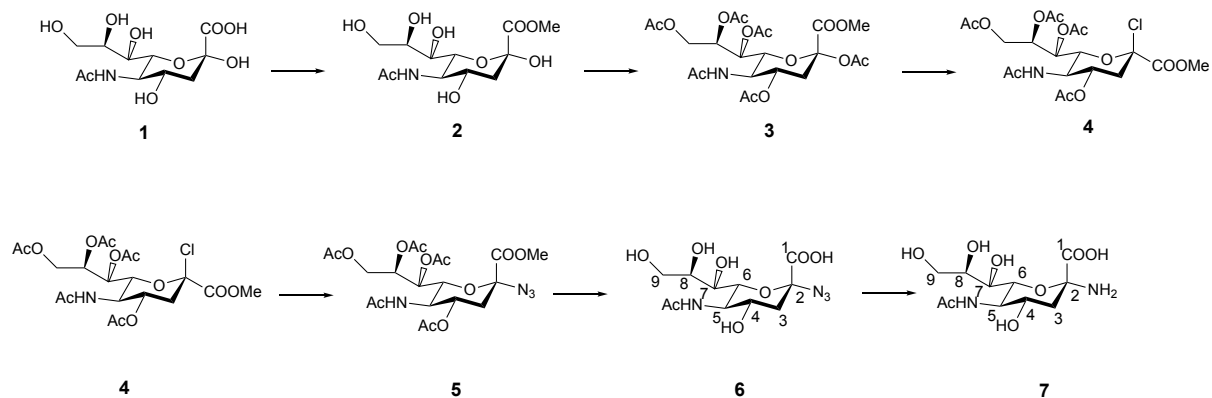


Figure S8. $\alpha,2$ -Amino-2-deoxy-*N*-acetyl-D-neuraminic acid synthesis

*Methyl 2,4,7,8,9-penta-O-acetyl-5-(acetamido)-2,3,5-trideoxy-D-glycero-β-D-galacto-non-2-
ulopyranosonate (3)*

Compound **3** was prepared according to the literature.³ Briefly, *N*-acetyl neuraminic acid (**1**) (5g, 16 mmol) and Dowex 50WX8 200 (H⁺) resin (12 g) were stirred in anhydrous MeOH (120 mL) at rt overnight. The mixture was filtered and the resin extensively washed with MeOH; the combined filtrates were evaporated under reduced pressure to dryness to give compound **2** as a white solid (5.8 g). Compound **2** (2 g, 6.1 mmol) was suspended in acetic anhydride (16 mL) and the mixture cooled down to 0°C in ice bath. Then, pyridine (14 mL) was added dropwise and the reaction was left to warm up to rt overnight. After TLC (toluene:acetone, 1:1) showed complete conversion, the reaction was evaporated under reduced pressure to dryness and co-evaporated with toluene (3x). The residue was dissolved in dichloromethane and the organic phase washed successively with 10% HCl solution, sat. NaHCO₃ and water. The organic phase was dried over anhydrous MgSO₄, filtered and evaporated under reduced pressure to dryness to give compound **3** as a glassy solid (3.4 g, quantitative), and used directly in the next step.

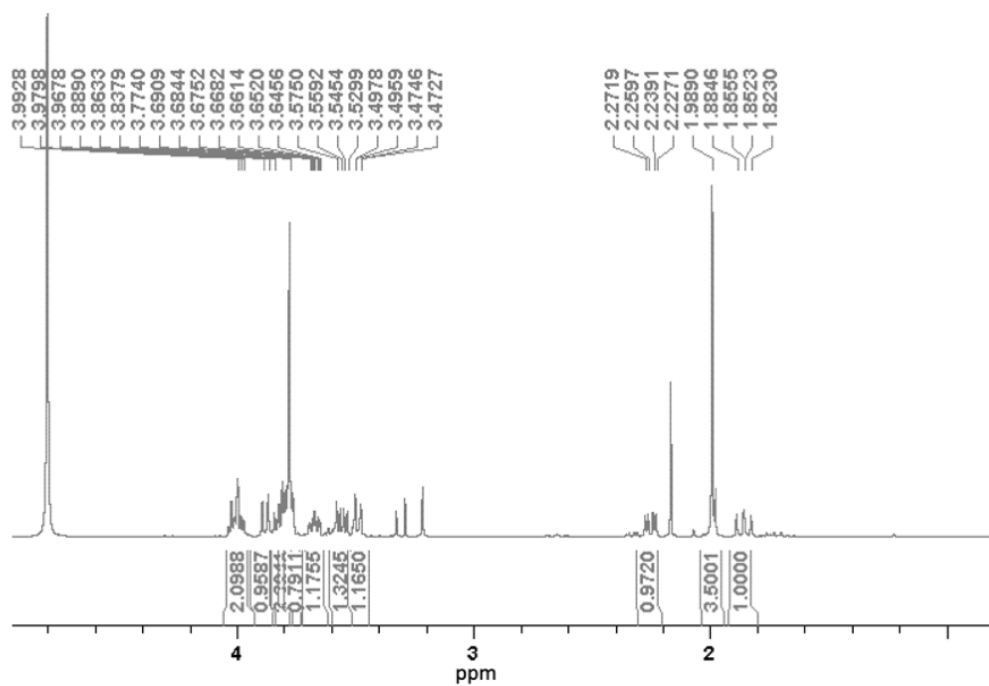


Figure S9. ¹H NMR spectrum of compound 2.

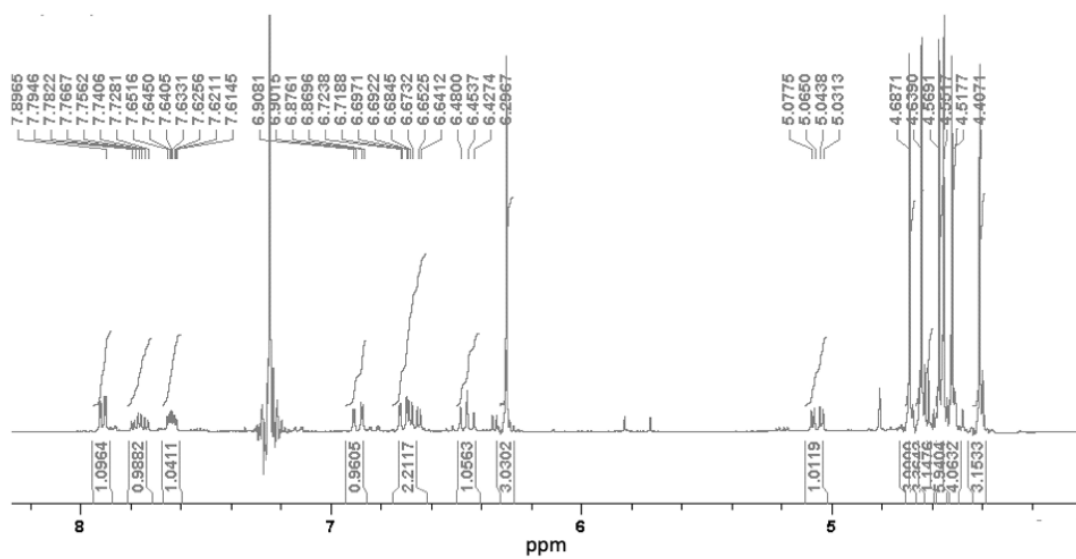


Figure S10. ¹H NMR spectrum of compound 3.

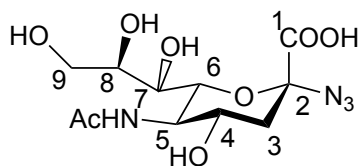
Methyl 4,7,8,9-tetra-O-acetyl-2-chloro-5-(acetamido)-2,3,5-trideoxy-D-glycero-β-D-galactonon-2-ulopyranosonate (4)

Synthesis was conducted following an established procedure.⁴ Anhydrous MeOH (3 mL, 11.5 eq) was added dropwise to a round bottom flask containing AcCl (5.5 mL, 12 eq) cooled with an ice bath. The resulting mixture was added to a solution of compound **3** (3.4 g, 1 eq) in 30 mL of anhydrous dichloromethane and 5.5 mL of AcCl (12 eq) cooled with an ice bath. The reaction was allowed up to rt and stirred overnight. After TLC (elution with 100% EtOAc for 3 times) showed complete conversion of the starting material, the volatile were evaporated under reduced pressure to dryness and the oily residue co-evaporated with toluene (3x) to give compound **4** as a glassy solid (3.2 g, quantitative). It was used directly in the next step.

Methyl 4,7,8,9-tetra-O-acetyl-2-azido-5-(acetamido)-2,3,5-trideoxy-D-glycero-β-D-galactonon-2-ulopyranosonate (5)

Synthesis was conducted following an established procedure.⁵ To a solution of halide **4** (1 g, 1 eq), TBAHS (0.665 g, 1 eq) and NaN₃ (0.637 g, 5 eq) in dichloromethane (1 mL/100mg of halide), saturated NaHCO₃ (1 mL/100 mg of halide) was added. The two-phase mixture was stirred vigorously at rt overnight after which time TLC showed complete conversion (TLC 100 % EtOH). To the crude reaction mixture, EtOAc was added (10 times the volume of dichloromethane); then, the organic phase was separated and successively washed with sat. NaHCO₃, water (2x) and brine. The combined organic extracts were dried over anhydrous Na₂SO₄, filtered, and evaporated under reduced pressure to dryness. Flash chromatography (Hex/EtOAc) afforded the product (**5**) as a white solid (0.750 g, 74 % yield). This was used directly in the next step.

2-azido-5-(acetamido)-3,5-dideoxy-D-glycero- α -D-galacto-non-2-ulopyranosonate (**6**). α 2-azido-2-deoxy-N-acetyl-D-neuraminic acid.



Compound **5** (0.4 g) was dissolved in MeOH:TEA:H₂O (4:1:5) (55 mL) and stirred at rt overnight. The reaction mixture was evaporated under reduced pressure to dryness, dissolved in water, and freeze-dried to afford the Neu5Ac azide (**6**) as a white solid (0.256 g, full conversion). A single anomer was obtained (α) based on the ¹³C shift at 90.9 of C2 (anomeric carbon), in agreement with literature value of 89.1 for the per-acetylated equivalent.⁵ There is no anomeric proton in his compound, hence the use of ¹³C.

δ_{H} (400 MHz, D₂O) 3.93-3.80 (3H, m, H⁴, H⁶, H⁹), 3.80-3.72 (1H, m, H⁵), 3.66-3.61 (1H, m, H⁸), 3.61-3.53(1H, m, H⁹), 3.39 (1H, q, *J* 7, H⁷), 2.68 (1H, dd, *J* 12.5, 4.5, H³), 2.03 (3H, s, CH₃), 1.63 (1H, t, *J* 12.5, H³). δ_{C} (400 MHz, D₂O) 175.1 (NHCO), 172.4 (C¹), 90.9 (C²), 73.8 (C⁶), 71.5 (C⁸), 68.1 (C⁷), 62.7 (C⁹), 51.6 (C⁵), 38.9 (C³), 22.0 (CH₃)

NB: The peaks at ~1.25 ppm and ~3.25 ppm in the proton NMR and ~9 ppm and ~45 ppm are triethylamine salt impurities

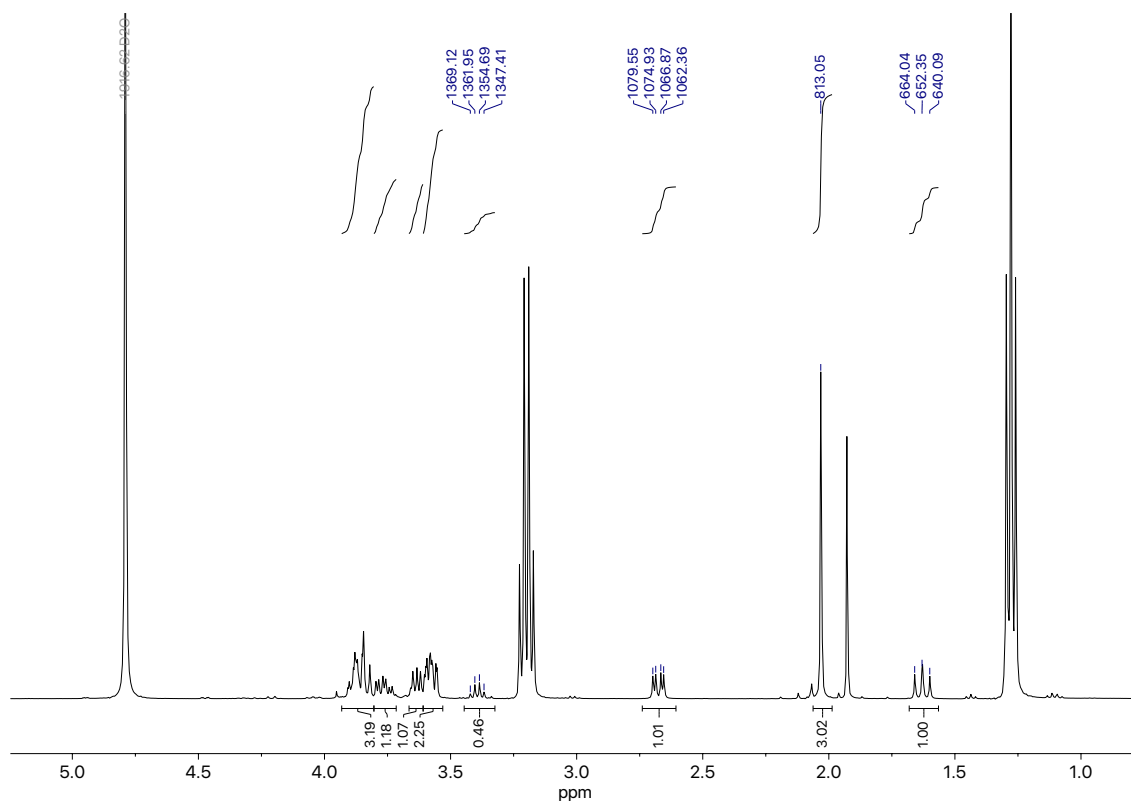


Figure S11. ^1H NMR spectrum of α 2-azido-2-deoxy-*N*-acetyl-D-neuraminic acid.

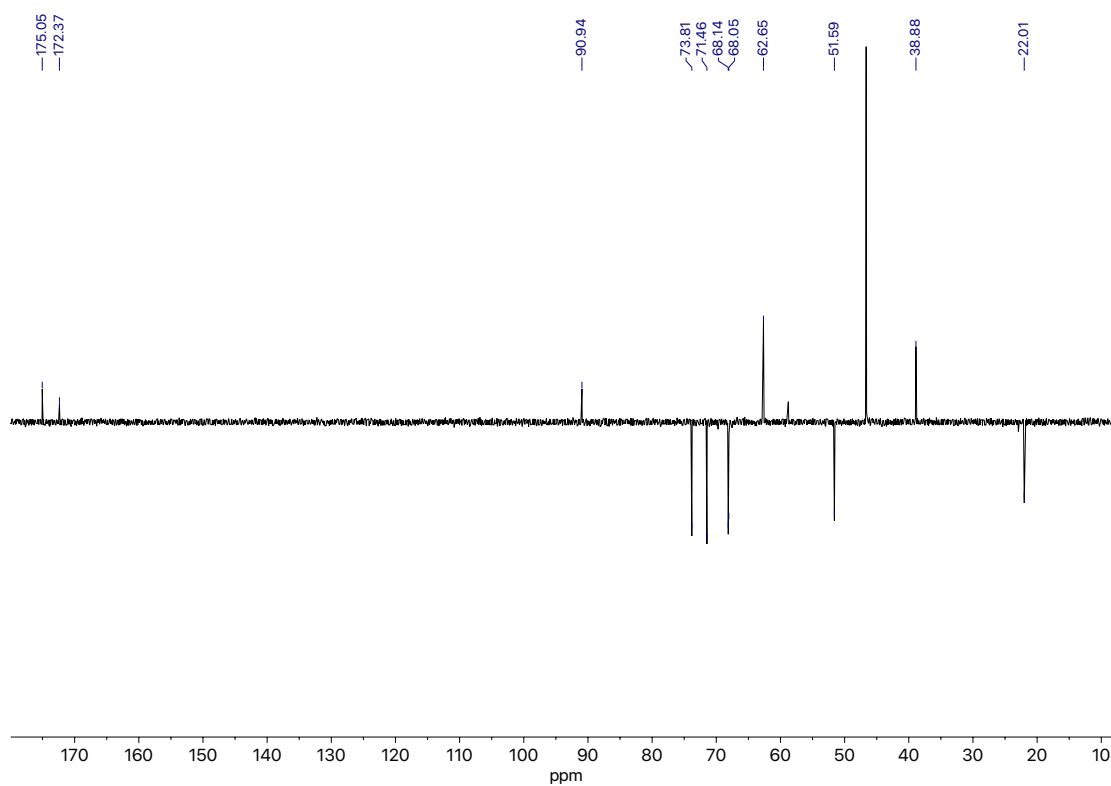
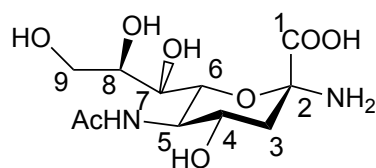


Figure S12. ^{13}C NMR spectrum of α 2-azido-2-deoxy-*N*-acetyl-D-neuraminic acid.

α 2-Amino-2-deoxy-N-acetyl-D-neuraminic acid (7).



2-Azido-2-deoxy-N-acetyl-D-neuraminic acid (40 mg, 0.120 mmol) was dissolved in methanol (5 mL) under nitrogen. Pd(OH)₂/C (20 wt %, 8.4 mg, 0.012 mmol) and hydrazine hydrate (50 %, 19.2 μ L, 0.299 mmol) were then added and the reaction heated to reflux for 4 hours. The reaction mixture was then cooled, filtered (to remove Pd/C) and concentrated *in vacuo* (to remove hydrazine) to give the product as a colourless oil (35 mg). A single anomer was identified in the ¹³C spectra with a chemical shift of 96.1, compared to 89.1 in the azido precursor, consistent with no anomeric inversion during the reduction of azide to amine.

δ_{H} (500 MHz, D₂O) 3.93 – 3.98 (1H, m, H⁴), 3.89 – 3.93 (1H, m, H⁶), 3.84 (1H, q, J 10.0, H⁵), 3.75 (1H, dd, J 12.0, 2.5, H^{9a}), 3.67 (1H, ddd, J 9.0, 6.5, 2.5, H⁸), 3.50 – 3.55 (1H, m, H^{9b}), 3.42 – 3.45 (1H, m, H⁷), 2.15 (1H, dd, J 13.0, 5.0, H^{3a}), 1.96 (3H, s, CH₃), 1.75 (1H, dd, J 13.0, 11.5, H^{3b}). δ_{C} NMR (126 MHz, D₂O) 175.8 (C=OCH₃), 174.7 (C¹), 96.1 (C²), 70.2, 70.2 (C⁶ and C⁸), 68.4 (C⁷), 67.1 (C⁴), 63.2 (C⁹), 52.2 (C⁵), 39.2 (C³), 22.1 (CH₃).

NB: The peaks at ~2.7 ppm and ~2.9 ppm in the proton NMR are DMF impurities

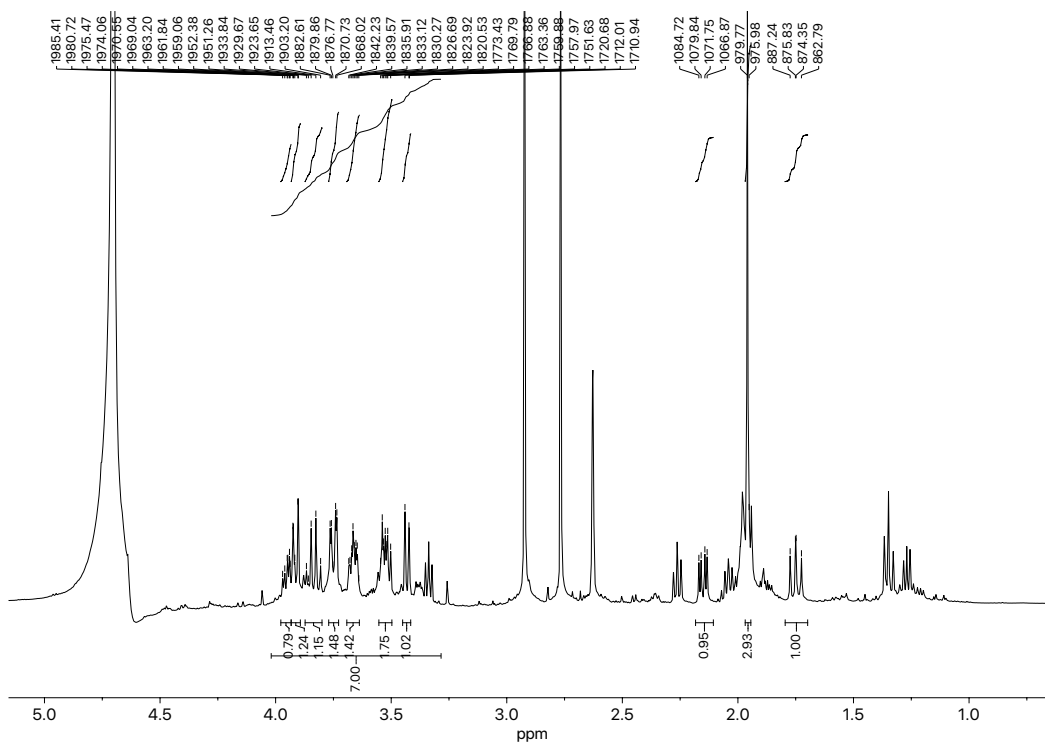


Figure S13. ^1H NMR spectrum of 2-Amino-2-deoxy-*N*-acetyl-*D*-neuraminic acid.

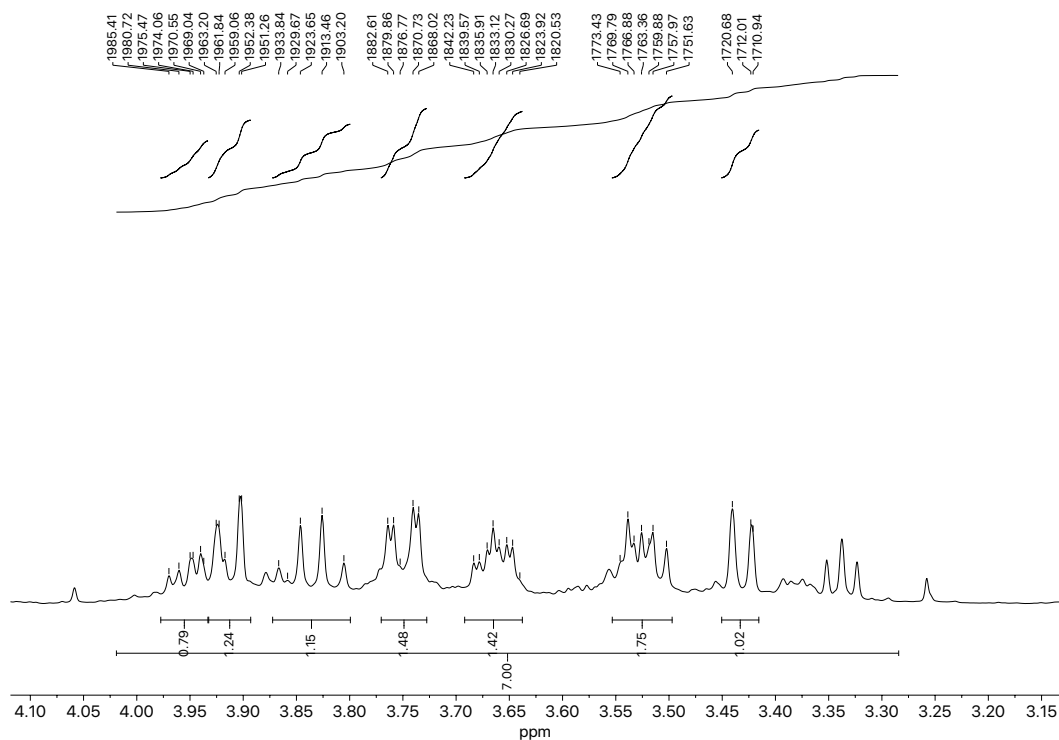


Figure S14. Zoom in of ^1H NMR spectrum (4.15 ppm to 3.15 ppm) of 2-amino-2-deoxy-*N*-acetyl-*D*-neuraminic acid.

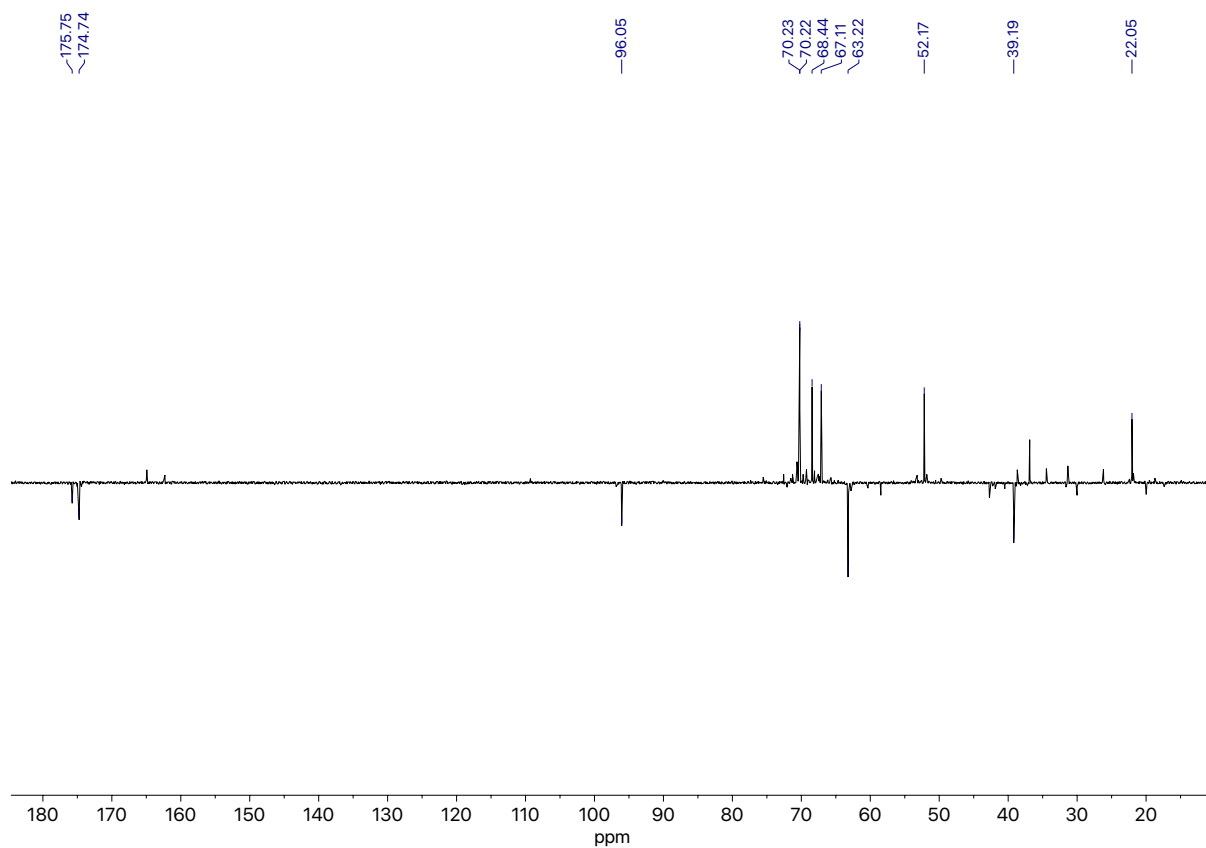


Figure S15. ^{13}C NMR spectrum of 2-amino-2-deoxy-*N*-acetyl-D-neuraminic acid. A single anomeric signal was observed (96 ppm).

*Citrate-stabilised 16nm Gold Nanoparticle Synthesis*⁶

To 500 mL of water was added 0.163 g (0.414 mmol) of gold(III) chloride trihydrate, the mixture was heated to reflux and 14.6 mL of water containing 0.429 g (1.46 mmol) of sodium citrate tribasic dihydrate was added. The reaction was allowed to reflux for 30 minutes before cooling to room temperature over 3 hours. The solution was centrifuged at 13 krpm for 30 minutes and the pellet resuspended in 40 mL of water to give an absorbance at 520 nm of ~1Abs.

Citrate-stabilised 35 nm Gold Nanoparticle Synthesis

35 nm gold nanoparticles were synthesised by a modified step growth method developed by Bastús *et al.*⁷ A solution of 2.2 mM sodium citrate in Milli-Q water (150 mL) was heated under reflux for 15 min under vigorous stirring. After boiling had commenced, 1 mL of H_{Au}Cl₄ (25 mM) was injected. The colour of the solution changed from yellow to bluish gray and then to soft pink in 10 min, 1 mL was taken for DLS and UV/Vis analysis. Immediately after the synthesis of the Au seeds and in the same reaction vessel, the reaction was cooled until the temperature of the solution reached 90 °C. Then, 1 mL of a H_{Au}Cl₄ solution (25 mM) was injected. After 20 min, the reaction was finished. This process was repeated twice. After that, the sample was diluted by adding 85 mL of MilliQ water and 3.1 mL of 60 mM sodium citrate. This solution was then used as a seed solution, and three further portions of 1.6 mL of 25 mM H_{Au}Cl₄ were added with 20 min between each addition. Following completion of this step 1 mL was taken for DLS and UV/Vis analysis. The sample was diluted by adding 135 mL of MilliQ water and 4.9 mL of 60 mM sodium citrate. This solution was then used as a seed solution, and the process was repeated with three further additions of 2.5 mL of 25 mM H_{Au}Cl₄, this solution was analysed by DLS and UV/Vis and target size of 35 nm was reached and the solution was cooled and a sample taken for TEM analysis.

This process of H₂AuCl₄ additions followed by dilution was repeated until a size of 55 nm and 70 nm was reached as determined by UV/Vis and DLS.

Gold Nanoparticle Polymer Coating Functionalisation – 16 nm

100 mg of glycopolymer was agitated overnight with 10 mL of 16 nm AuNPs ~1Abs at UV_{max}. The solution was centrifuged at 13 krpm for 30 minutes and the pellet resuspended in 10mL of water, the solution was centrifuged again at 13 krpm for 30 minutes and the pellet resuspended in 1 mL aliquots and centrifuged at 14.5 krpm for 10 minutes. The pellets were combined into a 1 mL solution with an absorbance at 520 nm of ~10 Abs.

Gold Nanoparticle Polymer Coating Functionalisation – 35, 55 and 70 nm

100 mg of glycopolymer was agitated overnight with 10 mL of 35 nm AuNPs ~1Abs at UV_{max}. The solution was centrifuged at 8 krpm for 30 minutes and the pellet resuspended in 10mL of water, the solution was centrifuged again at 8 krpm for 30 minutes and the pellet resuspended in 1 mL aliquots and centrifuged at 8 krpm for 10 minutes. The pellets were combined into a 1 mL solution with an absorbance at UV_{max} of ~10 Abs.

BSA blocking of Nanoparticle surface

1 mL of UV_{max} at 2.5 Abs AuNPs were centrifuged at 15,00 rpm for 30 mins and supernatant was removed and replaced with 1 mL 1 mg/mL BSA for 30 minutes. The blocking agent was then removed by centrifugation (2 × 30 minutes at 15,000 krpm for 16 nm AuNPs and 2 × 30 minutes at 8,000 rpm for 35 nm AuNPs). The particles were then taken to an Absorbance of ~10 at UV_{max}.

Expression and purification of SARS-COV-2 Spike (S1) in HEK293 Cells

Codon-optimised SARS-COV-2 Spike (S1) subunit (amino acids 1-685) with a C-terminal 10x polyhistidine tag was expressed under control of a CMV promoter (pCMV3-S1-10xHis, Sino Biological, #VG40591-CH). HEK293 cells were grown in suspension to a density of 1.0×10^6 cells/mL in FreeStyle 293 Expression Medium (Thermo Scientific, #12338018), then transfected with 0.5 μ g of pCMV3-S1-10xHis, 1.5 μ g of linear polyethyleneimine (Alfa Aesar, #43896.01) and 50 μ L Opti-MEM-I per 1 mL of cells (Thermo Scientific, #31985-062). After transfection, cells were grown to a density of 2.0×10^6 cells/mL and supplemented with 4 mM valproic acid (Sigma Aldrich, #P4543). 96 hours post transfection, the media was cleared by centrifugation, 6,000 x g in a Fiberlite F10-4 x 1000 LEX rotor (Thermo Scientific, #096-041053) for 10 minutes.

To purify Spike S1, cleared media was adjusted to 20 mM HEPES pH 7.5 and 10 mM imidazole, and was loaded on to a 5 mL HisTrap HP column (Cytiva, #17524801) at a flow rate of 20 mL/min for ~16 hours. A purification buffer comprising 20 mM HEPES, 300 mM NaCl and 1 mM DTT +/- 1 M imidazole was used (for buffer lines A and B respectively), and the column was washed with 30 CVs of 2% buffer B (20 mM imidazole) before eluting the protein over a 2-50% gradient over 30 CVs. Fractions containing Spike (S1) were pooled and concentrated using a 10 KDa molecular-weight cut-off spin concentrator (Sigma Aldrich, #UFC910008), before being buffer exchanged into 20 mM HEPES 7.5, 300 mM NaCl, 10% glycerol using a 5 mL HiTrap desalting column (Cytiva, #29048684). Peak fractions were pooled, and the final concentration was measured by absorbance at 280 nm, yielding a concentration of 1.25 mg/mL. Aliquots of protein were snap-frozen in liquid nitrogen and stored at -80°C.

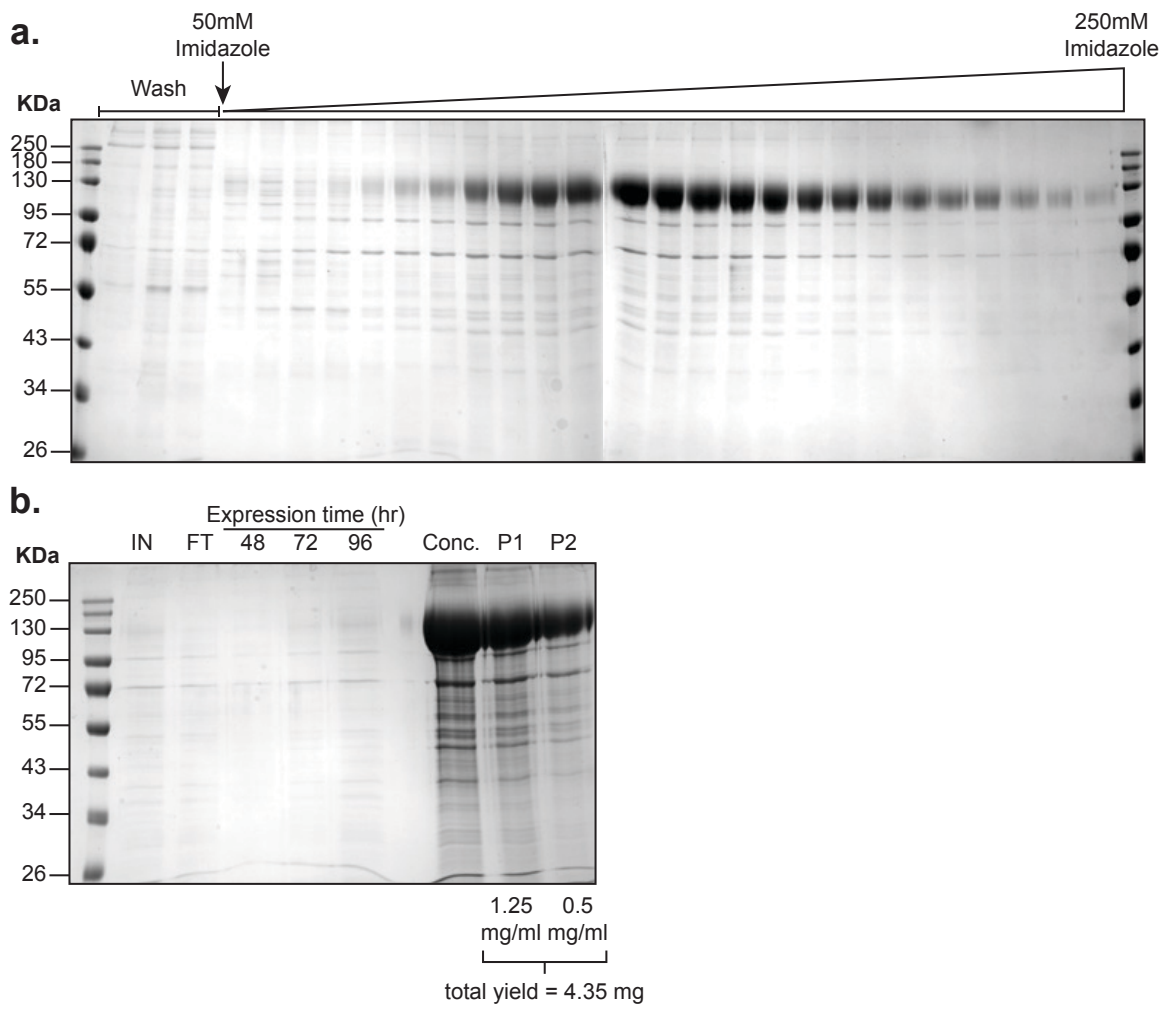


Figure S16. Gel electrophoresis of expressed spike protein. P1 and P2 were used here.

Recombinant Expression and Purification of SARS-COV-2,S1 (first 300 amino acids) for Thermal Shift Assay

A pET21a plasmid encoding for a hexahistidine-tag, SUMO-tag and the first 300 amino acids of SARS-COV-2,S1 was purchased from Genscript Inc. The plasmid was transformed into competent *Escherichia coli* BL21(DE3) cells (New England Biolabs). A colony was selected to inoculate 100 mL of LB-medium containing $100 \mu\text{g}\cdot\text{mL}^{-1}$ kanamycin and was grown overnight at 37°C under continuous shaking of 180 rpm. The following day, 10 mL of the preculture was added to 1 L of LB-medium (supplemented with $100 \mu\text{g}\cdot\text{mL}^{-1}$ kanamycin) in a 2.5 L Ultra Yield™ flask and grown at 37°C with a shaking speed of 180 rpm till an OD600 of 0.6 was reached. The temperature was then reduced to 16°C and the cells incubated for another hour before adding IPTG to a final concentration of 0.2 mM. The overexpression of the protein was allowed to take place overnight following which the cells were centrifuged at 5000 g for 10 minutes at 4°C . Pelleted cells were resuspended in PBS supplemented with Pierce protease inhibitor mini-tablets. The suspension was passed through a STANSTED ‘Pressure Cell’ FPG12800 homogenizer in order to lyse the cells. The cell lysate was centrifuged at 48,000 g and the supernatant was passed through a $0.45 \mu\text{m}$ filter before being added to a 3 mL column of IMAC cOmplete His-Tag Purification Resin (Roche) pre-equilibrated with PBS. The column was washed with 20 column volumes of PBS. Bound protein was eluted using 6 mL of 300 mM Imidazole in PBS. Further purification of was achieved using a HiLoad 16/600 Superdex 200 pg gel filtration column (GE Healthcare) with PBS as the running buffer. Purity was estimated using SDS-PAGE and protein concentration determined using Thermo Scientific Pierce BCA assay kit. Various volumes of the protein contained in PBS solution were aliquoted into 1.5 mL microcentrifuge tubes and snap-frozen in liquid nitrogen to store at -80°C until required.

Synthesis of Low Concentration SARS-COV-2,S1-coated Polystyrene Nanoparticle Virus Mimics

12.5 μL of 0.5 mg/mL SC2 S1 from Pool 2 and 125 μL of polystyrene nanoparticles were added to 1000 μL 10 mM HEPES saline buffer (0.15 M NaCl). This was agitated for 1 hour. It was not centrifuged before use in testing. This gave a maximum SC2 S1 concentration on polystyrene of 5.5 $\mu\text{g}/\text{mL}$.

The low concentration naked polystyrene control was made up as above except the SC2 S1 protein was replaced with distilled water of equal volume (12.5 μL).

Synthesis of High Concentration SARS-COV-2,S1-coated Polystyrene Nanoparticle Virus Mimics

30 μL of 0.5 mg/mL SC2 S1 from Pool 2 and 125 μL of polystyrene nanoparticles were added to 845 μL 10 mM HEPES saline buffer (0.15 M NaCl). This was agitated for 1 hour. It was not centrifuged before use in testing. This gave a maximum SC2 S1 concentration on polystyrene of 15 $\mu\text{g}/\text{mL}$.

The high concentration naked polystyrene control was made up as above except the SC2 S1 protein was replaced with distilled water of equal volume (12.5 μL).

Lateral Flow Strip Production, Running and Analysis Protocols

Protocol for manufacturing lateral flow strips

Backing cards were cut to size by removal of 20 mm using a guillotine. Nitrocellulose was added to the backing card by attaching the plastic backing of the nitrocellulose to the self-adhesive on the card. The wick material was then added to the backing card so it overlaps with the nitrocellulose by ~5 mm. The lateral flow strips were cut to size of width 2-3 mm.

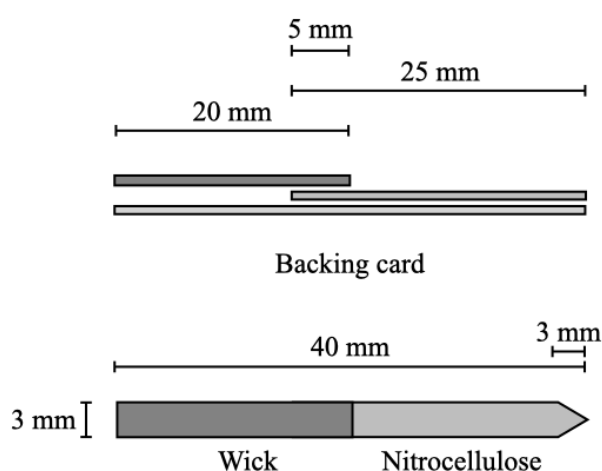


Figure S17. Lateral flow strip dimensions

Protocol for test line addition to the lateral flow strips

1 μL of the test line solution was added to the test strip using a micropipette fitted with 10 μL tip, the test line was spotted ~1 cm from the non-wick end of the strip. The strips were dried at 37 $^{\circ}\text{C}$ in an oven for 30 minutes. The tests strips were allowed to cool to room temperature before testing.

Protocol for running lateral flow test without target analyte in buffer

The running buffer of total volume 50 μL was made as follows; 5 μL AuNPs (OD10), 5 μL lateral flow assay buffer – 10 \times HEPES buffer, 40 μL water. The running solution was then

agitated on a roller for 5 minutes. 45 μL of this solution was added to a 0.2 mL PCR tube, standing vertically.

A small “v” (~3 mm) was cut into the test strips at the non-wick end and the strips added to the PCR tubes so they protrude from the top and the immobile phase (1 cm from non-wick end) is not below the solvent line. There was one test per tube. All tests were run in triplicate.

The tests were run for 20 minutes before removal from the tubes. The test strips were allowed to dry at room temperature for ~5 minutes. The test strips were mounted test-face down onto a clear and colourless piece of acetate sheeting.

Protocol for running lateral flow test with polystyrene nanoparticle virus mimic analyte in buffer

The running buffer of total volume 50 μL was made as follows; 5 μL AuNPs (OD10), 5 μL lateral flow assay buffer – 10 \times HEPES buffer, 40 μL polystyrene solution. The running solution was then agitated on a roller for 5 minutes. 45 μL of this solution was added to a 0.2 mL PCR tube, standing vertically.

A small “v” (~3 mm) was cut into the test strips at the non-wick end and the strips added to the PCR tubes so they protrude from the top and the immobile phase (1 cm from non-wick end) is not below the solvent line. There was one test per tube. All tests were run in triplicate.

The tests were run for 20 minutes before removal from the tubes. The test strips were allowed to dry at room temperature for ~5 minutes. The test strips were mounted test-face down onto a clear and colourless piece of acetate sheeting.

Standard protocol for lateral flow strip analysis

The acetate sheets were scanned using a Kyocera TASKalfa 5550ci printer to a pdf file that was converted to a jpeg, scans were taken within 1 hour of strip drying. The jpeg was analysed

in Image J 1.51 using the plot profile function to create a data set exported to Microsoft Excel for Mac. The data was exported to Origin 2019 64Bit and trimmed to remove pixel data not from the strip surface. The data was aligned and averaged (mean). The data was then reduced by number of groups to 100 data points (nitrocellulose and wick) and plotted as Grey value (scale) vs Relative distance along the 100 data points.

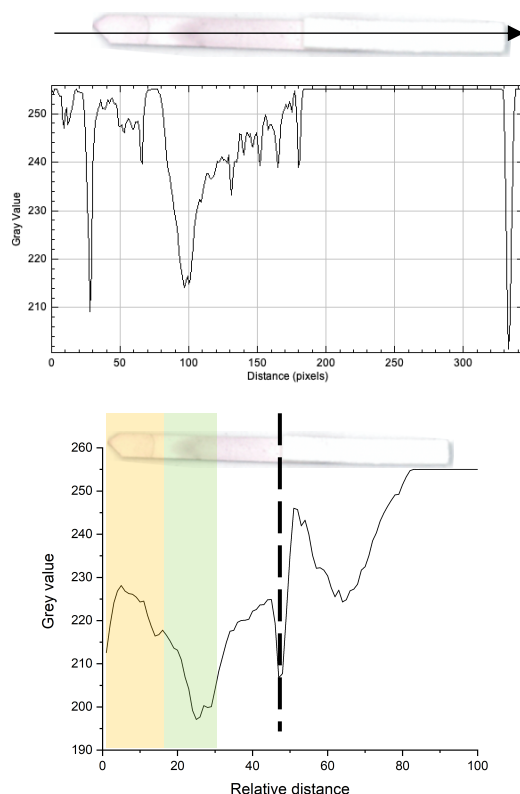


Figure S18. Representative dipstick (Top), raw grey value plot (Middle) and processed grey value plot (Bottom)

Lateral flow signal to noise analysis

Relative distance pixel 15 to 35 (area around the test line) was averaged (mean) to provide average noise around the test line for strips vs. 2,3'-sialyllactosamine-BSA (1 mg/mL) as a test line. The signal value was determined by selecting the lowest grey value between 15 to 35 relative distance pixels for strips vs. SARS-COV-2,S1 (0.39 mg/mL) as a testline. Equation 1 was then used to determine the signal to noise ratio.

$$\text{Signal to Noise} = \frac{255 - \text{Signal}}{255 - \text{Noise}}$$

Equation 1. Equation for determining signal to noise ratio

NB: 255 is the grey value for the blank nitrocellulose surface.

Lateral flow signal intensity analysis

Relative distance pixel 15 to 35 (area around the test line), excluding pixels that contributed to the signal peak were averaged (mean). This average was subtracted from the lowest grey value between 15 to 35.

Silver Staining Procedure

Staining solution was prepared as kit guidelines. 2 mL of solution A and 2 mL of solution B were added to a watch glass and mixed thoroughly. The wick of the strip was removed and the nitrocellulose strip immersed for 1 minute. Samples were removed from the solution, washed with still water and dried room temperature for 10 minutes before scanning with a Kyocera TASKalfa 5550ci printer to a pdf file that was converted to a jpeg.

Lateral flow assay buffer - 10× HEPES buffer (10% PVP₄₀₀) in 100 mL H₂O

2.38 g (100 mmol.dm⁻³) of HEPES, 8.77 g (1.50 mol.dm⁻³) of NaCl, 0.011 g (1.0 mmol.dm⁻³) of CaCl₂, 0.8 g (0.8% w/v., 123 mmol.dm⁻³) of NaN₃, 0.5 g (0.5% w/v., 4.07 mmol.dm⁻³) of Tween-20 and 10 g (10% w/v.) of poly(vinyl pyrrolidone)₄₀₀ (PVP₄₀₀, Average Mw ~40,000) was dissolved in 100 mL of water. The buffer is not pH adjusted. All experiments with 2,3'- and 2,6'-Sialyllactosamine (2,6SL) functionalised PHEA polymers used a 1% PVP₄₀₀ buffer.

Neuraminic acid (NeuNAc) functionalised PHEA polymers of varying lengths on 35nm AuNPs with BSA versus a test line of SARS-COV2,S1 protein (SC2, 0.39 mg/mL), SARS-COV1 spike protein (SC1, 0.4 mg/mL) or neuraminic acid-BSA (NeuNAc-BSA, 1 mg/mL)

also used a 1% PVP₄₀₀ buffer. Neuraminic acid (NeuNAc) functionalised PHEA polymers of varying lengths on 16nm and 35nm AuNPs verses a test line of SARS-COV2,S1 protein (SC2, 0.39 mg/mL) or 2,3'-sialyllactosamine BSA (2,3SL-BSA, 1mg/mL) also used a 1% PVP₄₀₀ buffer.

All other experiments with neuraminic acid glycopolymer functionalised AuNPs used a 10× HEPES buffer (20% PVP₄₀₀) buffer to further decrease background noise.

The percentage of PVP₄₀₀ in the buffer is listed in the supplementary figure and table headings.

Lateral Flow Complete Device Production, Running and Analysis Protocols

Protocol for manufacturing lateral flow complete devices

Nitrocellulose was added to the backing card by attaching the plastic backing of the nitrocellulose to the self-adhesive on the card. The wick material was then added to the backing card so it overlaps with the nitrocellulose by ~5 mm. The strips were then cut to size of width ~3 mm so they sit in the cassettes without the need for excess force to fit. Tests lines were then added before addition of the conjugate pad. 1 µL of the test line solution was added to the nitrocellulose strip using a micropipette fitted with 10 µL tip, the test line was spotted ~1 cm from the non-wick end of the nitrocellulose surface. A control line was added ~1.5 cm from non-wick end of the nitrocellulose surface. The strips were dried at 37 °C in an oven for 30 minutes. The tests strips were allowed to cool to room temperature before addition of the conjugate pad. The conjugate pad was added to the backing card so it overlaps with the nitrocellulose by ~3.5 mm. The sample pad, was cut to size of 20 mm by 6 mm and was added to the backing card, overlapping with the conjugate pad by ~6.5 mm and straddling the backing card evenly. The completed strip was then added to the cassettes and sealed.

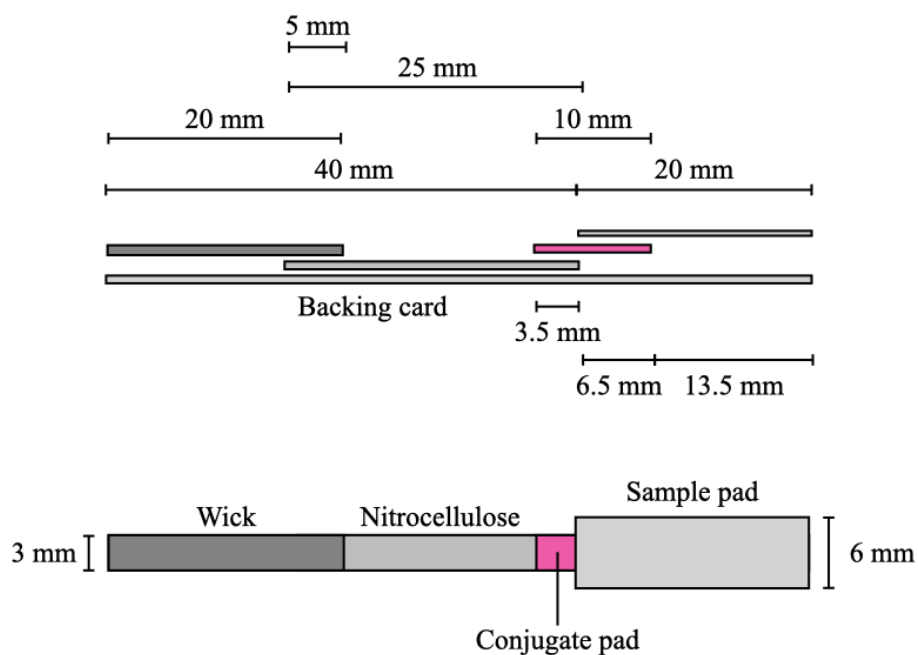


Figure S19. Lateral flow complete strip dimensions

Protocol for Conjugate Pad Production

Strips of the conjugate pad material were agitated for 30 minutes in a solution of 0.1% Tween-20 (blocking solution). The strips were then patted dry and baked overnight at 37 °C in an oven overnight. The conjugate pads were cut to size (3 mm width) and placed individually into the wells of a 384-well microplate. 20 μ L 1 \times conjugate pad buffer solution containing OD1 (unless otherwise specified) AuNPs was added to the top of each conjugate pad in the wells. The pads were dried for 3 hours at 37 °C in an oven before curing overnight in an airtight box containing desiccant. The completed pads were always stored in an airtight box containing desiccant.

10 \times Conjugate Pad Buffer

10% w/v. of poly(vinyl pyrrolidone)₄₀₀ (Average Mw \sim 40,000 g.mol⁻¹), 50% w/v. trehalose, 10% w/v. sucrose and 0.1% w/v. Tween-20 were added to distilled water and allowed to dissolve.

Protocol for running lateral flow test without target analyte in buffer

8 μL 10 \times HEPES buffer (20% PVP₄₀₀) was added to 72 μL distilled water. 80 μL was added to the sample pad and allowed to absorb. The test was run for 10 minutes before scanning in the cassettes by a Kyocera TASKalfa 5550ci printer to a pdf file that was converted to a jpeg. After \sim 1 hour the strips were removed from the cassettes, and added to acetate sheets. These were scanned using a Kyocera TASKalfa 5550ci printer to a pdf file that was converted to a jpeg, acetate scans were taken within 1 hour of strip drying. The jpegs were analysed in Image J 1.51 using the plot profile function to create a data set exported to Microsoft Excel for Mac. The data was exported to Origin 2019 64Bit and trimmed to remove pixel data not from the strip surface. The data was aligned and averaged (mean). The data was then reduced by number of groups to 100 data points (just the nitrocellulose surface) and plotted as Grey value (scale) vs Relative distance along the 100 data points.

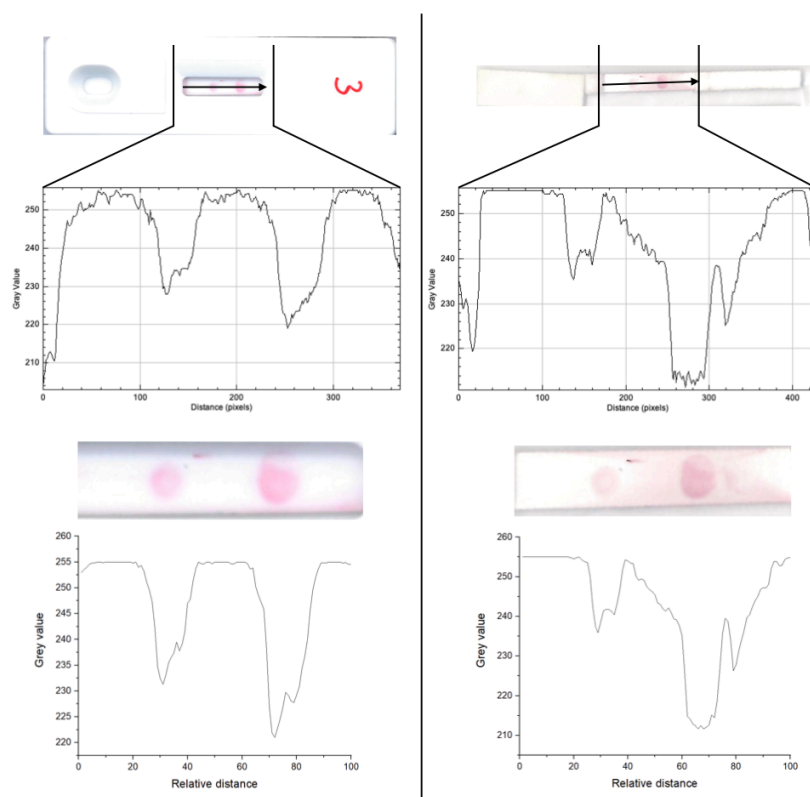


Figure S20. Representative cassette (Top left) and strip (Top right), raw grey value plot (Middle) and processed grey value plot (Bottom)

Lateral flow signal to noise analysis

Relative distance pixel 1 to 10 and 51 to 60 (area around the test line) was averaged (mean) to provide average noise around the test line for strips. The signal value was determined by selecting the lowest grey value between 11 to 50 relative distance pixels. Equation 1 was then used to determine the signal to noise ratio.

Lateral flow signal intensity analysis

Relative distance pixel 1 to 10 and 51 to 60 (area around the test line), excluding pixels that contributed to the signal peak were averaged (mean). This average was subtracted from the lowest grey value between 11 to 50.

Additional Data and Figures

Sequence Alignment comparison for coronaviruses.

The multiple sequence alignment was undertaken using Clustal Omega⁸ with the following GenBank accession numbers:

Coronavirus	GenBank accession numbers
HCoV-OC43	AAT84354.1
SARS-CoV-1	AAP13441.1
IBV-CoV	AAW33786.1
MERS-CoV	AYM48030.1
SARS-CoV-2	QHD43416.1

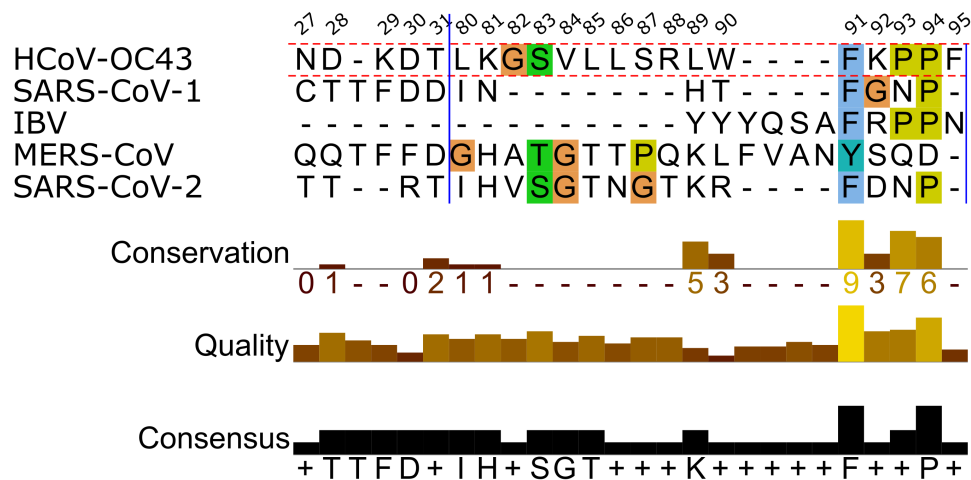


Figure S21. Sequence alignments of coronavirus spike proteins from SARS-COV-1, IBV, MERS-COV, and SARS-COV-2 with respect to the known sialic acid binding groove of HCOV-OC43.

Glycan Synthesis additional data.

The synthetic schemes for the glycans used here are shown in Figure S22. To confirm reduction of the azides to amines, TLC staining with ninhydrin was undertaken, as shown in Figure S23/24.

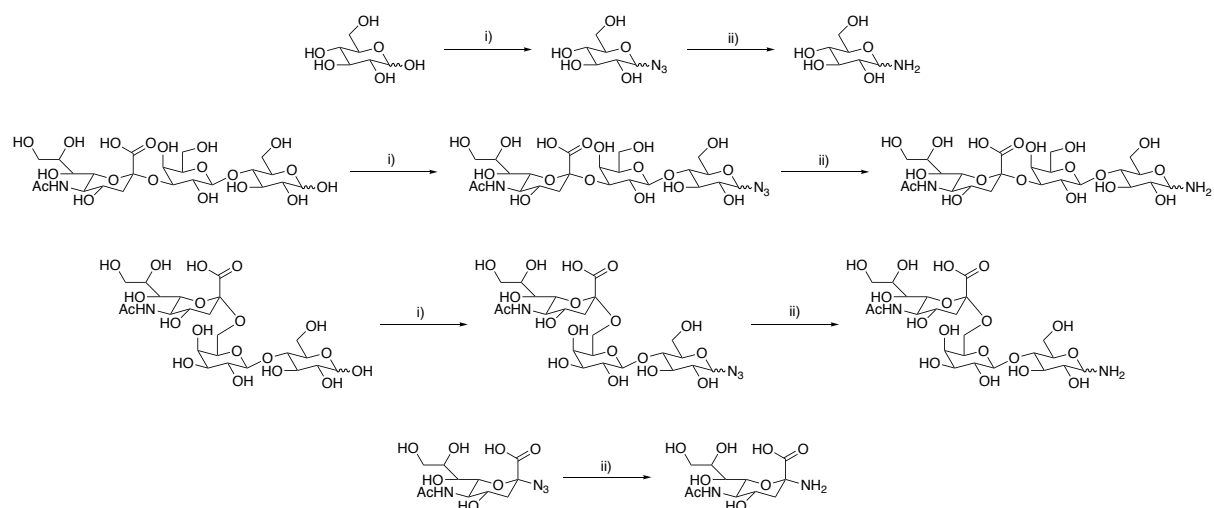


Figure S22. Glycan synthesis. i) 5 eq. Et_3N , 3 eq. 2-azido-1,3-dimethylimidazolium hexafluorophosphate (ADMP), 4:1 $\text{D}_2\text{O}/\text{MeCN}$, 0 °C 3h, 4 °C 16h. ii) 2.5 eq. H_2NNH_2 , 0.1 eq. $\text{Pd}(\text{OH})_2/\text{C}$, MeOH, reflux, 16h.

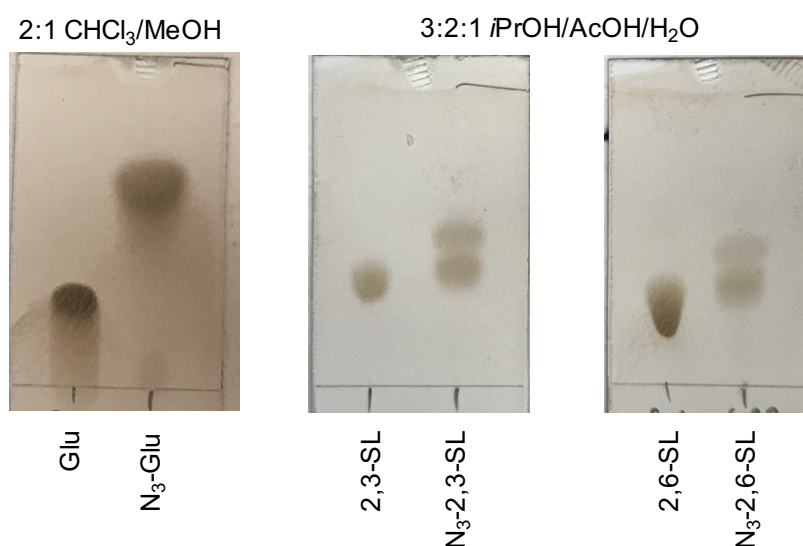


Figure S23. TLC's from ADMP reaction to form azido-glycans. TLC plates were stained with 5% H_2SO_4 in EtOH, then heated to visualise the spots.

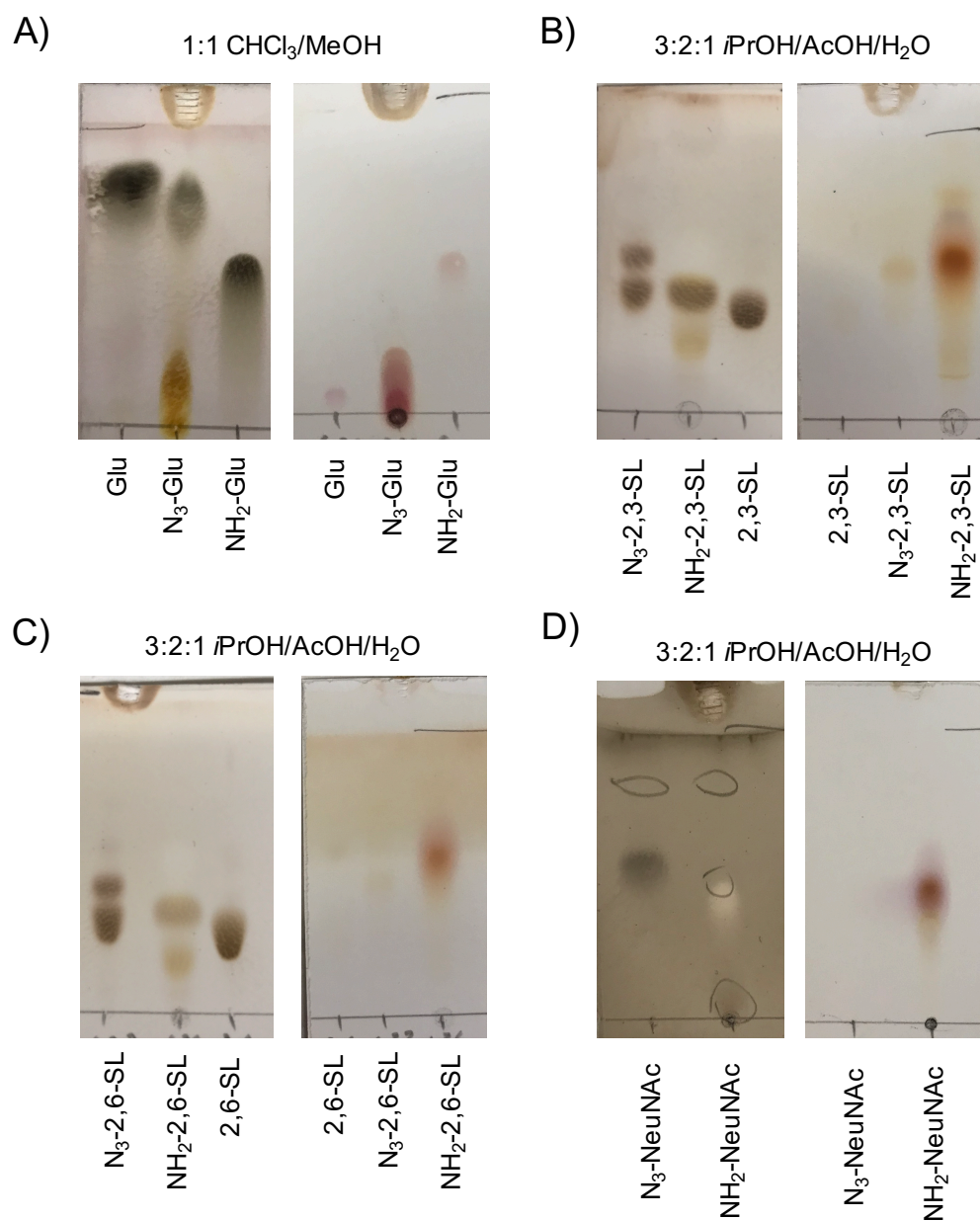


Figure S24. TLC's from reduction reactions to form amino-glycans. TLC's were stained with either 5% H₂SO₄ in EtOH (left hand TLC) or ninhydrin (right hand TLC), then heated to visualise the spots. A) Glucose, B) 2,3'-sialyllactose (2,3-SL), C) 2,6'-sialyllactose (2,6-SL), D) N-acetylneuraminic acid.

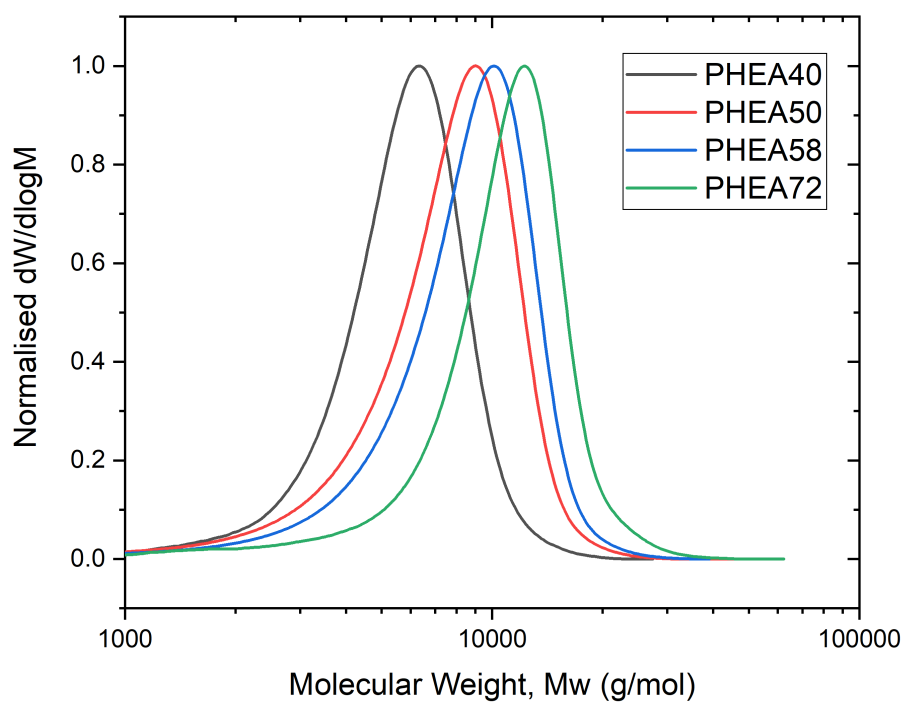


Figure S25. Normalised size exclusion chromatography RI molecular weight distributions of telechelic PHEA obtained in DMF versus PMMA standards.

NB: For PHEA72; $M:CTA = 30$, $M_{N(theo)} = 5100 \text{ g}\cdot\text{mol}^{-1}$, $M_{N(SEC)} = 8900 \text{ g}\cdot\text{mol}^{-1}$, $M_{N(NMR)} = 7800 \text{ g}\cdot\text{mol}^{-1}$ and $D = 1.28$

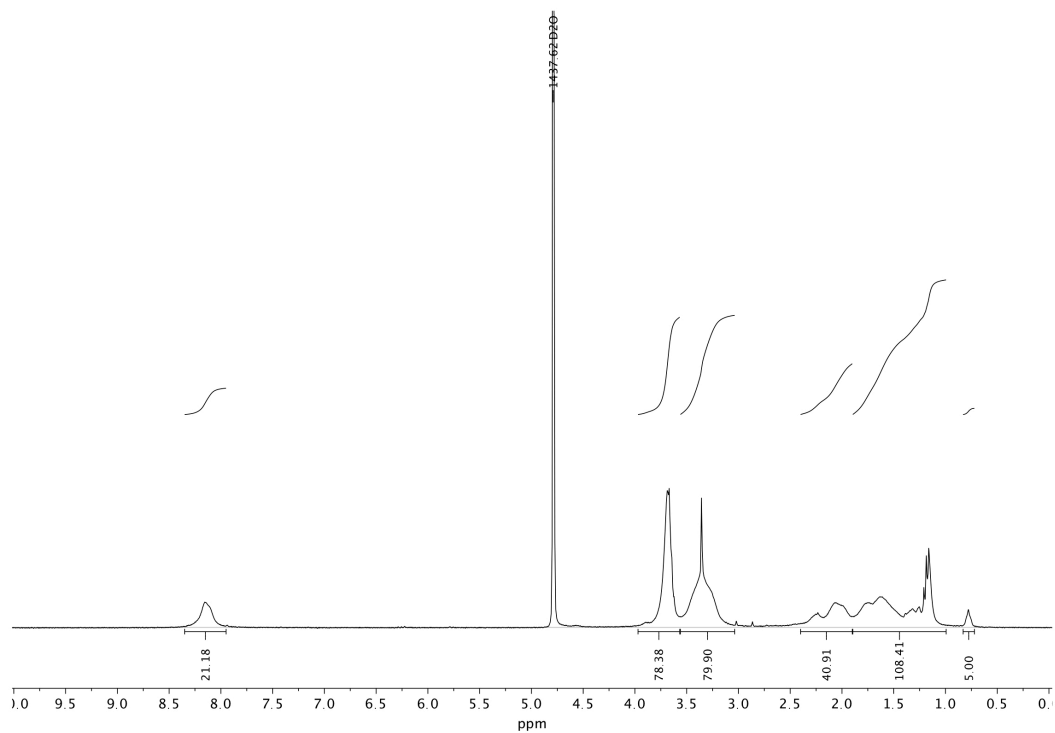


Figure S26. ^1H NMR spectrum of DP40 PHEA

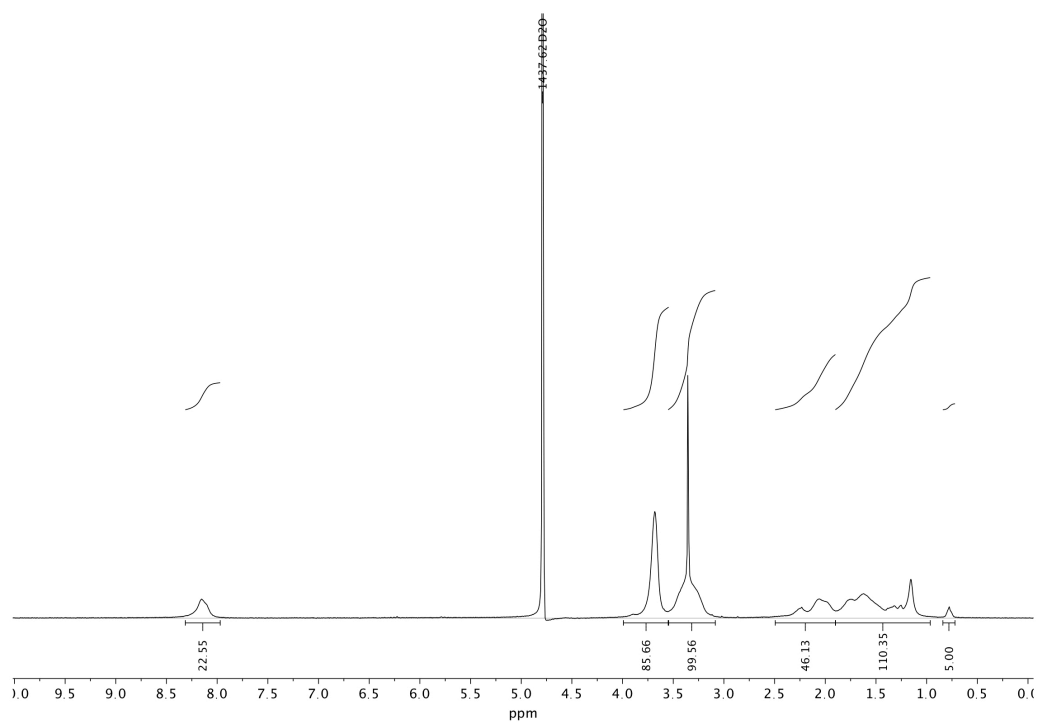


Figure S27. ^1H NMR spectrum of DP50 PHEA

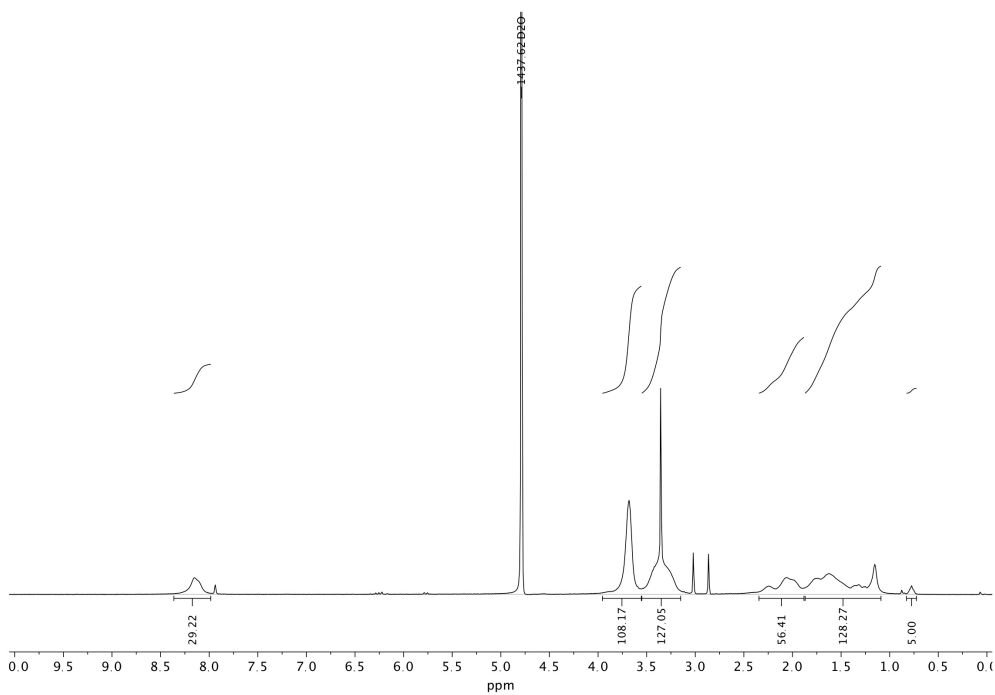


Figure S28. ^1H NMR spectrum of DP58 PHEA

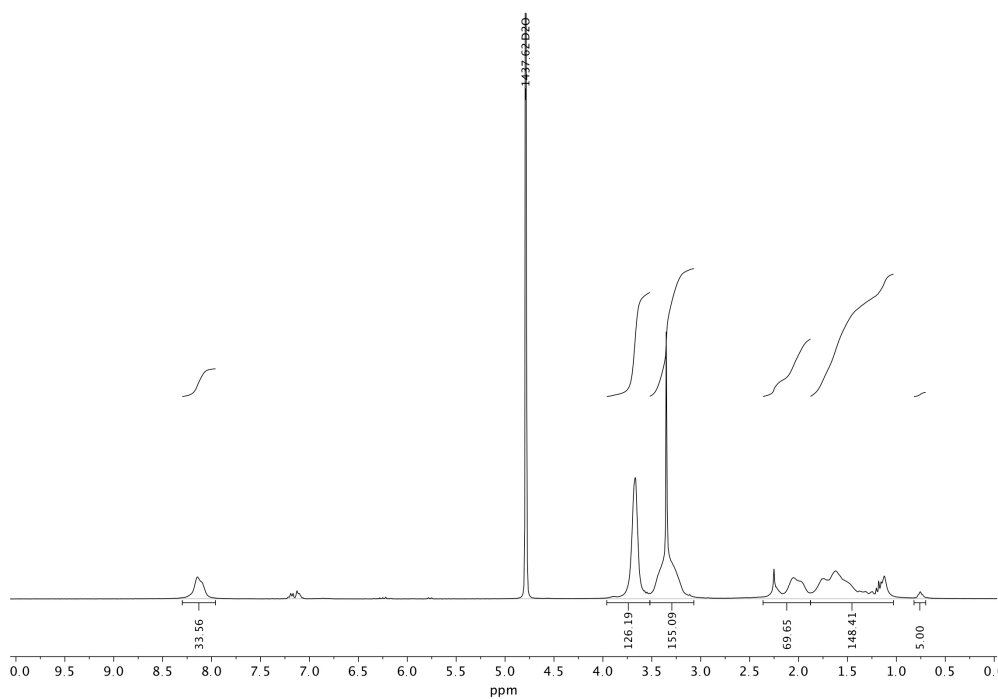


Figure S29. ^1H NMR spectrum of DP72 PHEA

Nanoparticle Characterization

The citrate-stabilized gold nanoparticles were characterized by DLS, UV/VIS and TEM. Example images and histogram analyses (from >100 particles) are shown below. Note 16 nm particles with sialyllactose were not colloiddally stable and not used, as indicated in main text.

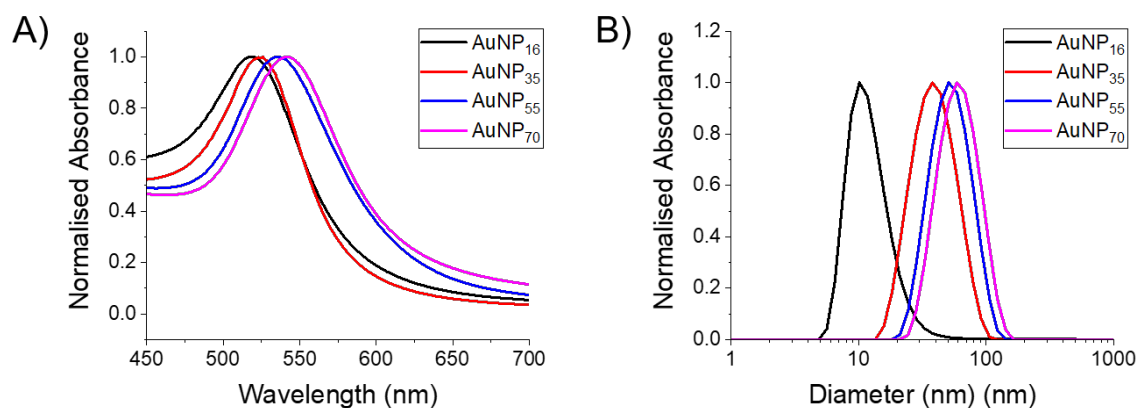


Figure S30. Characterization of uncoated AuNPs used in this study A) UV/Vis and B) DLS.

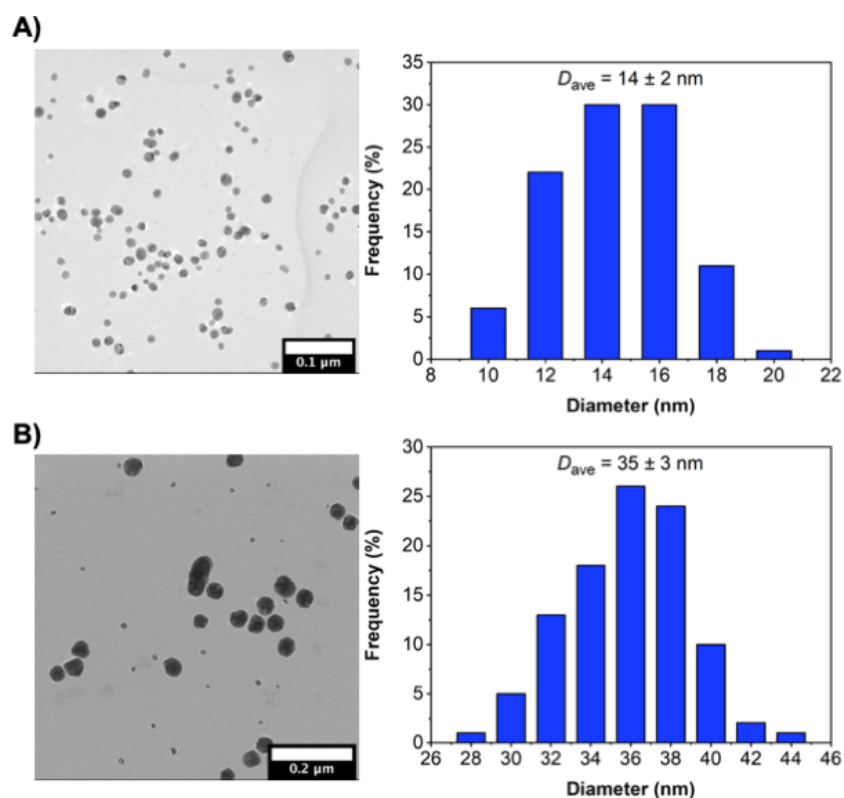


Figure S31. TEM images (Left) and histograms (right) of citrate stabilized AuNPs. A) 16 nm AuNP and B) 35 nm AuNP. Histograms from analysis of analysis of >100 particles

Code	UVmax ^(a) (nm)	A _{SPR} /A ₄₅₀ ^(b)	D _h ^(c) (nm)	D _{h(DLS)} ^(d) (nm)
Citrate AuNP ₁₆	519	1.64	16	20.7±0.8
NeuNAc- PHEA ₅₀ AuNP ₁₆	527	1.66	16	40.9±0.5
NeuNAc- PHEA ₅₈ AuNP ₁₆	526	1.68	18	44.2±0.8
Citrate AuNP ₃₅	526	1.91	35	34.5±0.5
NeuNAc- PHEA ₅₀ AuNP ₃₅	531	1.98	45	46.2±0.7
NeuNAc- PHEA ₅₈ AuNP ₃₅	531	1.99	45	55.3±0.8

Table S1. Characterization of unfunctionalized and functionalised AuNPs used in this study.

SPR absorption maximum; (b) Absorbance ratio of SPR to 450 nm; (c) Estimated from UV-Vis⁹; (d) From dynamic light scattering; (e) From TEM, from average of >100 particles, showing ±S.D.

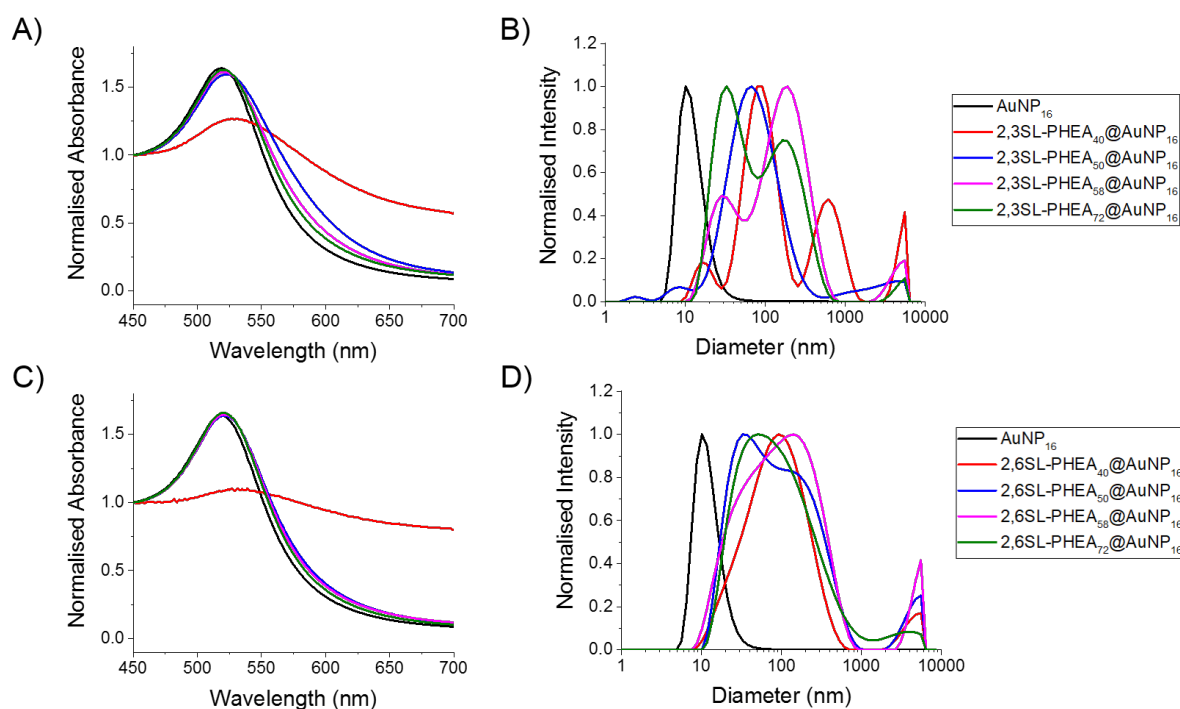


Figure S32. Characterization of 16 nm AuNPs functionalised with α 2,3'-sialyllactose by A) UV/Vis and B) DLS and functionalised with α 2,6'-sialyllactose by C) UV/Vis and D) DLS.

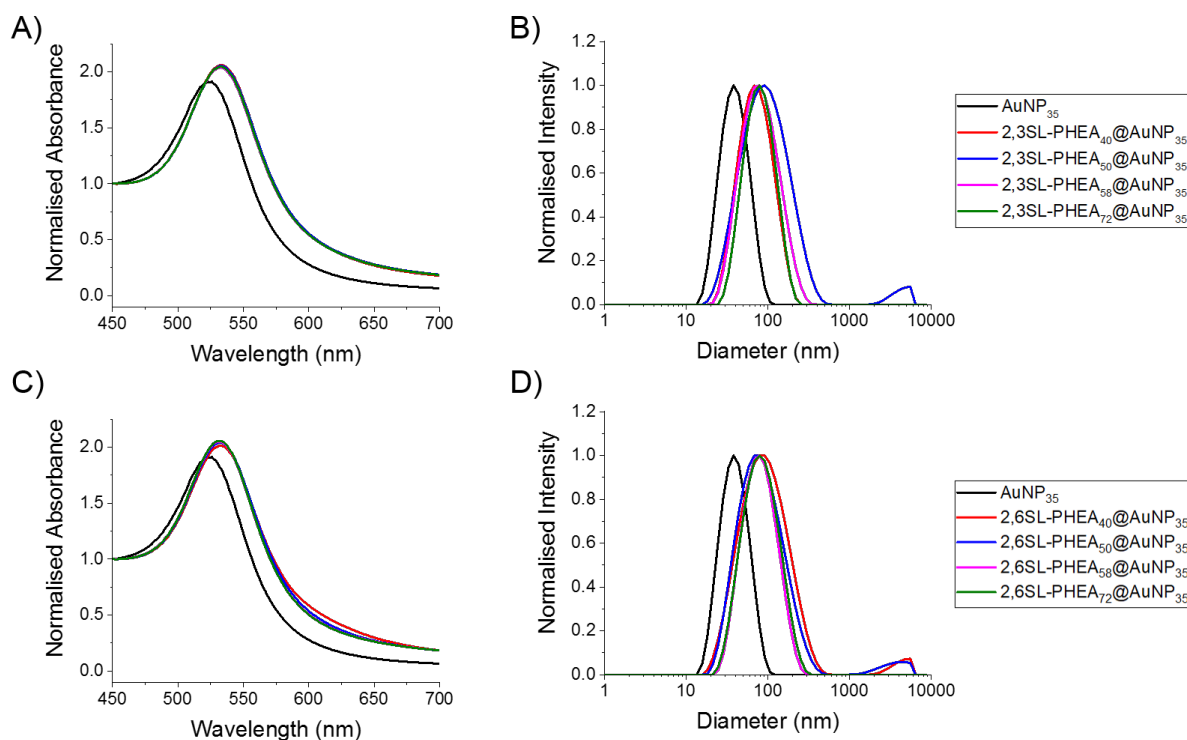


Figure S33. Characterisation of 35 nm AuNPs functionalised with α 2,3'-sialyllactose by A) UV/Vis and B) DLS and functionalised with α 2,6'-sialyllactose by C) UV/Vis and D) DLS.

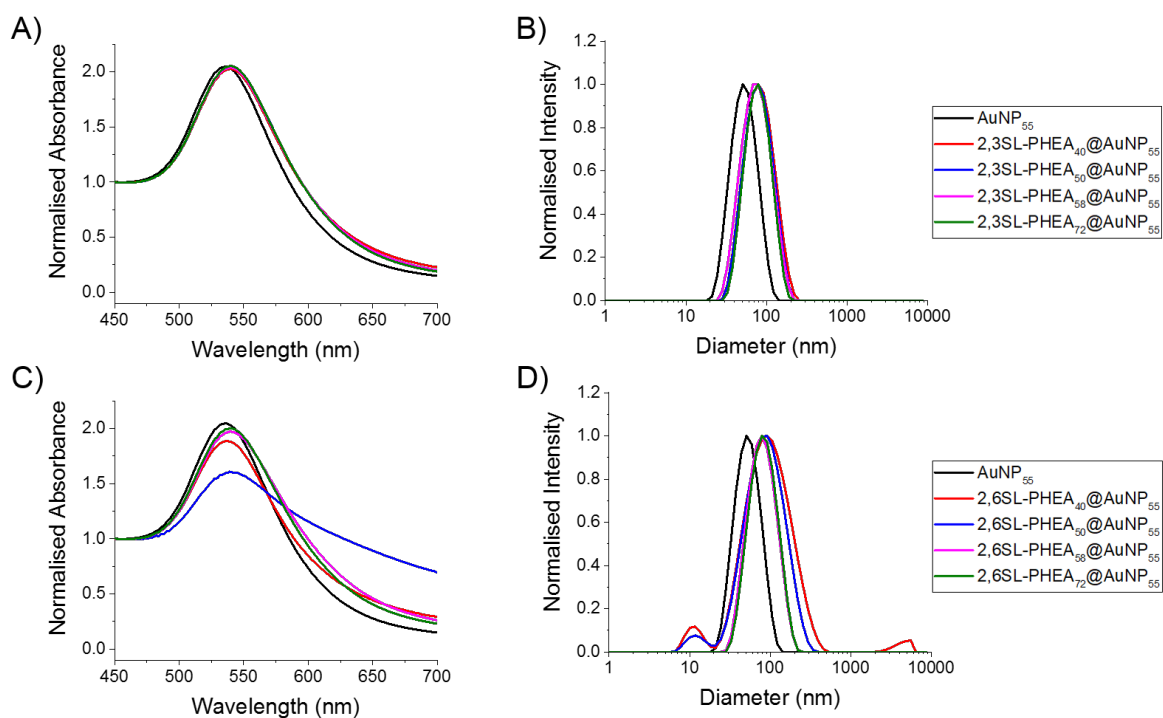


Figure S34. Characterisation of 55 nm AuNPs functionalised with α 2,3'-sialyllactose by A) UV/Vis and B) DLS and functionalised with α 2,6'-sialyllactose by C) UV/Vis and D) DLS.

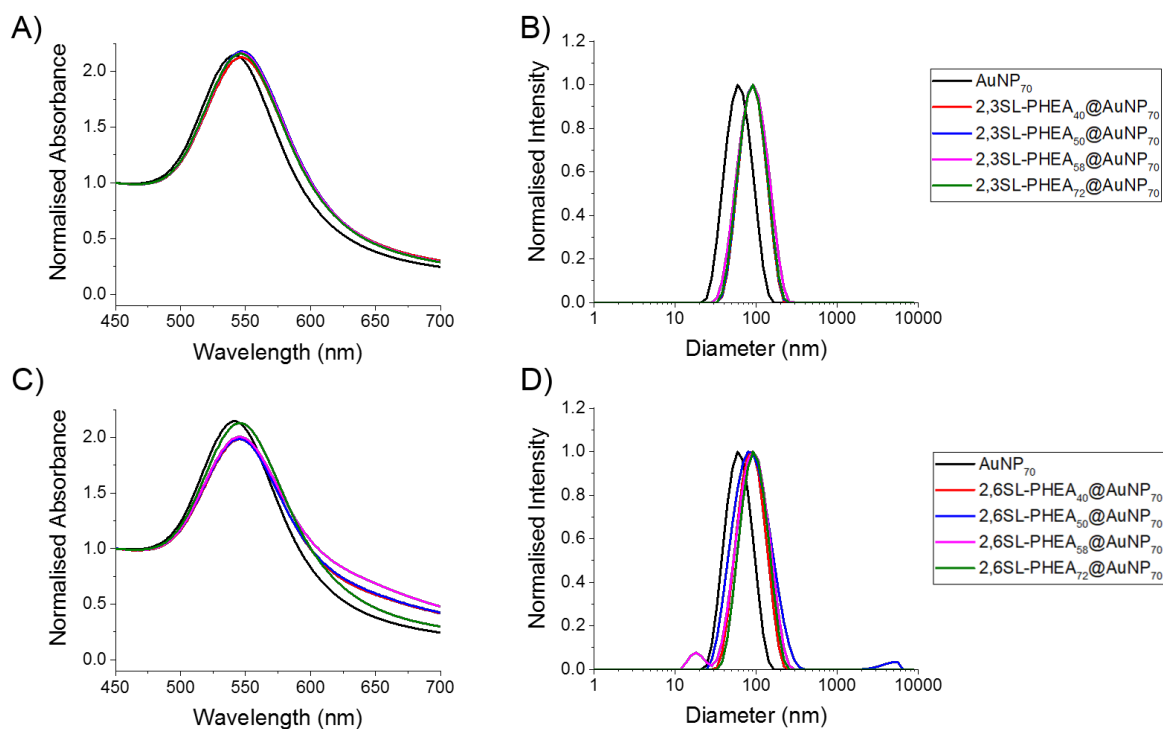


Figure S35. Characterisation of 70 nm AuNPs functionalised with α 2,3'-sialyllactose by A) UV/Vis and B) DLS and functionalised with α 2,6'-sialyllactose by C) UV/Vis and D) DLS.

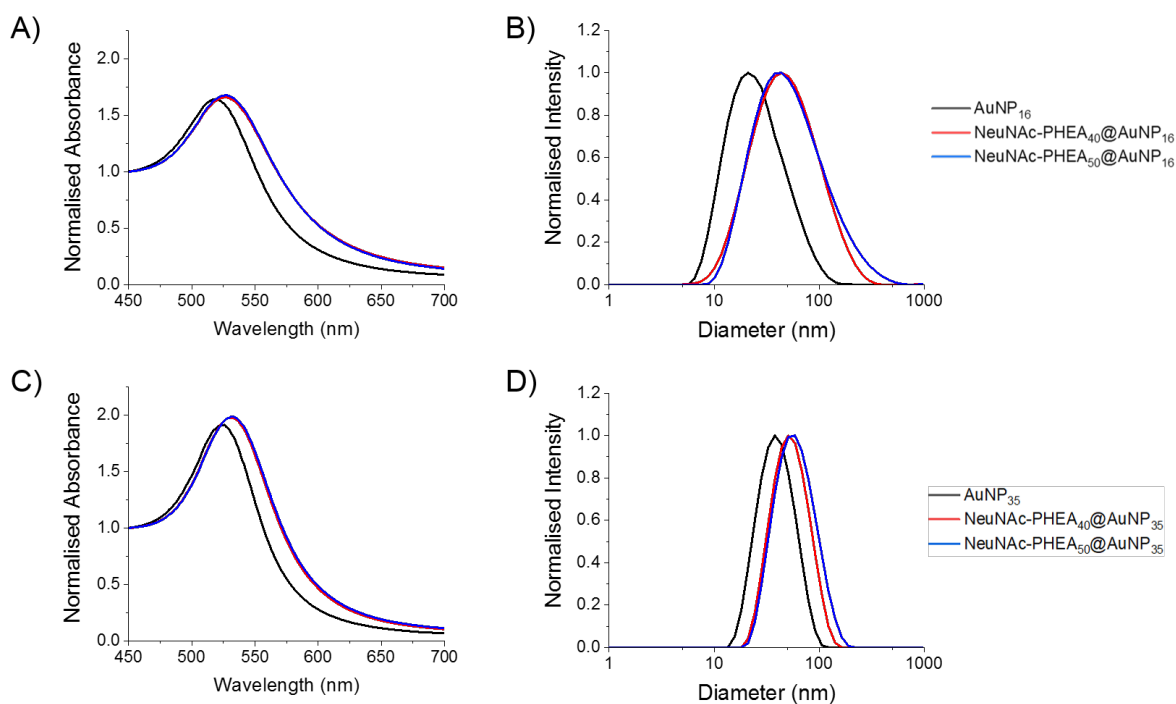


Figure S36. Characterisation of NeuNAc-functionalised 16 nm AuNPs by A) UV/Vis and B) DLS and 35 nm AuNPs by C) UV/Vis and D) DLS.

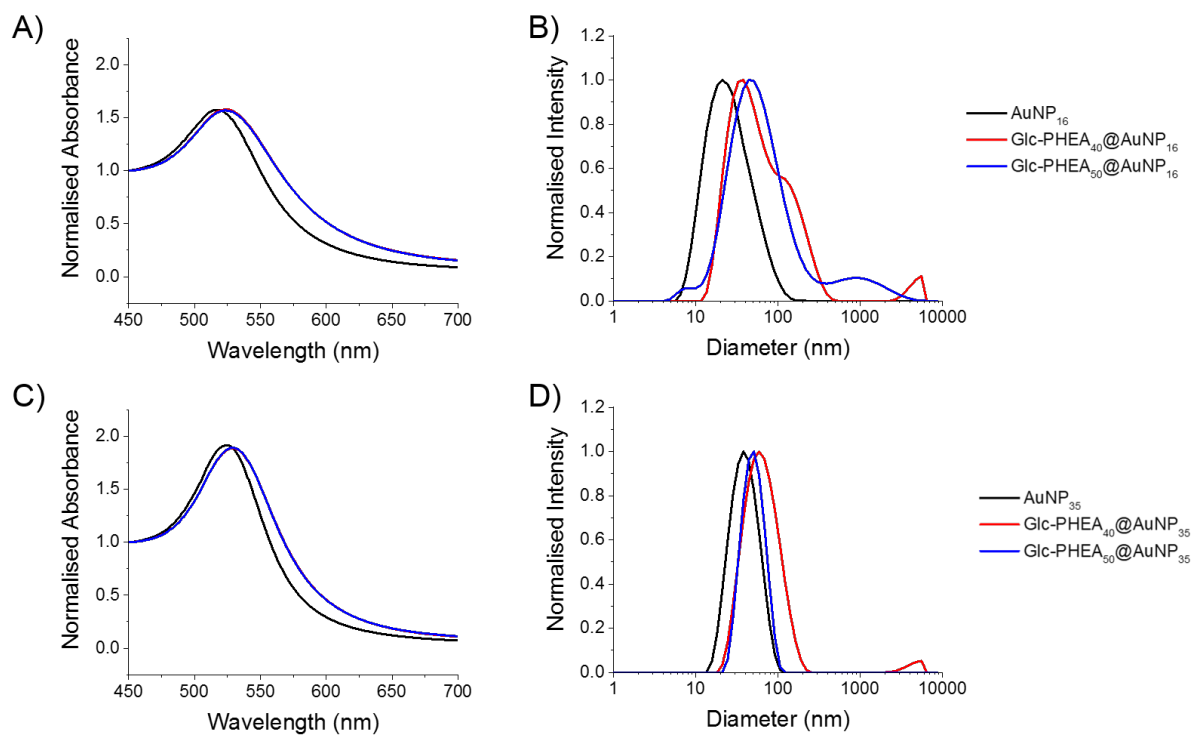


Figure S37. Characterisation of Glc-functionalised 16 nm AuNPs by A) UV/Vis and B) DLS and 35 nm AuNPs by C) UV/Vis and D) DLS.

BSA-Glycan Conjugate Test-Line Validation

To ensure the (commercial) glycosylated BSA's were suitable test lines for capture of the protein analytes BLI was undertaken. SBA or SARS-COV-2,S1 were immobilized (as described in experimental) and the BSA flowed over. The SBA was used as a control for the process.

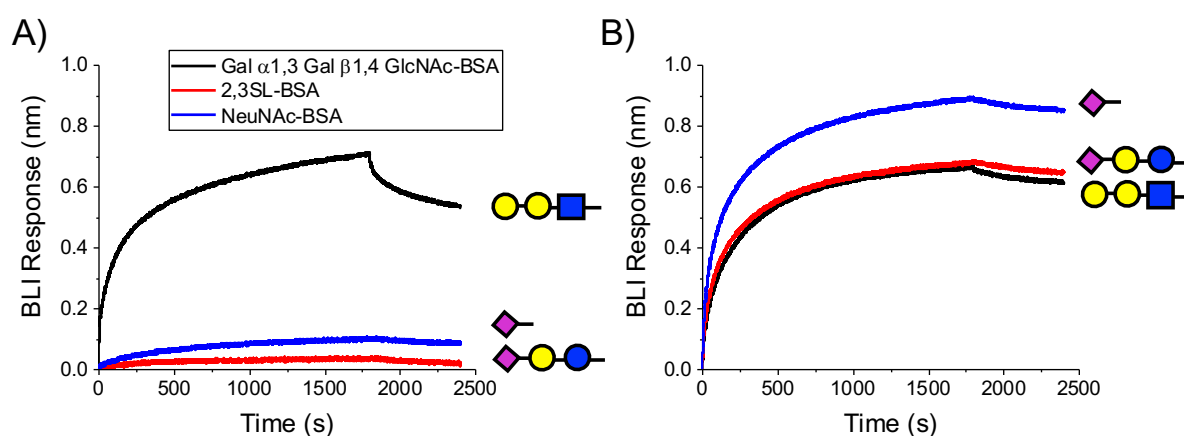


Figure S38. Bi-layer interferometry analysis of testline BSA derivatives (Gal α 1,3 Gal β 1,4 GlcNAc-BSA (Black), 2,3'sialyllactose-BSA (Red) and NeuNAc-BSA (blue)). In each case the BSA system is applied at 0.1 mg/mL against BLI sensors with the following immobilized A) SBA and B) SARS-CoV-2,S1.

Lateral Flow Strips and Plotted Data

None of the images in this supplementary information have been enhanced













AuNP system	Test line	Strips
NeuNAc-PHEA40AuNP16	1mg/ml 2,3SL-BSA	
	0.39mg/ml SARS-COV2 S1	
NeuNAc-PHEA50AuNP16	1mg/ml 2,3SL-BSA	
	0.39mg/ml SARS-COV2 S1	
NeuNAc-PHEA58AuNP16	1mg/ml 2,3SL-BSA	
	0.39mg/ml SARS-COV2 S1	
NeuNAc-PHEA40AuNP35	1mg/ml 2,3SL-BSA	
	0.39mg/ml SARS-COV2 S1	
NeuNAc-PHEA50AuNP35	1mg/ml 2,3SL-BSA	
	0.39mg/ml SARS-COV2 S1	
NeuNAc-PHEA58AuNP35	1mg/ml 2,3SL-BSA	
	0.39mg/ml SARS-COV2 S1	

Table S2. Scans of lateral flow strips using neuraminic acid (NeuNAc) functionalised PHEA polymers of varying lengths on 16 nm and 35nm AuNPs verses a test line of SARS-COV2,S1 protein or 2,3'-sialyllactosamine BSA (2,3SL-BSA) on lateral flow strips. Buffer containing 1% PVP was used.

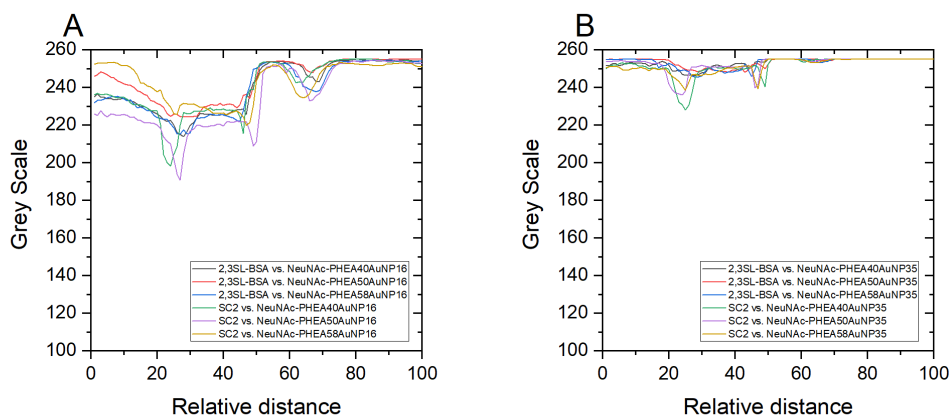


Figure S39. Analysis of scanned lateral flow strips. Neuraminic acid (NeuNAc) functionalised PHEA polymers of varying lengths on AuNPs of varying sizes versus a test line of SARS-COV-2,S1 protein (SC2, 0.39 mg/mL) or 2,3'-sialyllactosamine BSA (2,3SL-BSA, 1mg/mL). A) 16 nm AuNP and B) 35 nm AuNP. Buffer containing 1% PVP was used.

AuNP system	Test line	Strips
2,3SL-PHEA40AuNP16	1mg/ml 2,6SL-BSA	
	0.39mg/ml SARS-COV2 S1	
2,3SL-PHEA50AuNP16	1mg/ml 2,6SL-BSA	
	0.39mg/ml SARS-COV2 S1	
2,3SL-PHEA58AuNP16	1mg/ml 2,6SL-BSA	
	0.39mg/ml SARS-COV2 S1	
2,3SL-PHEA72AuNP16	1mg/ml 2,6SL-BSA	
	0.39mg/ml SARS-COV2 S1	
2,3SL-PHEA40AuNP35	1mg/ml 2,6SL-BSA	
	0.39mg/ml SARS-COV2 S1	
2,3SL-PHEA50AuNP35	1mg/ml 2,6SL-BSA	
	0.39mg/ml SARS-COV2 S1	
2,3SL-PHEA58AuNP35	1mg/ml 2,6SL-BSA	
	0.39mg/ml SARS-COV2 S1	
2,3SL-PHEA72AuNP35	1mg/ml 2,6SL-BSA	
	0.39mg/ml SARS-COV2 S1	

Table S3. Scans of lateral flow strips using 2,3'-sialyllactosamine (2,3SL) functionalised PHEA polymers of varying lengths on 16 nm and 35 nm AuNPs versus a test line of SARS-COV-2,S1 protein or 2,6'-sialyllactosamine BSA (2,6SL-BSA). Buffer containing 1% PVP was used. Black box indicates that condition was not ran due to particle instability in buffer.

AuNP system	Test line	Strips
2,3SL-PHEA40AuNP55	1mg/ml 2,6SL-BSA	
	0.39mg/ml SARS-COV2 S1	
2,3SL-PHEA50AuNP55	1mg/ml 2,6SL-BSA	
	0.39mg/ml SARS-COV2 S1	
2,3SL-PHEA58AuNP55	1mg/ml 2,6SL-BSA	
	0.39mg/ml SARS-COV2 S1	
2,3SL-PHEA72AuNP55	1mg/ml 2,6SL-BSA	
	0.39mg/ml SARS-COV2 S1	
2,3SL-PHEA40AuNP70	1mg/ml 2,6SL-BSA	
	0.39mg/ml SARS-COV2 S1	
2,3SL-PHEA50AuNP70	1mg/ml 2,6SL-BSA	
	0.39mg/ml SARS-COV2 S1	
2,3SL-PHEA58AuNP70	1mg/ml 2,6SL-BSA	
	0.39mg/ml SARS-COV2 S1	
2,3SL-PHEA72AuNP70	1mg/ml 2,6SL-BSA	
	0.39mg/ml SARS-COV2 S1	

Table S4. Scans of lateral flow strips using 2,3'-sialyllactosamine (2,3SL) functionalised PHEA polymers of varying lengths on 55 nm and 70 nm AuNPs versus a test line of SARS-COV-2,S1 protein or 2,6'-sialyllactosamine BSA (2,6SL-BSA) on lateral flow strips. Buffer containing 1% PVP was used. Black box indicates that condition was not ran due to particle instability in buffer.

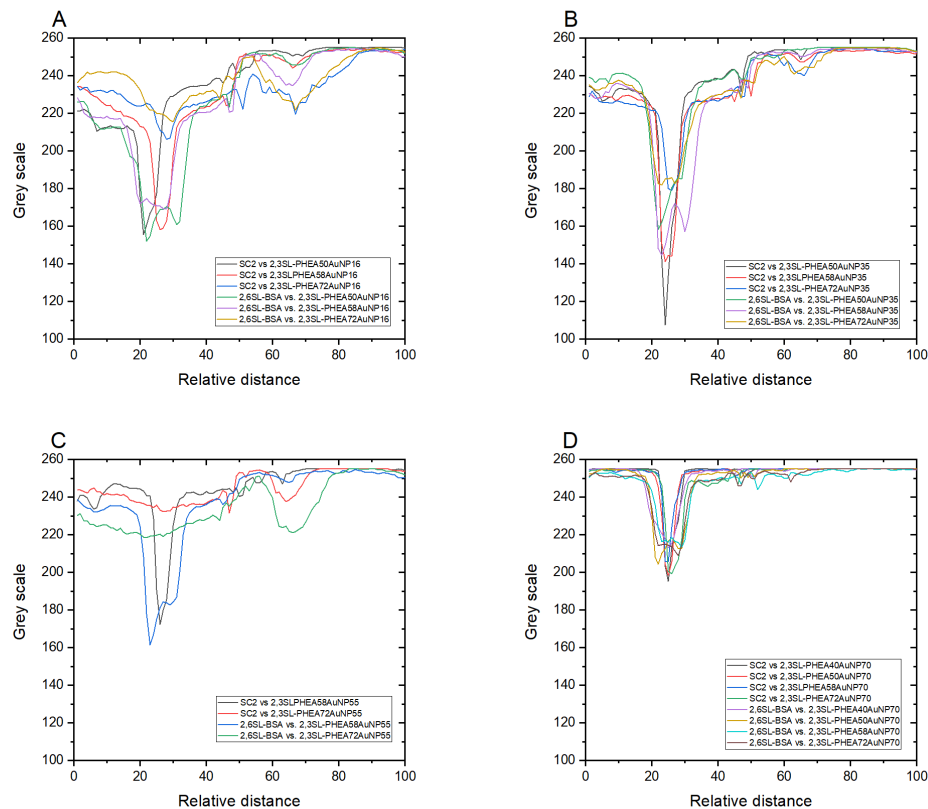


Figure S40. Analysis of scanned lateral flow strips. 2,3'-sialyllactosamine (2,3SL) functionalised PHEA polymers of varying lengths on AuNPs of varying sizes versus a test line of SARS-COV-2,S1 protein (SC2, 0.39 mg/mL) or 2,6'-sialyllactosamine BSA (2,6SL-BSA, 1mg/mL). A) 16 nm AuNP, B) 35 nm AuNP, C) 55 nm AuNP and D) 70 nm AuNP. Buffer containing 1% PVP was used.

AuNP system	Test line	Strips
2,6SL-PHEA40AuNP16	1mg/ml 2,6SL-BSA	
	0.39mg/ml SARS-COV2 S1	
2,6SL-PHEA50AuNP16	1mg/ml 2,6SL-BSA	
	0.39mg/ml SARS-COV2 S1	
2,6SL-PHEA58AuNP16	1mg/ml 2,6SL-BSA	
	0.39mg/ml SARS-COV2 S1	
2,6SL-PHEA72AuNP16	1mg/ml 2,6SL-BSA	
	0.39mg/ml SARS-COV2 S1	
2,6SL-PHEA40AuNP35	1mg/ml 2,6SL-BSA	
	0.39mg/ml SARS-COV2 S1	
2,6SL-PHEA50AuNP35	1mg/ml 2,6SL-BSA	
	0.39mg/ml SARS-COV2 S1	
2,6SL-PHEA58AuNP35	1mg/ml 2,6SL-BSA	
	0.39mg/ml SARS-COV2 S1	
2,6SL-PHEA72AuNP35	1mg/ml 2,6SL-BSA	
	0.39mg/ml SARS-COV2 S1	

Table S5. Scans of lateral flow strips using 2,6'-sialyllactosamine (2,6SL) functionalised PHEA polymers of varying lengths on 16 nm and 35 nm AuNPs versus a test line of SARS-COV-2,S1 protein or 2,6'-sialyllactosamine BSA (2,6SL-BSA) on lateral flow strips. Buffer containing 1% PVP was used. Black box indicates that condition was not ran due to particle instability in buffer.

AuNP system	Test line	Strips
2,6SL-PHEA40AuNP55	1mg/ml 2,6SL-BSA	
	0.39mg/ml SARS-COV2 S1	
2,6SL-PHEA50AuNP55	1mg/ml 2,6SL-BSA	
	0.39mg/ml SARS-COV2 S1	
2,6SL-PHEA58AuNP55	1mg/ml 2,6SL-BSA	
	0.39mg/ml SARS-COV2 S1	
2,6SL-PHEA72AuNP55	1mg/ml 2,6SL-BSA	
	0.39mg/ml SARS-COV2 S1	
2,6SL-PHEA40AuNP70	1mg/ml 2,6SL-BSA	
	0.39mg/ml SARS-COV2 S1	
2,6SL-PHEA50AuNP70	1mg/ml 2,6SL-BSA	
	0.39mg/ml SARS-COV2 S1	
2,6SL-PHEA58AuNP70	1mg/ml 2,6SL-BSA	
	0.39mg/ml SARS-COV2 S1	
2,6SL-PHEA72AuNP70	1mg/ml 2,6SL-BSA	
	0.39mg/ml SARS-COV2 S1	

Table S6. Scans of lateral flow strips using 2,6'-sialyllactosamine (2,3SL) functionalised PHEA polymers of varying lengths on 55 nm and 70 nm AuNPs verses a test line of SARS-COV-2,S1 protein or 2,6'-sialyllactosamine BSA (2,6SL-BSA) on lateral flow strips. Buffer containing 1% PVP was used. Black box indicates that condition was not ran due to particle instability in buffer.

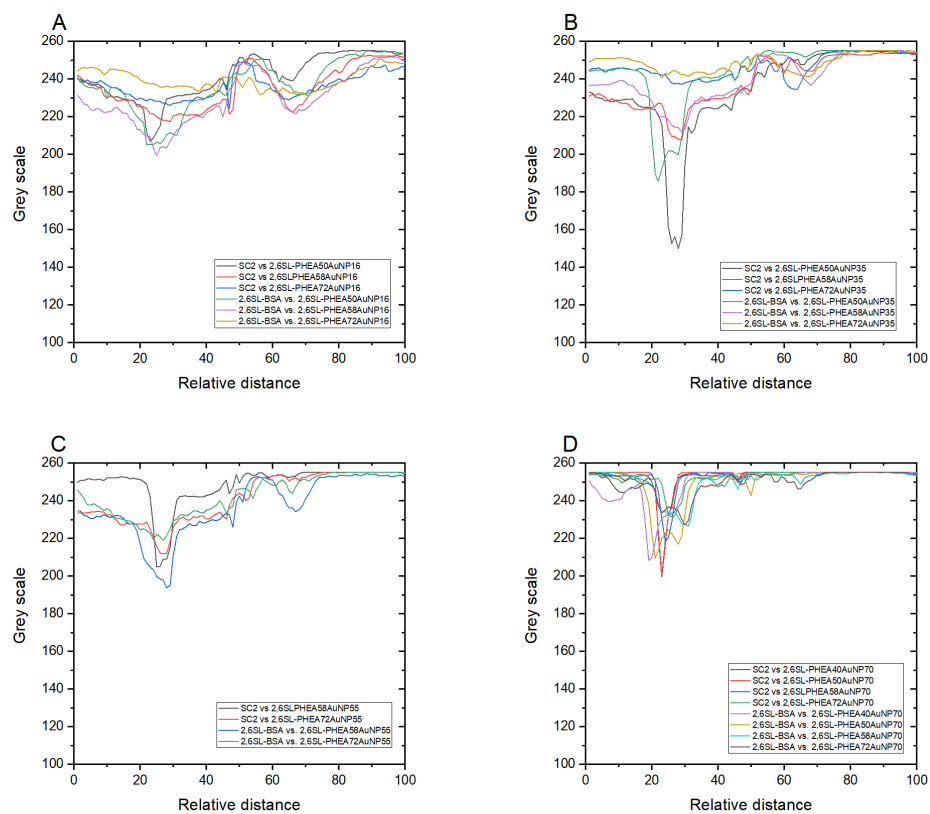


Figure S41. Analysis of scanned lateral flow strips. 2,6'-Sialyllactosamine (2,6SL) functionalised PHEA polymers of varying lengths on AuNPs of varying sizes versus a test line of SARS-COV-2,S1 protein (SC2, 0.39 mg/mL) or 2,6'-sialyllactosamine BSA (2,6SL-BSA, 1 mg/mL). A) 16 nm AuNP, B) 35 nm AuNP, C) 55 nm AuNP and D) 70 nm AuNP. Buffer containing 1% PVP was used.







Test line	AuNP system	
	NeuNAc-PHEA40AuNP35	NeuNAc-PHEA50AuNP35
1mg/ml NeuNAc-BSA		
0.39mg/ml SARS-COV2 S1		
0.4mg/ml SARS-COV1 Spike Protein		

Table S7. Scans of lateral flow strips using neuraminic acid (NeuNAc) functionalised PHEA polymers of varying lengths on 35 nm AuNPs versus a test line of SARS-COV-2,S1 protein or neuraminic acid-BSA (NeuNAc-BSA) on lateral flow strips. Buffer containing 1% PVP was used.

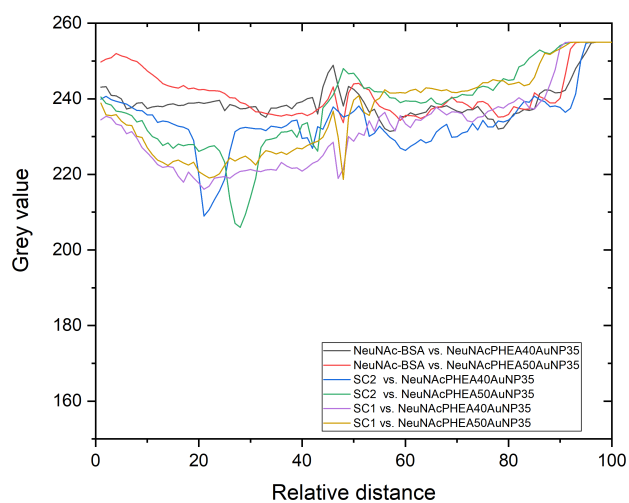


Figure S42. Analysis of scanned lateral flow strips. Neuraminic acid (NeuNAc) functionalised PHEA polymers of varying lengths on 35nm AuNPs with BSA versus a test line of SARS-COV-2,S1 protein (SC2, 0.39 mg/mL), SARS-COV-1 spike protein (SC1, 0.4 mg/mL) or neuraminic acid-BSA (NeuNAc-BSA, 1 mg/mL). Buffer containing 1% PVP was used.








Test line	AuNP system	
	NeuNAc-PHEA50AuNP35	
1mg/ml NeuNAc-BSA		
1mg/ml SBA		
1mg/ml SNA		
1mg/ml UEA		
1mg/ml RCA120		
1mg/ml WGA		
No test line		

Table S8. Scans of lateral flow strips using neuraminic acid (NeuNAc) functionalised PHEA50 on 35 nm AuNPs verses tests line of various lectins or neuraminic acid-BSA (NeuNAc-BSA) or no test line on lateral flow strips. Buffer containing 2% PVP was used.

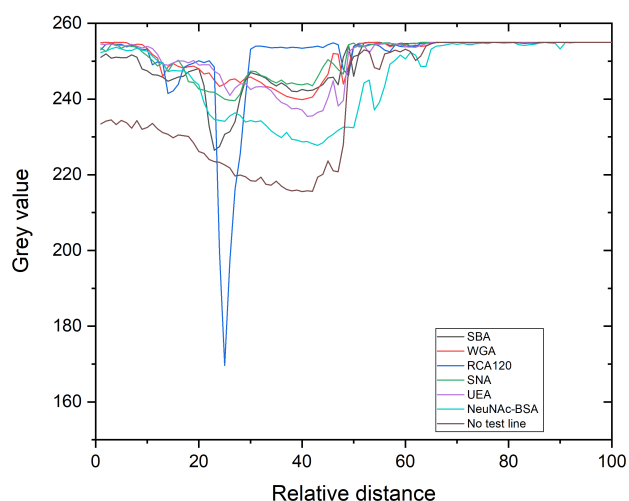


Figure S43. Analysis of scanned lateral flow strips. Neuraminic acid (NeuNAc) functionalised PHEA50 on 35 nm AuNPs verses tests line of various lectins or neuraminic acid-BSA (NeuNAc-BSA) or no test line on lateral flow strips. Buffer containing 2% PVP was used.

























Test line	AuNP system	
	NeuNAc-PHEA50AuNP35	Gal-PHEA72AuNP16
0.5mg/ml SC2 S1		
0.25mg/ml SC2 S1		
0.125mg/ml SC2 S1		
0.0625mg/ml SC2 S1		
0.03125mg/ml SC2 S1		
0.0156mg/ml SC2 S1		
0.0078mg/ml SC2 S1		
0.0039mg/ml SC2 S1		
0.00195mg/ml SC2 S1		
0.00098mg/ml SC2 S1		
0.00049mg/ml SC2 S1		
0.00024mg/ml SC2 S2		

Table S9. Scans of lateral flow strips using (NeuNAc) functionalised PHEA50 on 35 nm AuNPs and galactosamine (Gal) functionalised PHEA72 on 16nm AuNPs verses SARS COV-2,S1 protein (SC2 S1) at varying concentrations. Buffer containing 2% PVP was used.

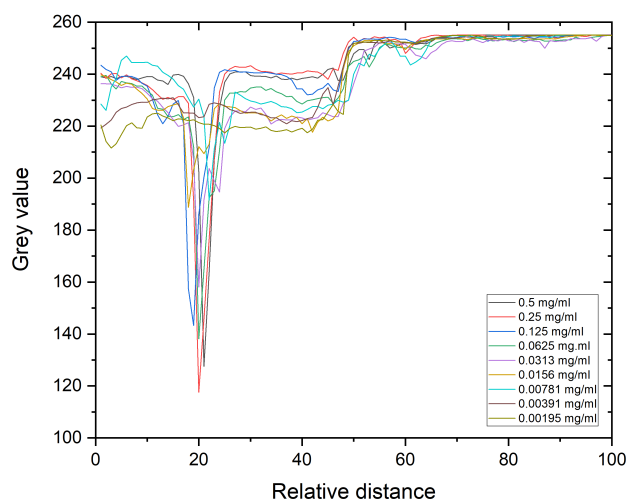


Figure S44. Analysis of scanned lateral flow strips. Neuraminic acid (NeuNAc) functionalised PHEA50 on 35 nm AuNPs versus a test line of SARS COV-2,S1 (SC2 S1) protein at varying concentrations on lateral flow strips. Buffer containing 2% PVP was used.

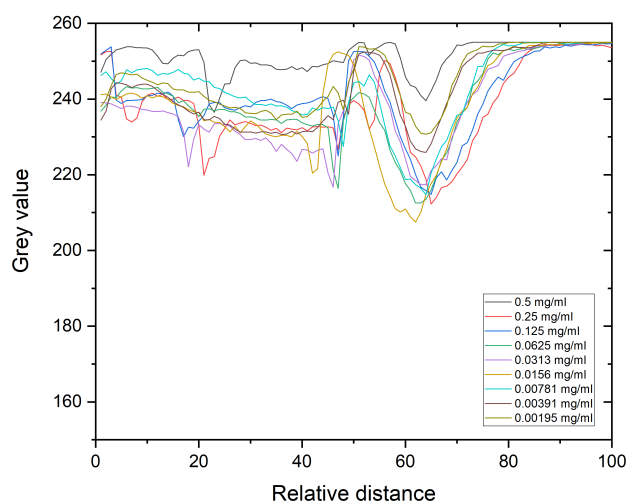


Figure S45. Analysis of scanned lateral flow strips. Galactosamine (Gal) functionalised PHEA72 on 16nm AuNPs versus a test line of SARS COV-2,S1 (SC2 S1) protein at varying concentrations on lateral flow strips. Buffer containing 2% wt/v PVP was used.

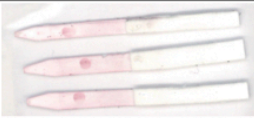





Test line	AuNP system	
	NeuNAc-PHEA50AuNP35	Gal-PHEA72AuNP16
1mg/ml SBA		
0.5mg/ml SBA		
0.25mg/ml SBA		

Table S10. – Scans of lateral flow strips using neuraminic acid (NeuNAc) functionalised PHEA50 on 35 nm AuNPs and galactosamine (Gal) functionalised PHEA72 on 16nm AuNPs verses soybean agglutinin (SBA) at varying concentrations. Buffer containing 2% wt/v PVP was used.

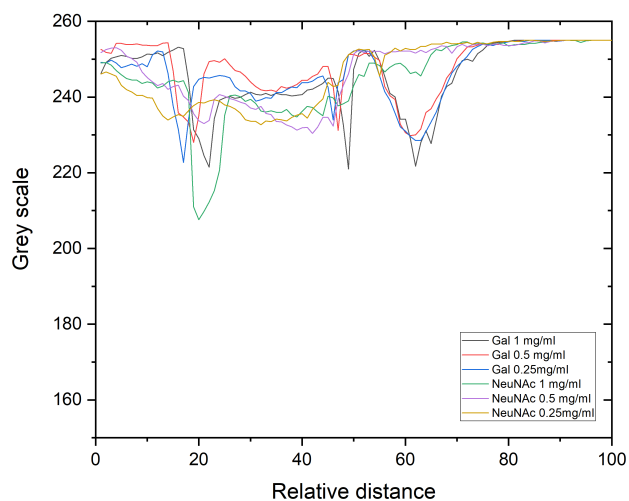


Figure S46. Analysis of scanned lateral flow strips. Neuraminic acid (NeuNAc) functionalised PHEA50 on 35 nm AuNPs and galactosamine (Gal) functionalised PHEA72 on 16nm AuNPs verses a test line of soybean agglutinin at varying concentrations on lateral flow strips. Buffer containing 2% wt/v PVP was used.








	AuNP system	Strips
High concentration SC2 S1 on polystyrene	NeuNAc-PHEA50AuNP35	
	Gal-2-PHEA72AuNP16	
Low concentration SC2 S1 on polystyrene	NeuNAc-PHEA50AuNP35	
	Gal-2-PHEA72AuNP16	
High concentration naked polystyrene	NeuNAc-PHEA50AuNP35	
Low concentration naked polystyrene	NeuNAc-PHEA50AuNP35	
No polystyrene	NeuNAc-PHEA50AuNP35	

Table S11. Analysis of scanned lateral flow strips. Scans of lateral flow strips using polystyrene viral mimics. A test line of 1 mg/mL NeuNAc-BSA and a control line of 1 mg/mL RCA₁₂₀ were used in all tests. Buffer containing 2% wt/v PVP was used.

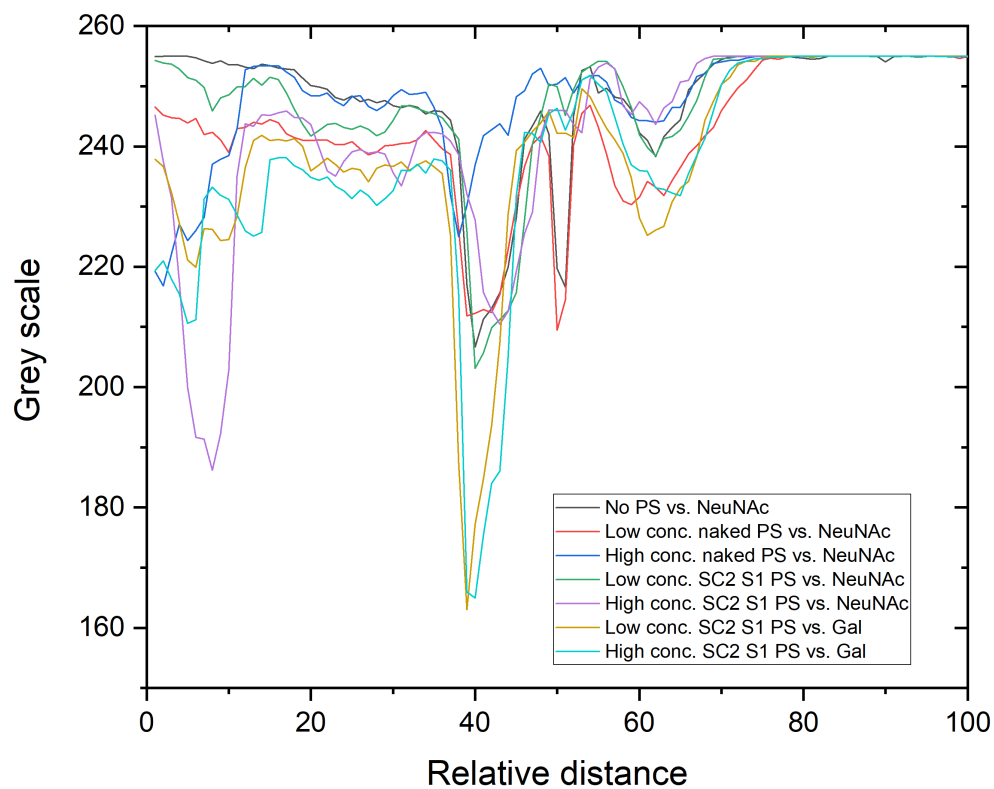


Figure S47. Analysis of scanned lateral flow strips. Polystyrene (PS) viral mimic strip data. Tests were done using NeuNAc PHEA50AuNP35 (NeuNAc) or Gal-2-PHEA72AuNP16 (Gal) particles. A test line of 1 mg/mL NeuNAc-BSA and a control line of 1 mg/mL RCA₁₂₀ were used in all tests. Buffer containing 2% wt/v PVP was used.

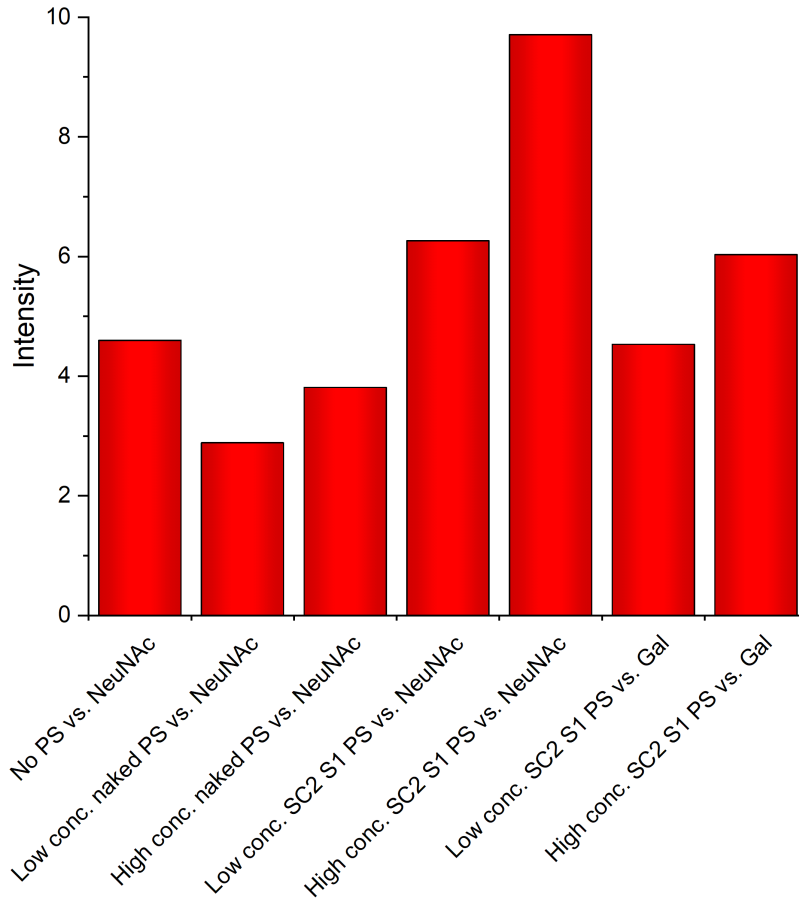


Figure S48. Analysis of scanned lateral flow strips using Polystyrene (PS) viral mimic. Tests were done using NeuNAc PHEA50AuNP35 (NeuNAc) or Gal-2-PHEA72AuNP16 (Gal) particles. A test line of 1 mg/mL NeuNAc-BSA and a control line of 1 mg/mL RCA₁₂₀ were used in all tests. Buffer containing 2% wt/v PVP was used.

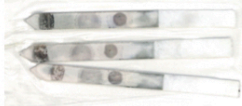

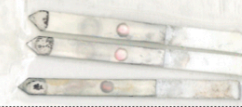
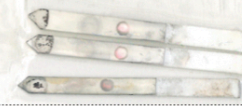

	AuNP system	Strips
High concentration SC2 S1 on polystyrene	NeuNAc-PHEA50AuNP35	
Low concentration SC2 S1 on polystyrene	NeuNAc-PHEA50AuNP35	
High concentration naked polystyrene	NeuNAc-PHEA50AuNP35	
Low concentration naked polystyrene	NeuNAc-PHEA50AuNP35	
No polystyrene	NeuNAc-PHEA50AuNP35	

Table S12. Analysis of scanned silver stained lateral flow strips. Scans of lateral flow strips using polystyrene viral mimics. A test line of 1 mg/mL NeuNAc-BSA and a control line of 1 mg/mL RCA₁₂₀ were used in all tests. Buffer containing 2% wt/v PVP was used.

The Gal-2-PHEA₇₂AuNP₁₆ could not be used as a fair silver staining comparison as they are 16 nm AuNPs not 35 nm AuNPs and hence nucleate differently and give very different signal intensities.

Lateral Flow Strips – Blocking Experiments

Blocking agent	Test line	AuNP System			
		NeuNAc-PHEA40AuNP16	NeuNAc-PHEA50AuNP16	NeuNAc-PHEA40AuNP35	NeuNAc-PHEA50AuNP35
BSA	1mg/ml 2,3SL-BSA				
	0.39mg/ml SARS-COV2 S1				

Table S13. Scans of lateral flow strips using neuraminic acid (NeuNAc) functionalised PHEA polymers of varying lengths on 16 nm or 35 nm AuNPs blocked with BSA verses a test line of SARS-COV2,S1 protein or 2,3'-sialyllactosamine BSA (2,3SL-BSA) on lateral flow strips. Buffer containing 1% wt/v PVP was used.

Test line	AuNP system		
	2,3SL-PHEA50AuNP16	2,3SL-PHEA58AuNP16	2,3SL-PHEA72AuNP16
1mg/ml 2,3SL-BSA			
0.39mg/ml SARS-COV2 S1			

Table S14. Scans of lateral flow strips using 2,3'-sialyllactosamine (2,3SL) functionalised PHEA polymers of varying lengths on 16 nm AuNPs blocked with BSA verses a test line of SARS-COV2,S1 protein or 2,3'-sialyllactosamine BSA (2,3SL-BSA) on lateral flow strips. Buffer containing 1% wt/v PVP was used.

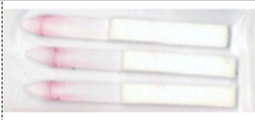





Test line	AuNP system		
	2,3SL-PHEA40AuNP35	2,3SL-PHEA50AuNP35	2,3SL-PHEA58AuNP35
1mg/ml 2,3SL-BSA			
0.39mg/ml SARS-COV2 S1			

Table S15. Scans of lateral flow strips using 2,3'-sialyllactosamine (2,3SL) functionalised PHEA polymers of varying lengths on 16 nm AuNPs blocked with BSA versus a test line of SARS-COV2,S1 protein or 2,3'-sialyllactosamine BSA (2,3SL-BSA) on lateral flow strips. Buffer containing 1% wt/v PVP was used.

BSA-blocking was carried out as this can improve the signal-to-noise in nanoparticle systems. While the BSA-blocking seemingly improved the signal-to-noise of the 2,3'-sialyllactosamine systems it did not improve the NeuNAc systems that already showed negligible non-specific binding to the off-target test line and the nitrocellulose surface. Therefore, it was unnecessary to BSA-block the optimised NeuNAc systems.

It is notable that BSA-blocking could be observed by XPS analysis. The amide to alkane ratio of the BSA-blocked particles was greater than the non-blocked particles showing the presence of protein. The N 1s to Au 4f was also far higher in the BSA-blocked systems than the non-BSA-blocked systems.

Lateral Flow Cassettes and Strips, and Plotted Data

Complete cassettes were made as described, to determine whether the NeuNAc-PHEA₅₀AuNP₃₅ particle system could be used in a cassette format.

Tests using SARS-COV-2,S1 as a test line gave good (near complete) resuspension of the AuNPs from the conjugate pad and bound the test line. The tests were run in a shorter time than the dipstick setup, taking 5-10 minutes to give a response. Similar limits of detection without further formulation steps were also seen, towards the SARS-COV-2,S1 test line. A series of tests were carried out to find the optimum OD of the AuNPs on the conjugate pad.

Attempts to use the virus polystyrene mimic were however unsuccessful as the high viscosity of the polystyrene solutions prevented good absorption of the polystyrene solution into the sample pad and good resuspension of the AuNPs from the conjugate pad.



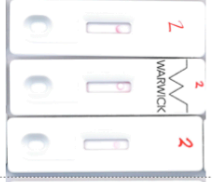


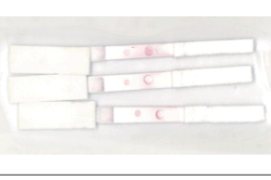
Test line	AuNP system	
	NeuNAc-PHEA ₅₀ AuNP ₃₅ Cassettes	NeuNAc-PHEA ₅₀ AuNP ₃₅ Strips
1mg/ml NeuNAc-BSA		
1mg/ml 2,3SL-BSA		
0.5mg/ml SC2 S1		

Table S16. Scans of lateral flow cassettes and strips from the cassettes using neuraminic acid (NeuNAc) functionalised PHEA₅₀ on 35 nm AuNPs versus a test line of SARS-COV₂,S1 protein (SC2 S1), neuraminic acid-BSA (NeuNAc-BSA) or 2,3'-sialyllactosamine-BSA (2,3SL-BSA) in cassettes and on complete lateral flow strips. A control line of 1 mg/mL RCA₁₂₀ was used in all tests. Buffer containing 2% wt/v PVP was used.

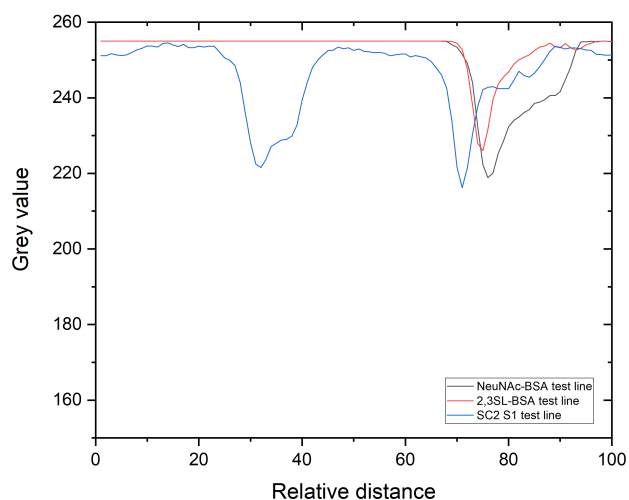


Figure S49. Analysis of scanned lateral flow cassettes. Neuraminic acid (NeuNAc) functionalised PHEA50 on 35 nm AuNPs versus test lines of Neuraminic acid-BSA (NeuNAc-BSA, 1 mg/mL), 2,3'-sialyllactosamine-BSA (2,3SL-BSA, 1 mg/mL) and SARS-COV-2,S1 (SC2 S1, 0.5 mg/mL) on lateral flow cassettes. A control line of 1 mg/mL RCA₁₂₀ was used in all tests. Buffer containing 2% wt/v PVP was used. Data taken from the strips before removal from the cassettes.

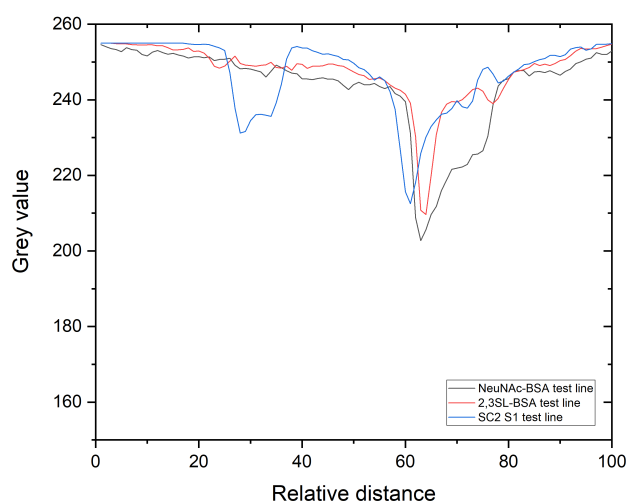


Figure S50. Analysis of scanned lateral flow strips from cassettes. Neuraminic acid (NeuNAc) functionalised PHEA50 on 35 nm AuNPs versus a test lines of Neuraminic acid-BSA (NeuNAc-BSA, 1 mg/mL), 2,3'-sialyllactosamine-BSA (2,3SL-BSA, 1 mg/mL) and SARS COV-2,S1 (SC2 S1, 0.5 mg/mL) on lateral flow cassettes. A control line of 1 mg/mL RCA₁₂₀ was used in all tests. Buffer containing 2% wt/v PVP was used. Data taken from the strips after removal from the cassettes.


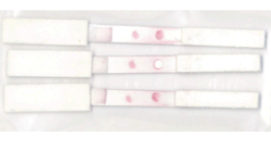

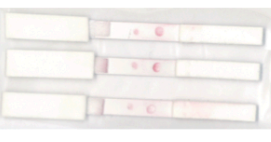



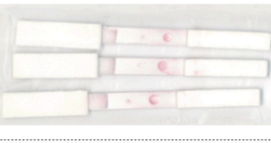

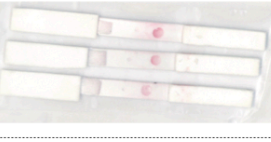
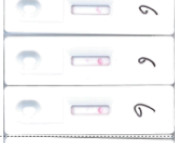

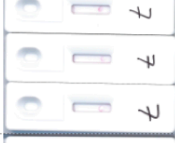

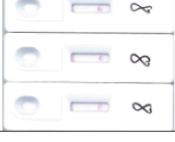

Test line	AuNP system	
	NeuNAc-PHEA ₅₀ AuNP35 Cassettes	NeuNAc-PHEA ₅₀ AuNP35 Strips
0.5mg/ml SC2 S1		
0.25mg/ml SC2 S1		
0.125mg/ml SC2 S1		
0.0625mg/ml SC2 S1		
0.03125mg/ml SC2 S1		
0.0156mg/ml SC2 S1		
0.0078mg/ml SC2 S1		
0.0039mg/ml SC2 S1		

Table S17. Scans of lateral flow cassettes and strips from the cassettes using neuraminic acid (NeuNAc) functionalised PHEA₅₀ on 35 nm AuNPs versus a test line of SARS-COV-2,S1 protein (SC2 S1) at varying concentrations, in cassettes and on complete lateral flow strips. A control line of 1 mg/mL RCA₁₂₀ was used in all tests. The sample pads were removed after the tests were run. Buffer containing 2% wt/v PVP was used.

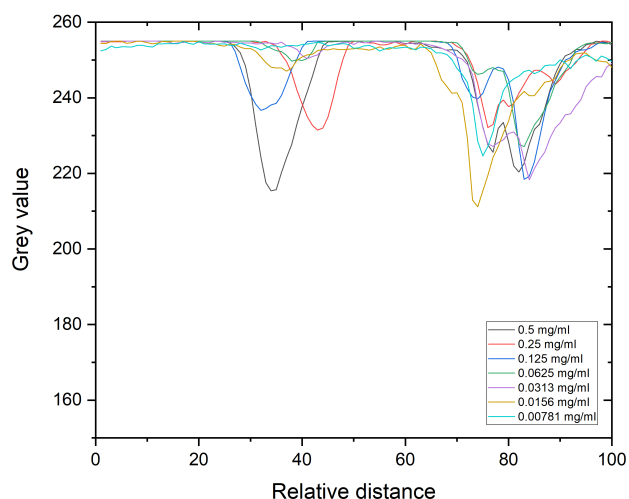


Figure S51. Analysis of scanned lateral flow from cassettes. Neuraminic acid (NeuNAc) functionalised PHEA₅₀ on 35 nm AuNPs versus a test line of SARS-COV-2,S1 (SC2 S1) at varying concentrations on lateral flow cassettes. A control line of 1 mg/mL RCA₁₂₀ was used in all tests. Buffer containing 2% wt/v PVP was used. Data taken from the strips before removal from the cassettes.

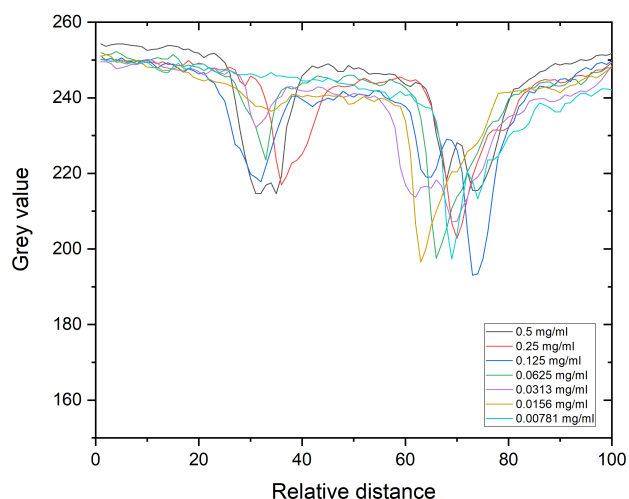


Figure S52. Analysis of scanned lateral flow strips from cassettes. Neuraminic acid (NeuNAc) functionalised PHEA₅₀ on 35 nm AuNPs versus a test line of SARS-COV-2,S1 (SC2 S1) at varying concentrations on lateral flow cassettes. A control line of 1 mg/mL RCA₁₂₀ was used in all tests. Buffer containing 2% wt/v PVP was used. Data taken from the strips after removal from the cassettes after ~1 hour.

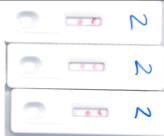
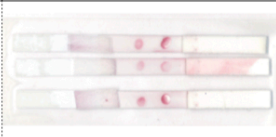
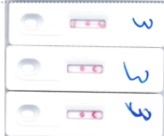


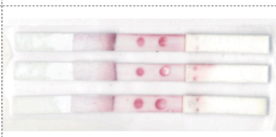

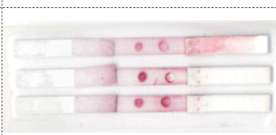
AuNP OD on Conjugate Pad	AuNP system	
	NeuNAc-PHEA ₅₀ AuNP ₃₅ Cassettes	NeuNAc-PHEA ₅₀ AuNP ₃₅ Strips
2		
3		
4		
5		

Table S18. Scans of lateral flow cassettes and strips from the cassettes using neuraminic acid (NeuNAc) functionalised PHEA₅₀ on 35 nm AuNPs at varying ODs versus a test line of 0.5 mg/mL SARS-COV-2,S1 protein (SC2 S1), in cassettes and on complete lateral flow strips. A control line of 1 mg/mL RCA₁₂₀ was used in all tests. The conjugate pads in these tests were not cured overnight. The sample pads were removed after the tests were run. Buffer containing 2% wt/v PVP was used.

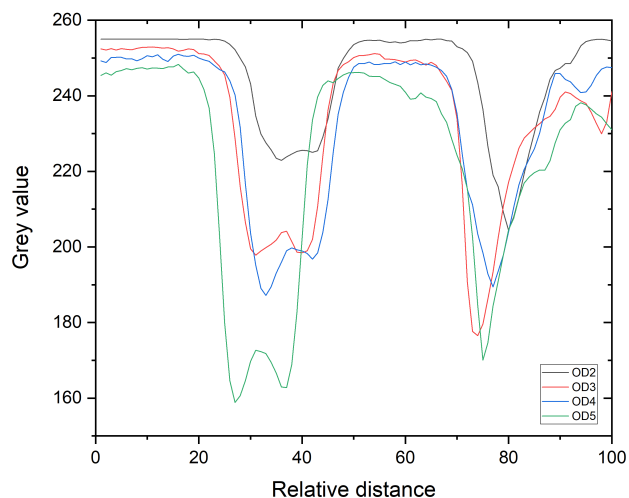


Figure S53. Analysis of scanned lateral flow cassettes. Neuraminic acid (NeuNAc) functionalised PHEA₅₀ on 35 nm AuNPs of varying ODs versus a test line of SARS-COV-2,S1 (SC2 S1, 0.5 mg/mL). A control line of 1 mg/mL RCA₁₂₀ was used in all tests. Buffer containing 2% wt/v PVP was used. Data taken from the strips before removal from the cassettes. Conjugate pads were not cured overnight.

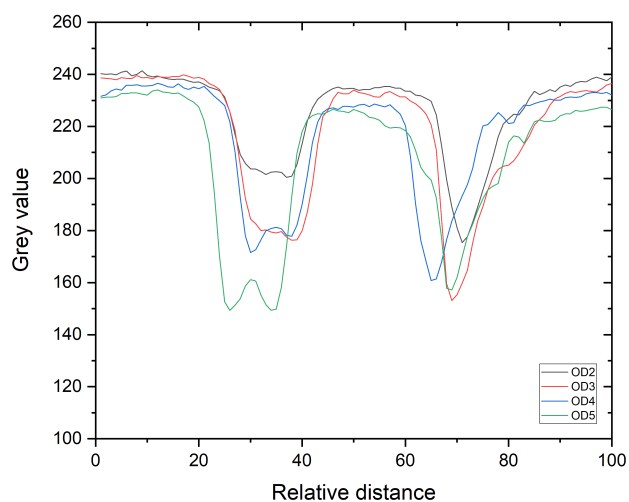


Figure S54. Analysis of scanned lateral flow strips from cassettes. Neuraminic acid (NeuNAc) functionalised PHEA₅₀ on 35 nm AuNPs of varying ODs versus a test line of SARS-COV-2,S1 (SC2 S1, 0.5 mg/mL). A control line of 1 mg/mL RCA₁₂₀ was used in all tests. Buffer containing 2% wt/v PVP was used. Data taken from the strips after removal from the cassettes after ~1 hour. Conjugate pads were not cured overnight.


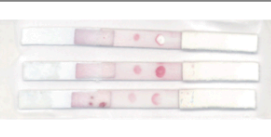

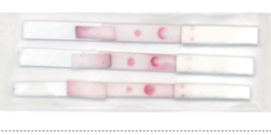




AuNP OD on Conjugate Pad	AuNP system	
	NeuNAc-PHEA ₅₀ AuNP ₃₅ Cassettes	NeuNAc-PHEA ₅₀ AuNP ₃₅ Strips
2		
3		
4		
5		

Table S19. Scans of lateral flow cassettes and strips from the cassettes using of neuraminic acid (NeuNAc) functionalised PHEA₅₀ on 35 nm AuNPs at varying ODs versus a test line of 0.5 mg/mL SARS-COV-2,S1 protein (SC2 S1), in cassettes and on complete lateral flow strips. A control line of 1 mg/mL RCA₁₂₀ was used in all tests. The conjugate pads in these tests were cured overnight. Buffer containing 2% wt/v PVP was used.

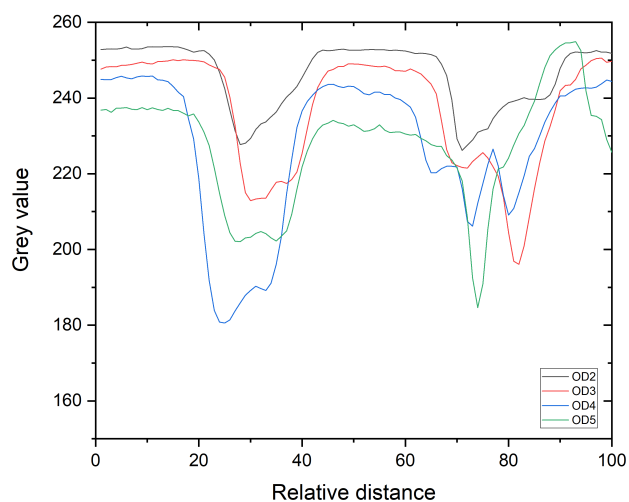


Figure S55. Analysis of scanned lateral flow cassettes. Neuraminic acid (NeuNAc) functionalised PHEA₅₀ on 35 nm AuNPs of varying ODs versus a test line of SARS-COV-2,S1 (SC2 S1, 0.5 mg/mL) on lateral flow cassettes. A control line of 1 mg/mL RCA₁₂₀ was used in all tests. Buffer containing 2% PVP was used. Data taken from the strips before removal from the cassettes. Conjugate pads were cured overnight.

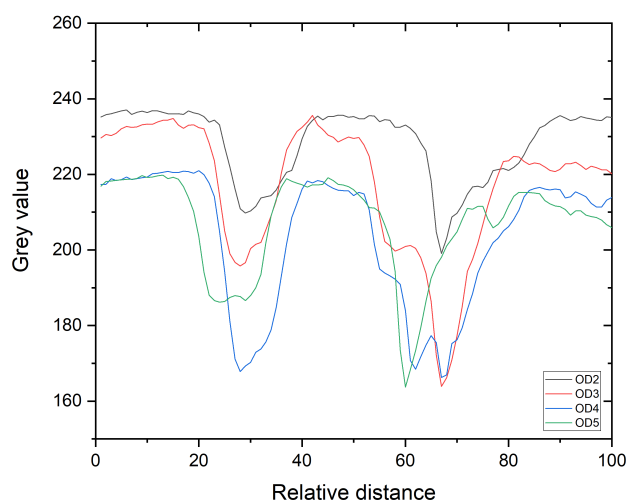


Figure S56. Analysis of scanned lateral flow strips from cassettes. Neuraminic acid (NeuNAc) functionalised PHEA₅₀ on 35 nm AuNPs of varying ODs versus a test line of SARS-COV-2,S1 (SC2 S1, 0.5 mg/mL) on lateral flow cassettes. A control line of 1 mg/mL RCA₁₂₀ was used in all tests. Buffer containing 2% PVP was used. Data taken from the strips after removal from the cassettes after ~1 hour. Conjugate pads were cured overnight.

Test line	AuNP system	
	NeuNAc-PHEA50AuNP35 Cassettes	NeuNAc-PHEA50AuNP35 Strips
0.25mg/ml SC2 S1		
0.125mg/ml SC2 S1		
0.0625mg/ml SC2 S1		
0.03125mg/ml SC2 S1		
0.0156mg/ml SC2 S1		
0.0078mg/ml SC2 S1		

Table S20. Scans of lateral flow cassettes and strips from the cassettes using neuraminic acid (NeuNAc) functionalised PHEA₅₀ on 35 nm AuNPs at OD3 versus a test line of SARS-COV-2,S1 protein (SC2 S1) at varying concentrations, in cassettes and on complete lateral flow strips. A control line of 1 mg/mL RCA₁₂₀ was used in all tests. The conjugate pads in these tests were cured overnight. Buffer containing 2 % wt/v PVP was used.

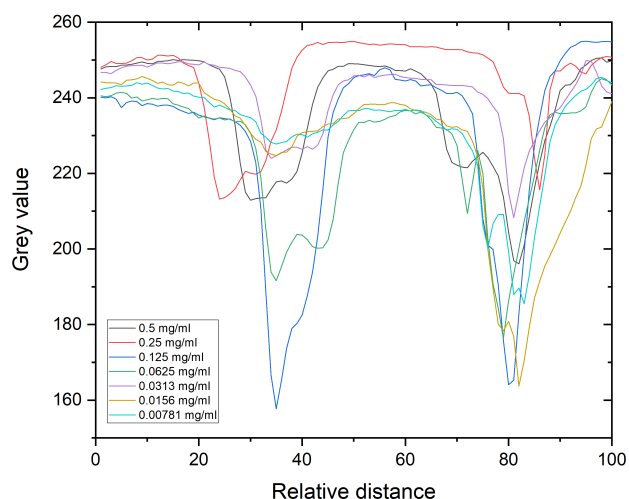


Figure S57. Analysis of scanned lateral flow cassettes. Neuraminic acid (NeuNAc) functionalised PHEA₅₀ on 35 nm AuNPs at OD3 versus a test line of SARS-COV-2,S1 (SC2 S1) at varying concentrations on lateral flow cassettes. A control line of 1 mg/mL RCA₁₂₀ was used in all tests. Buffer containing 2% PVP was used. Data taken from the strips before removal from the cassettes. Conjugate pads were cured overnight. Data for 0.5 mg/mL taken from Table S19.

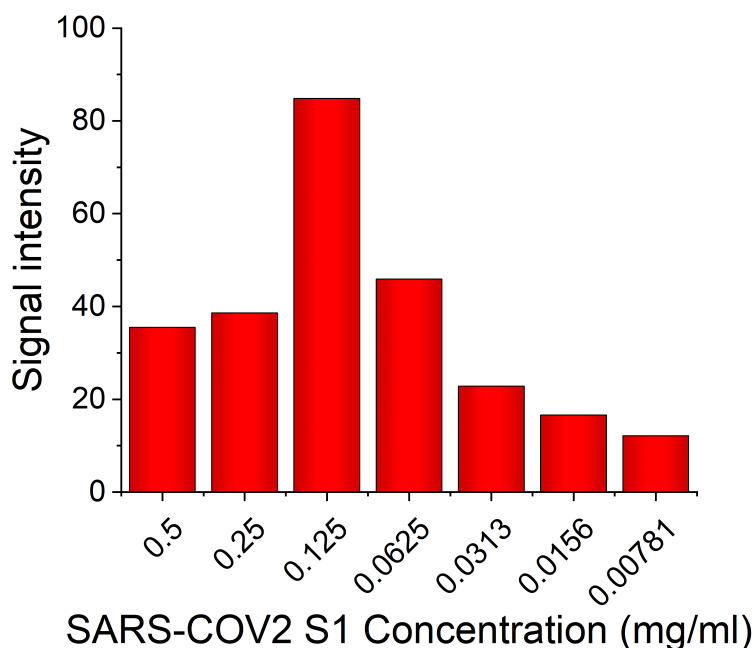


Figure S58. Analysis of scanned lateral flow cassettes. Signal intensity plot of Neuraminic acid (NeuNAc) functionalised PHEA₅₀ on 35 nm AuNPs at OD3 versus a test line of SARS-COV-2,S1 (SC2 S1) at varying concentrations on lateral flow cassettes. A control line of 1 mg/mL RCA₁₂₀ was used in all tests. Buffer containing 2% PVP was used. Data taken from the strips before removal from the cassettes. Conjugate pads were cured overnight. Data for 0.5 mg/mL taken from Table S19.

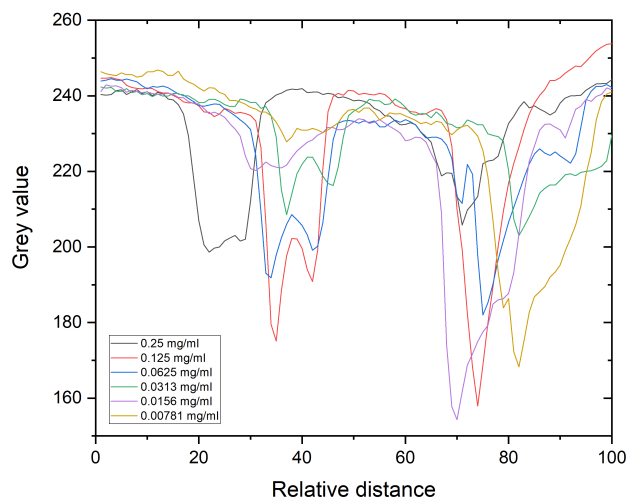


Figure S59. Analysis of scanned lateral flow from cassettes. Neuraminic acid (NeuNAc) functionalised PHEA₅₀ on 35 nm AuNPs at OD3 versus a test line of SARS-COV-2,S1 (SC2 S1) at varying concentrations on lateral flow cassettes. A control line of 1 mg/mL RCA₁₂₀ was used in all tests. Buffer containing 2% PVP was used. Data taken from the strips after removal from the cassettes after ~1 hour. Conjugate pads were cured overnight.

Cassettes from Pseudotyped Lentivirus Experiments









Titre, TU/ml	Particles	Cassettes after 20 minute run	Cassettes after ~17 hours
1.5×10^5	NeuNAc-PHEA50AuNP35		
1.5×10^4	NeuNAc-PHEA50AuNP35		
1.5×10^3	NeuNAc-PHEA50AuNP35		
1.5×10^5	Gal-PHEA72AuNP16		

Table S21. Photos of lateral flow cassettes and strips from the cassettes versus a test line of Spike (SARS-COV2) pseudotyped lentivirus at varying concentrations. A control line of 5 mg/mL RCA₁₂₀ was used in NeuNAc-PHEA50AuNP35 (OD3) tests and a control line of 5 mg/mL RCA₁₂₀ was used in Gal-PHEA72AuNP16 (OD3) tests. The conjugate pads in these tests were cured overnight. Buffer containing 2 % wt/v PVP was used in NeuNAc-PHEA50AuNP35 tests and 1 % wt/v PVP was used in Gal-PHEA72AuNP16 tests.

NB: Photos were taken of the cassettes rather than scans due biosafety measures.

Lateral Flow Influenza Controls

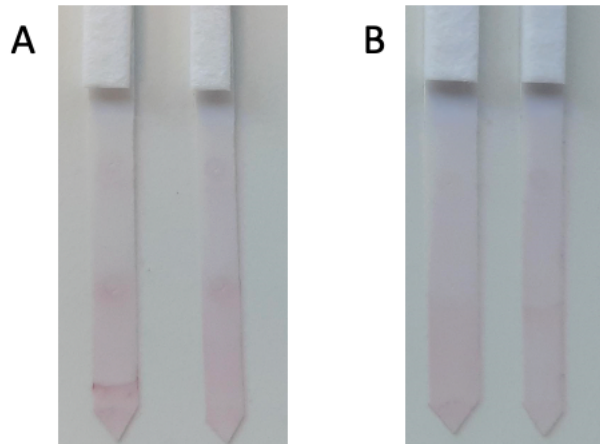


Figure S60. Photos of lateral flow strips of NeuNAc-PHEA₅₀AuNP35 versus a test line of propiolactone-deactivated Influenza viruses (50 HGU). A) H3N2 B) H5N1

Analyzed XPS (x-ray Photoelectron Spectroscopy) data

All nanoparticle used here were analysed by XPS. Fitted XPS are provided below.

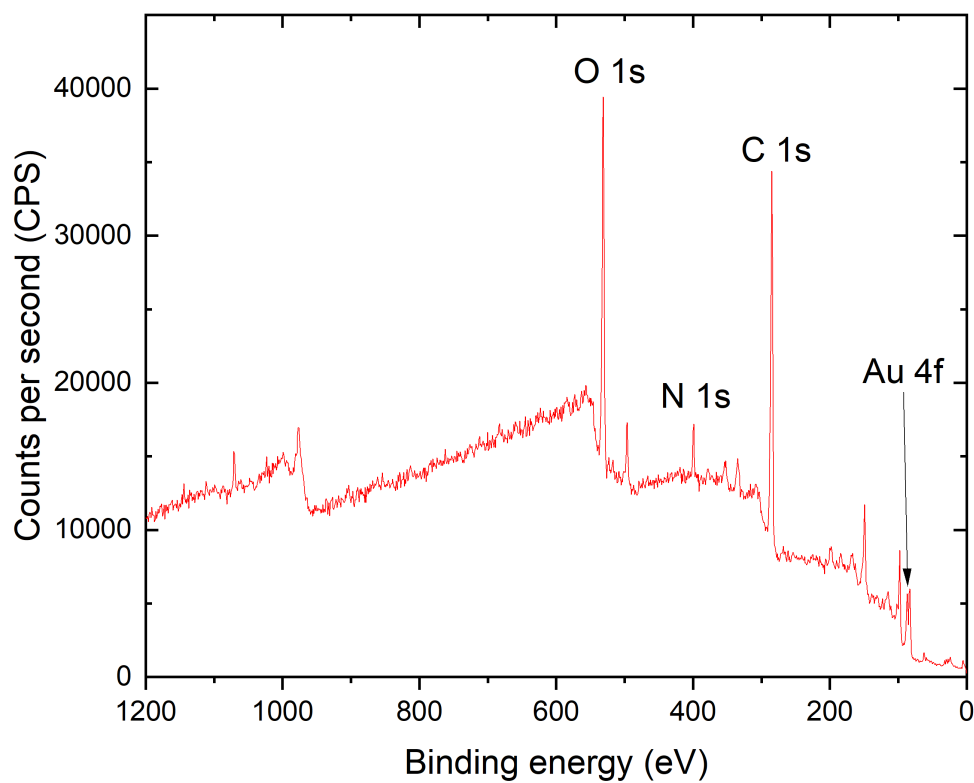


Figure S61. Representative XPS survey scan of glycopolymer functionalised AuNP (neuraminic acid PHEA50@AuNP16)

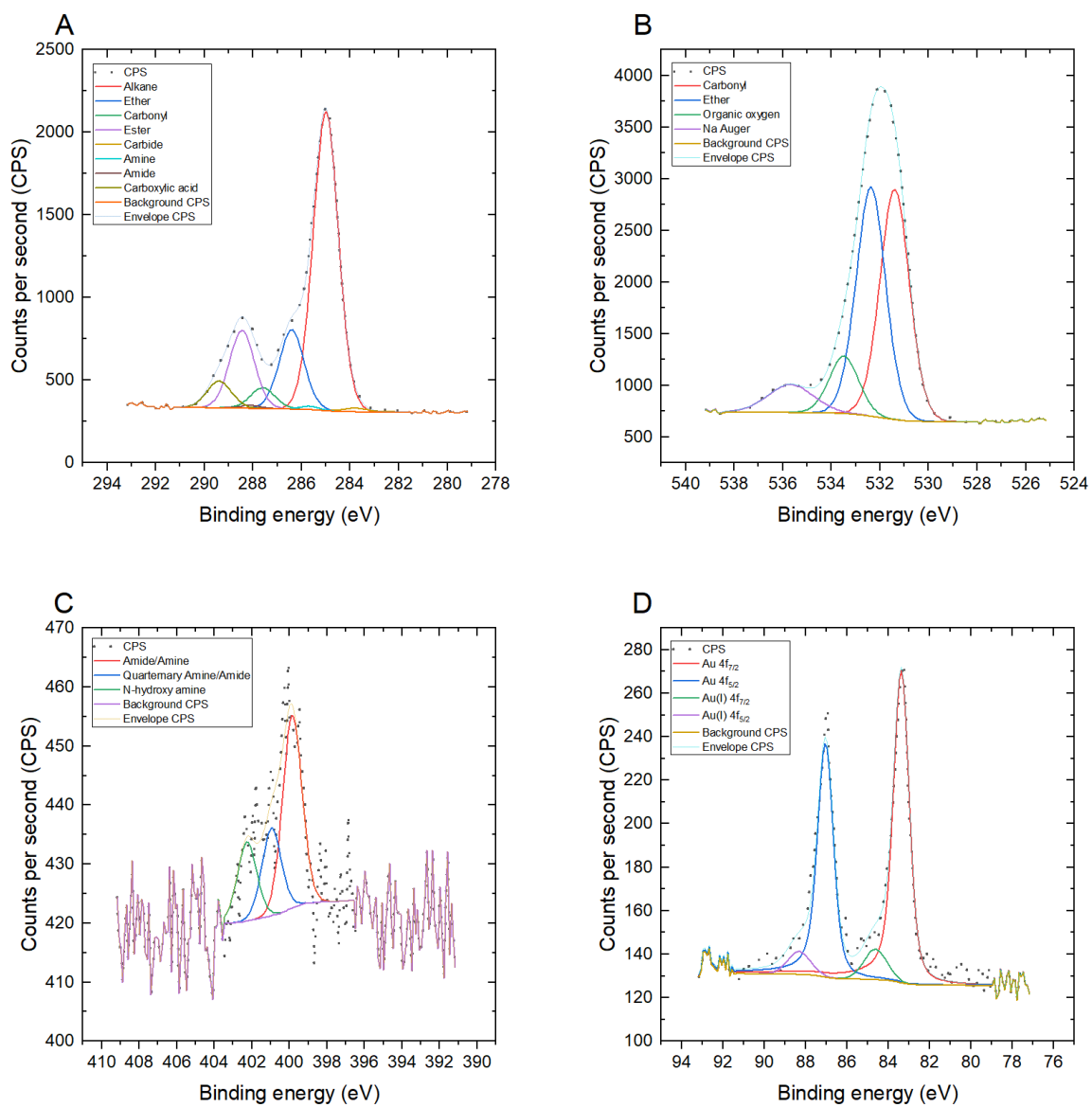


Figure S62. XPS of citrate stabilized 16nm AuNP A) C 1s B) O 1s C) N 1s and D) Au 4f

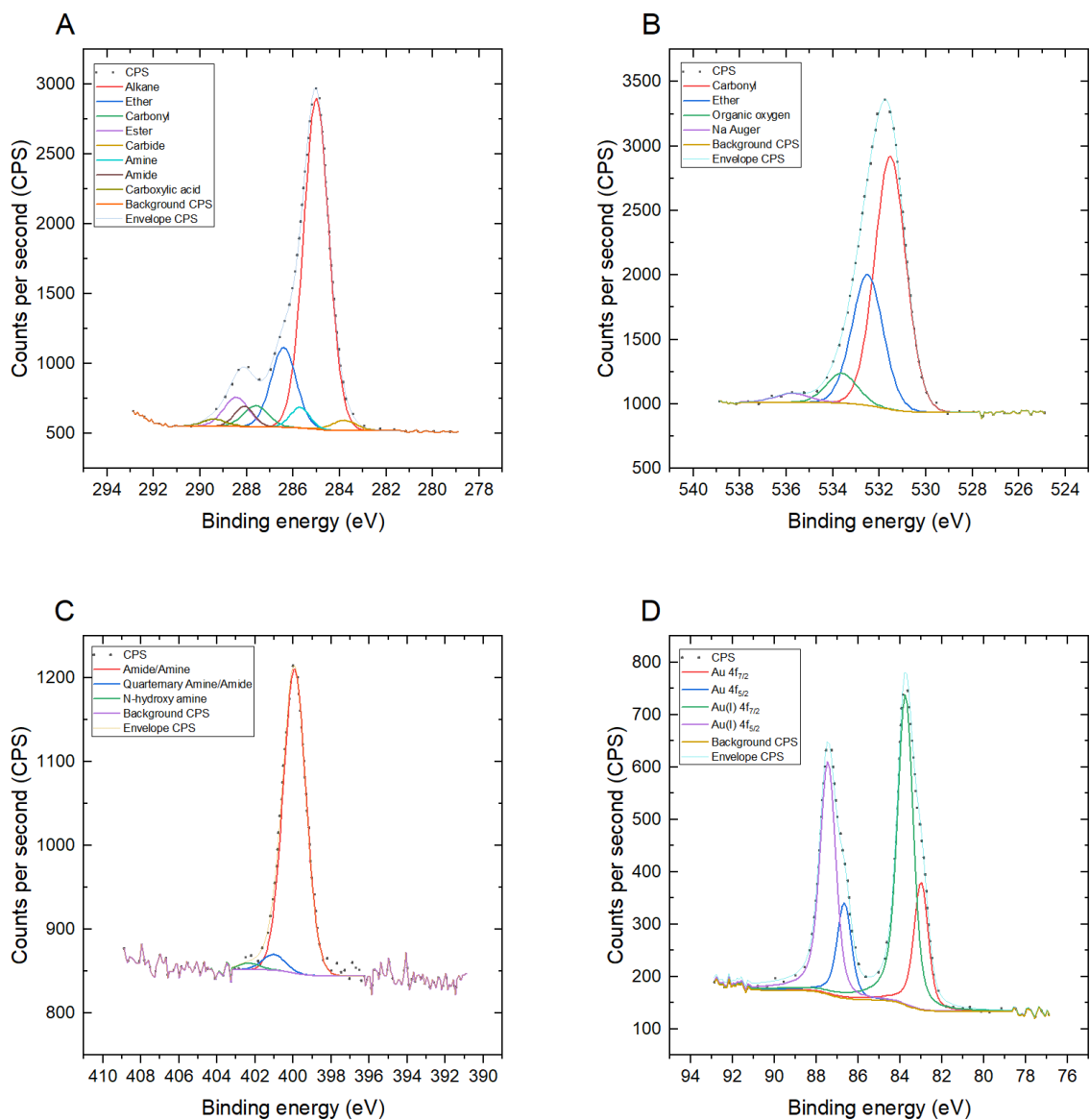


Figure S63. XPS of neuraminic acid PHEA40@AuNP16 A) C 1s B) O 1s C) N 1s and D) Au 4f

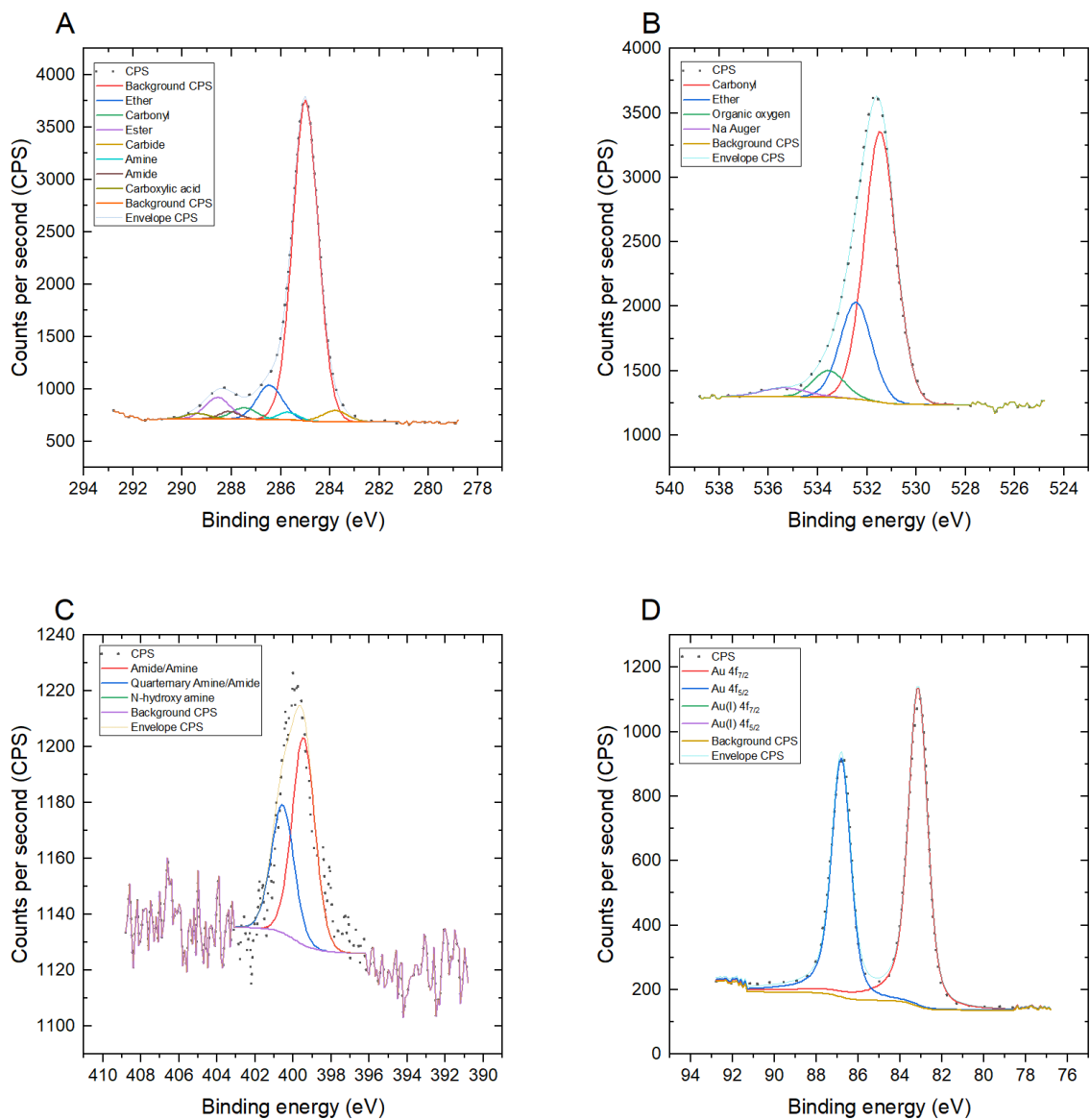


Figure S64. XPS of 2,3'-sialyllactosamine PHEA50@AuNP16 A) C 1s B) O 1s C) N 1s and D) Au 4f

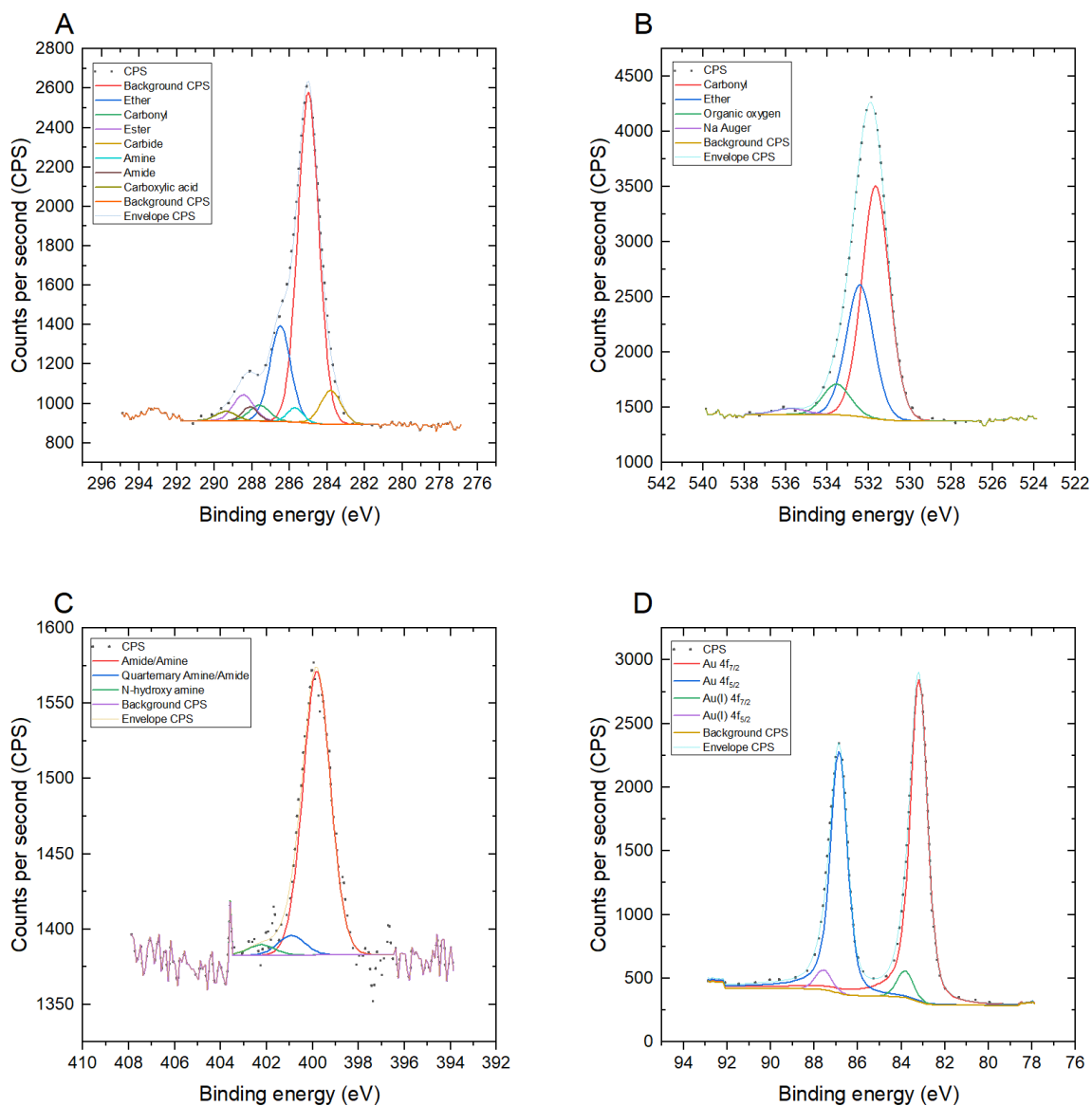


Figure S65. XPS of 2,6'-sialyllactosamine PHEA50@AuNP16 A) C 1s B) O 1s C) N 1s and D) Au 4f

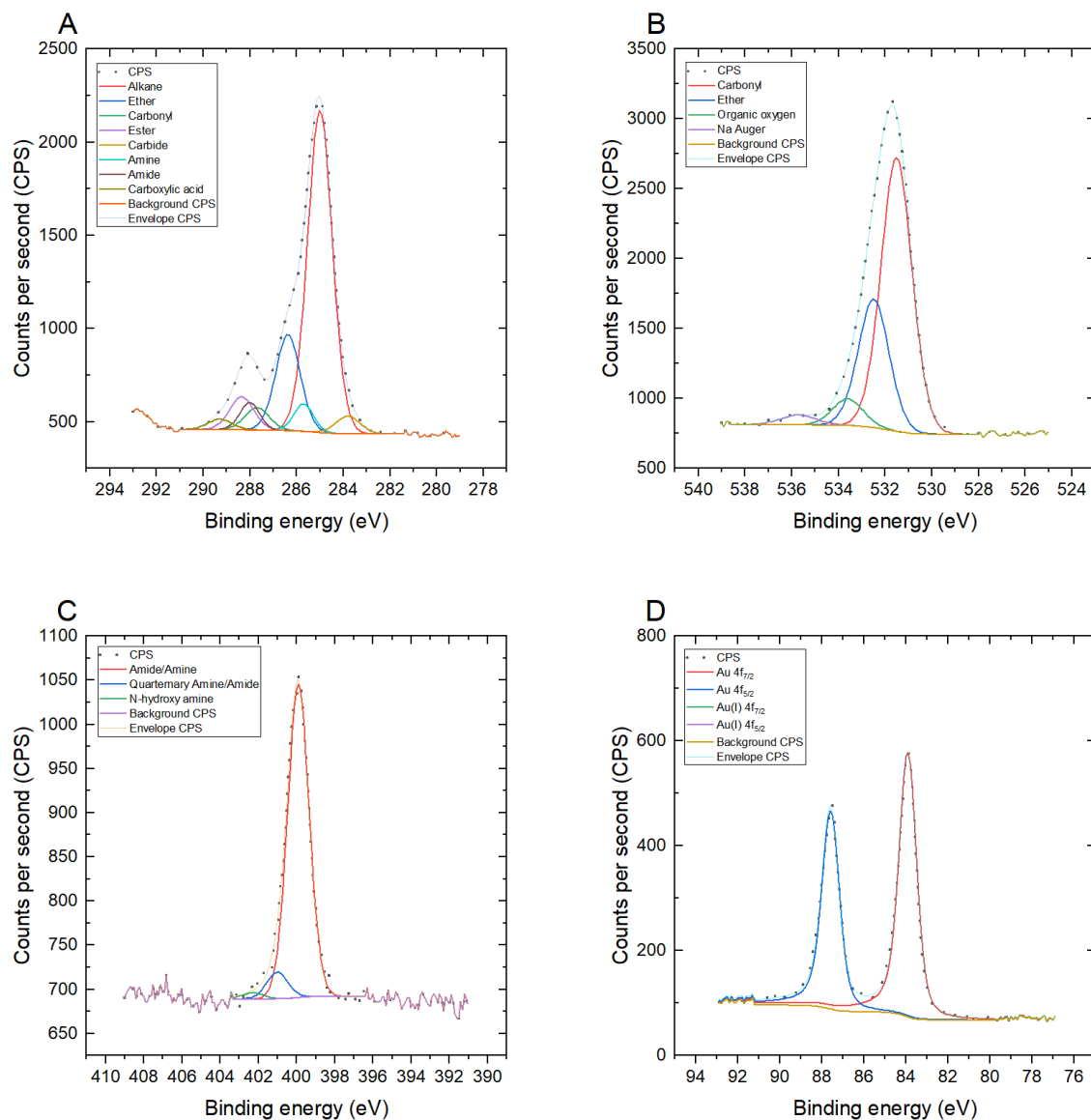


Figure S66. XPS of neuraminic acid PHEA50@AuNP16 A) C 1s B) O 1s C) N 1s and D) Au 4f

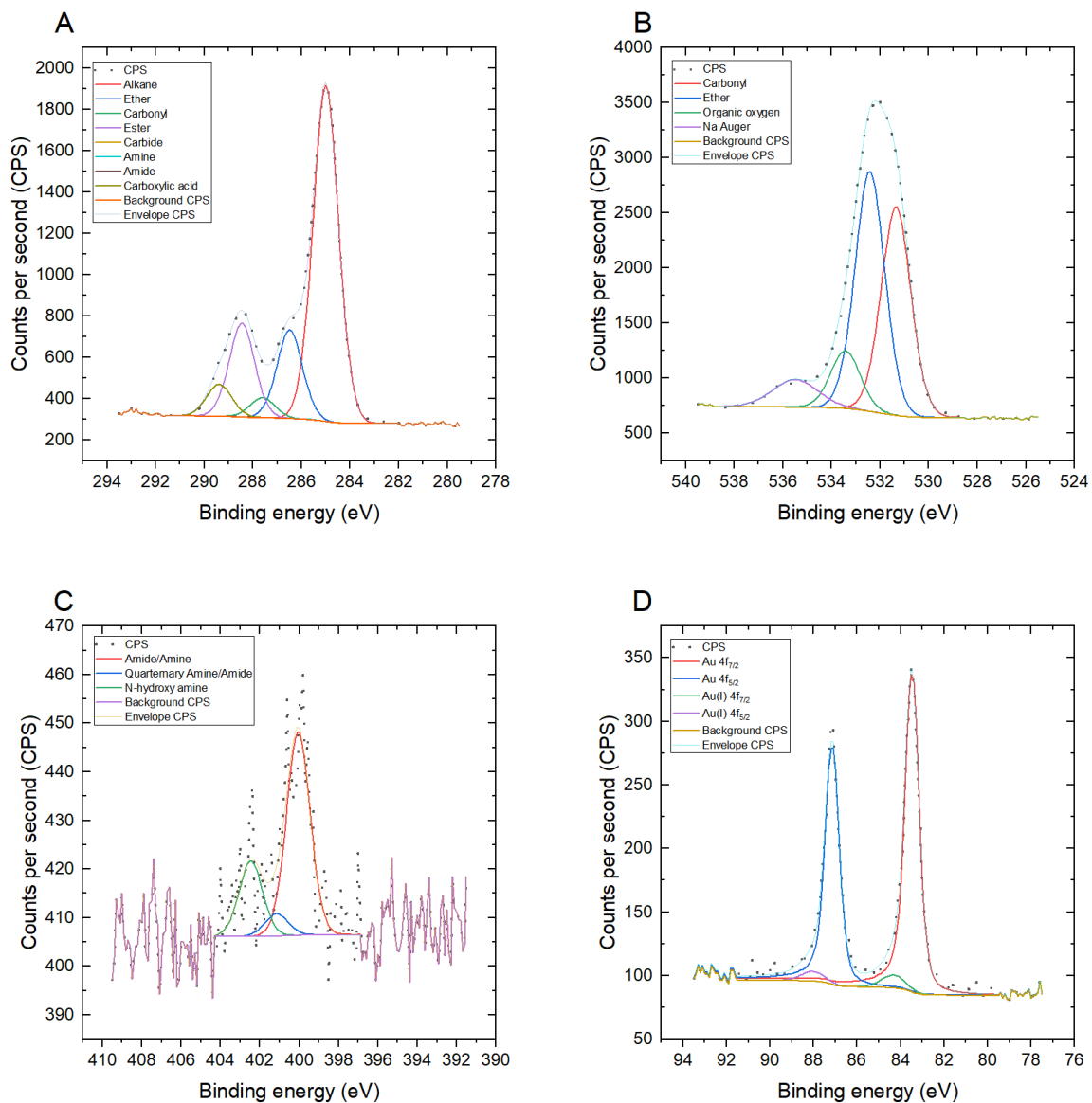


Figure S67. XPS of citrate stabilized 35nm AuNP A) C 1s B) O 1s C) N 1s and D) Au 4f

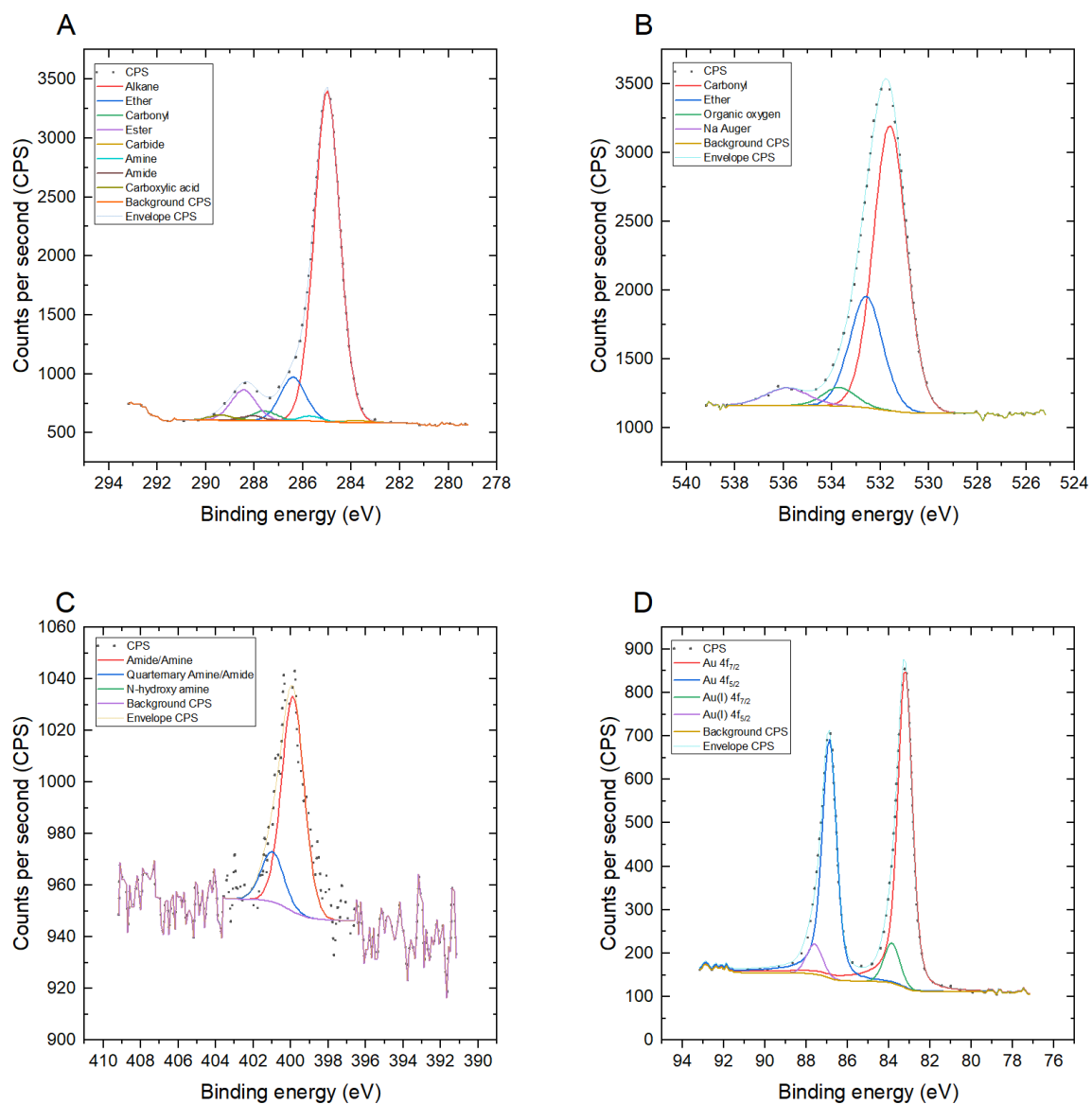


Figure S68. XPS of 2,3'-sialyllactosamine PHEA40@AuNP35 A) C 1s B) O 1s C) N 1s and D) Au 4f

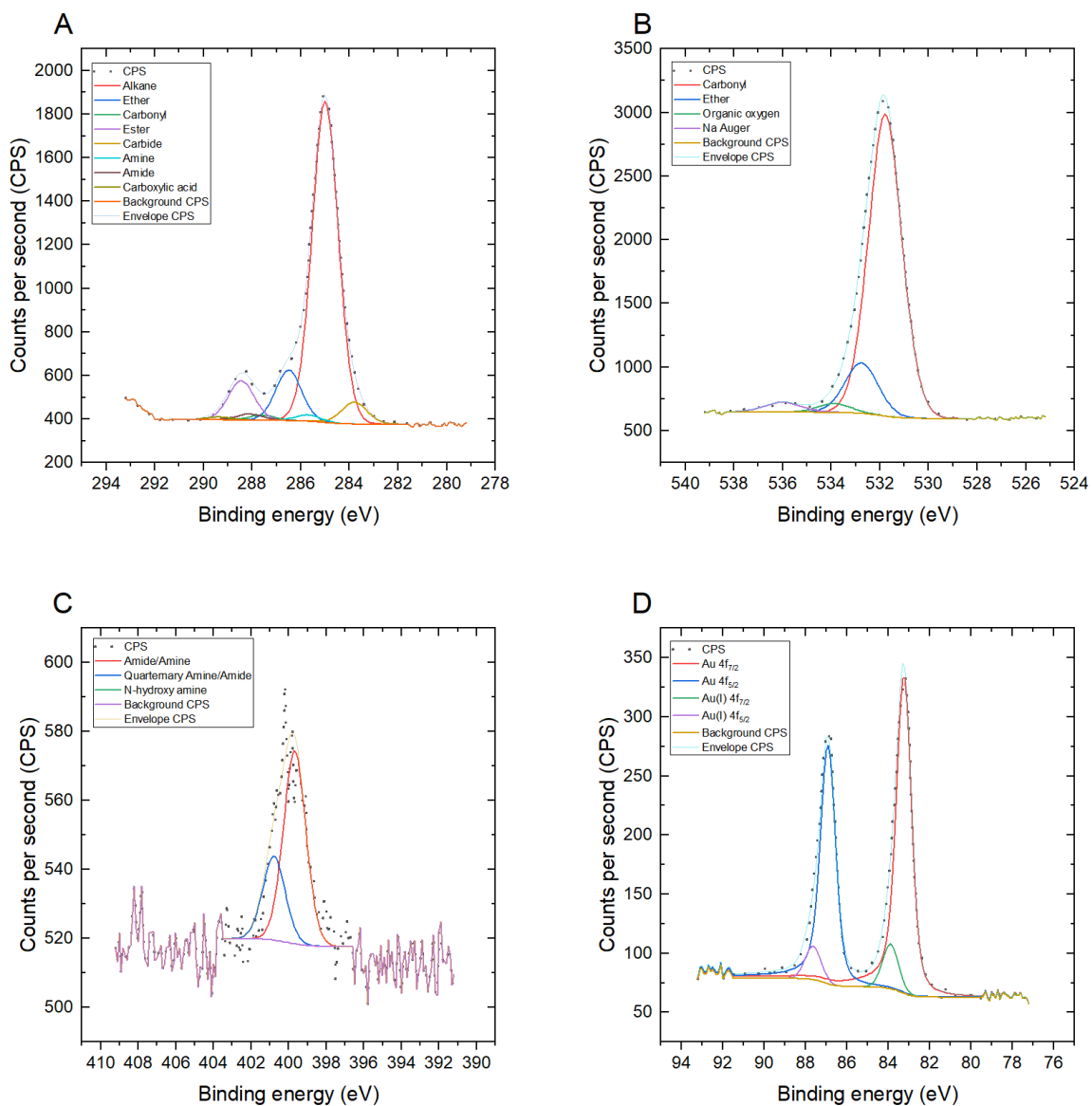


Figure S69. XPS of 2,6'-sialyllactosamine PHEA40@AuNP35 A) C 1s B) O 1s C) N 1s and D) Au 4f

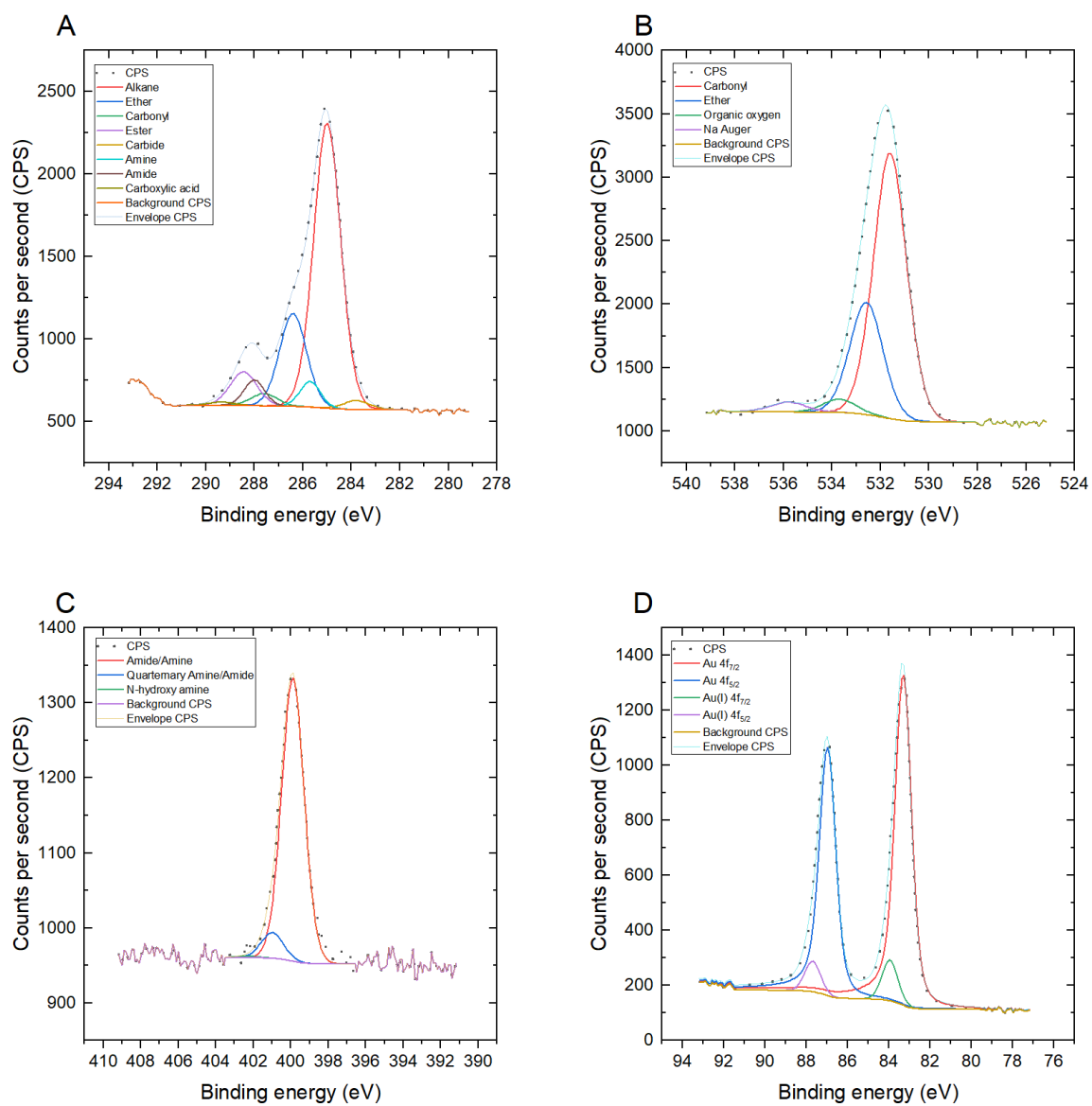


Figure S70. XPS of neuraminic acid PHEA40@AuNP35 A) C 1s B) O 1s C) N 1s and D) Au 4f

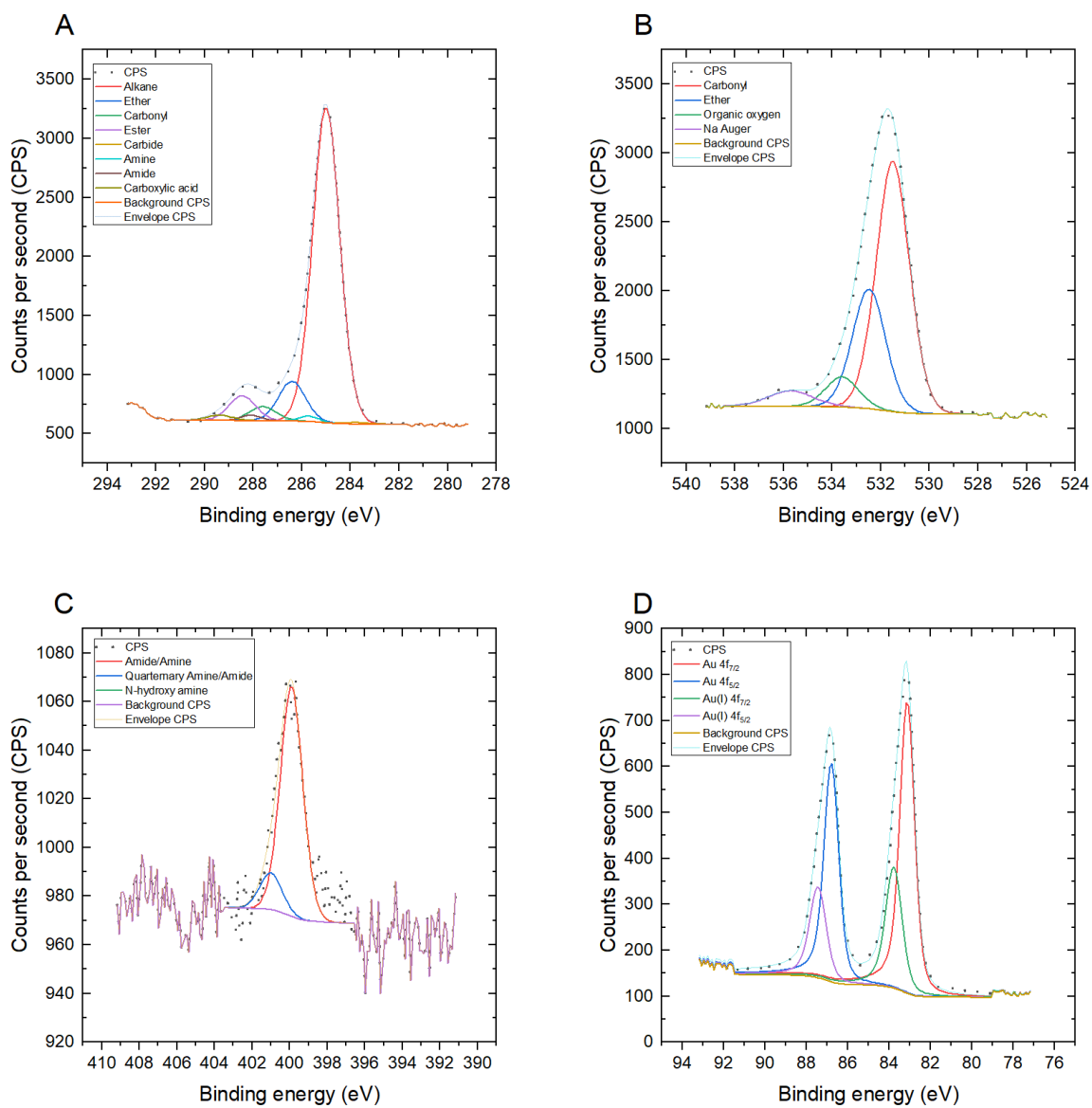


Figure S71. XPS of 2,3'-sialyllactosamine PHEA50@AuNP35 A) C 1s B) O 1s C) N 1s and D) Au 4f

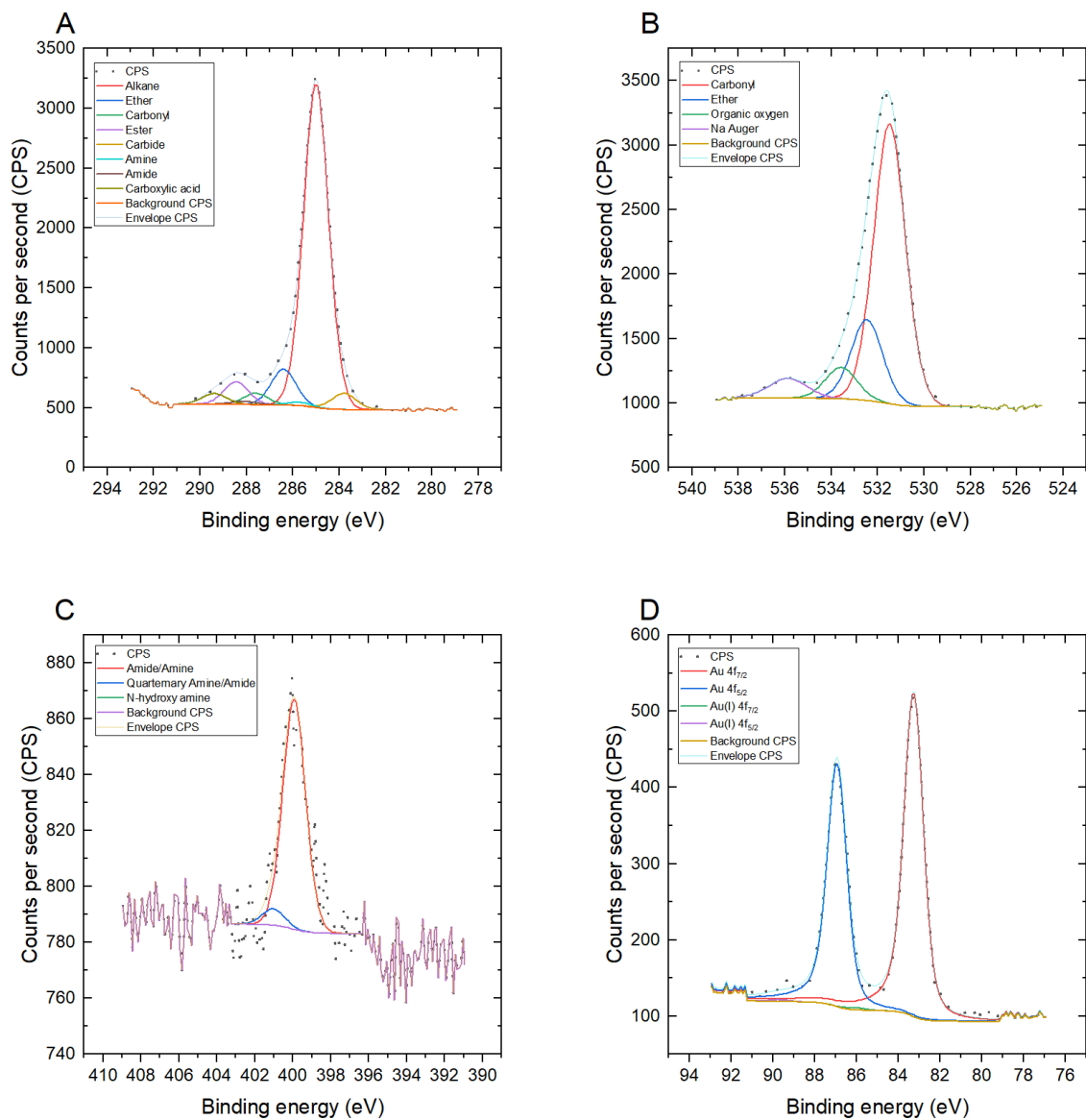


Figure S72. XPS of 2,6'-sialyllactosamine PHEA50@AuNP35 A) C 1s B) O 1s C) N 1s and D) Au 4f

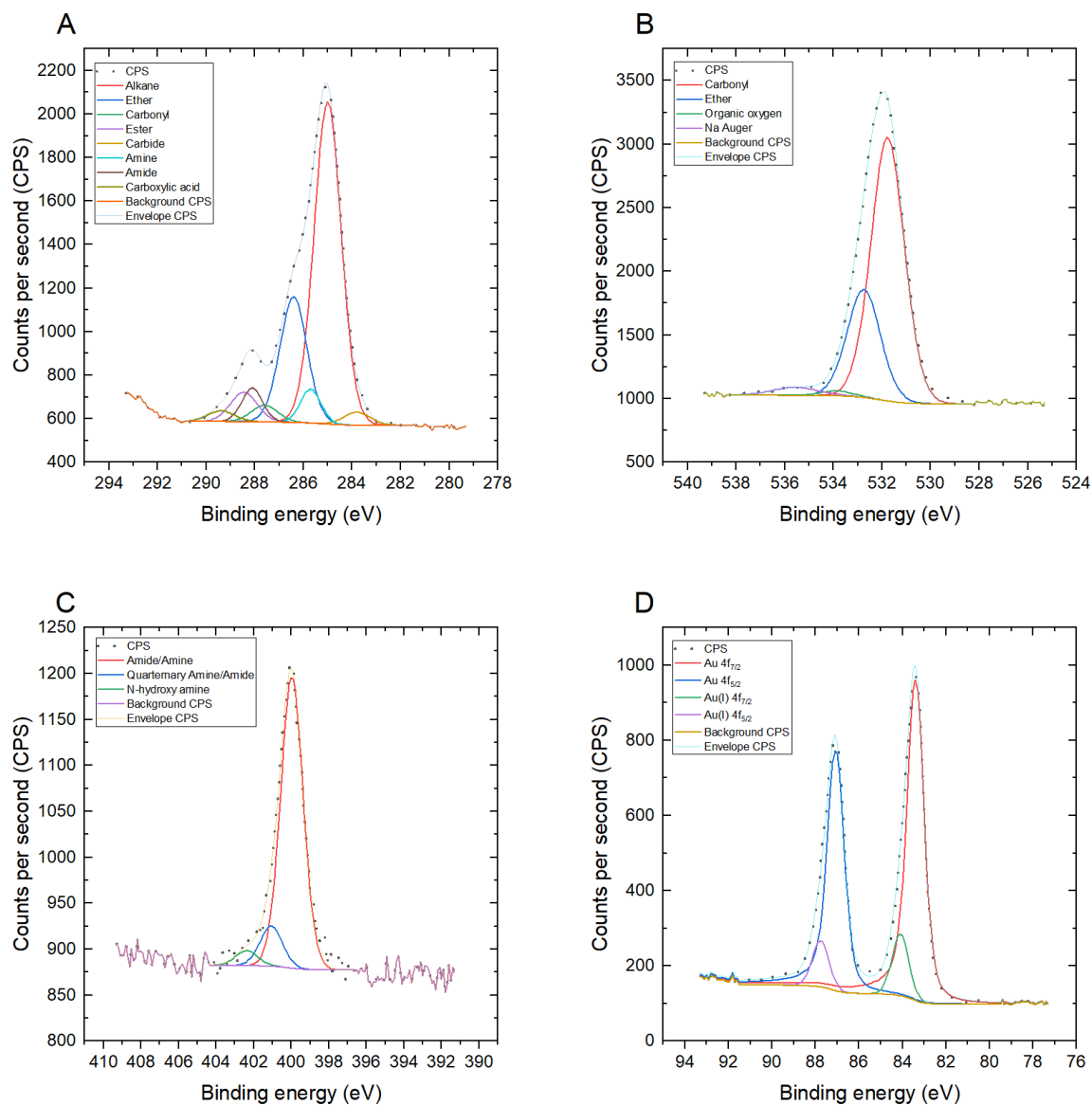


Figure S73. XPS of neuraminic acid PHEA50@AuNP35 A) C 1s B) O 1s C) N 1s and D) Au 4f

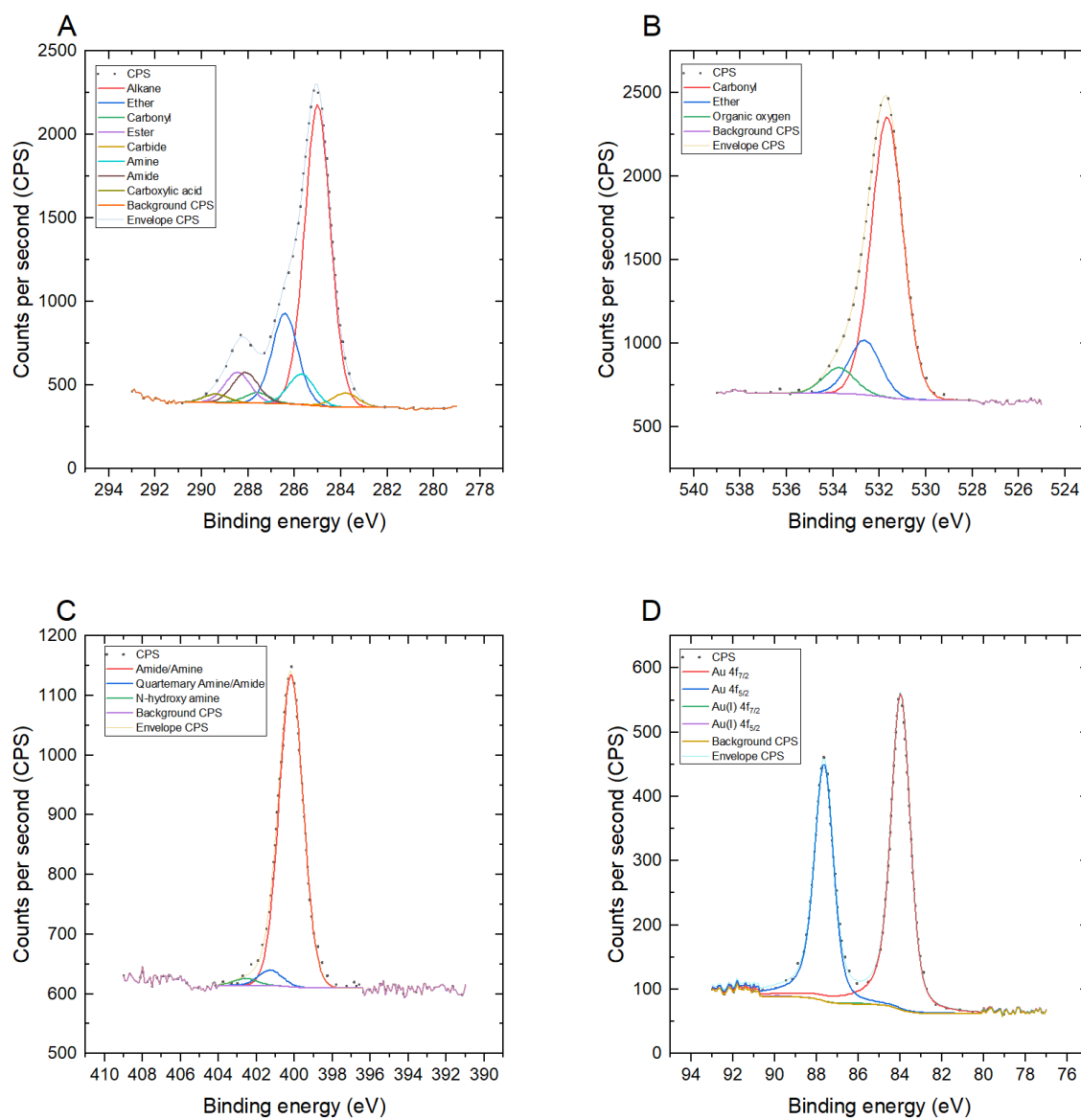


Figure S74. XPS of BSA-blocked neuraminic acid PHEA40@AuNP16 A) C 1s B) O 1s C) N 1s and D) Au 4f

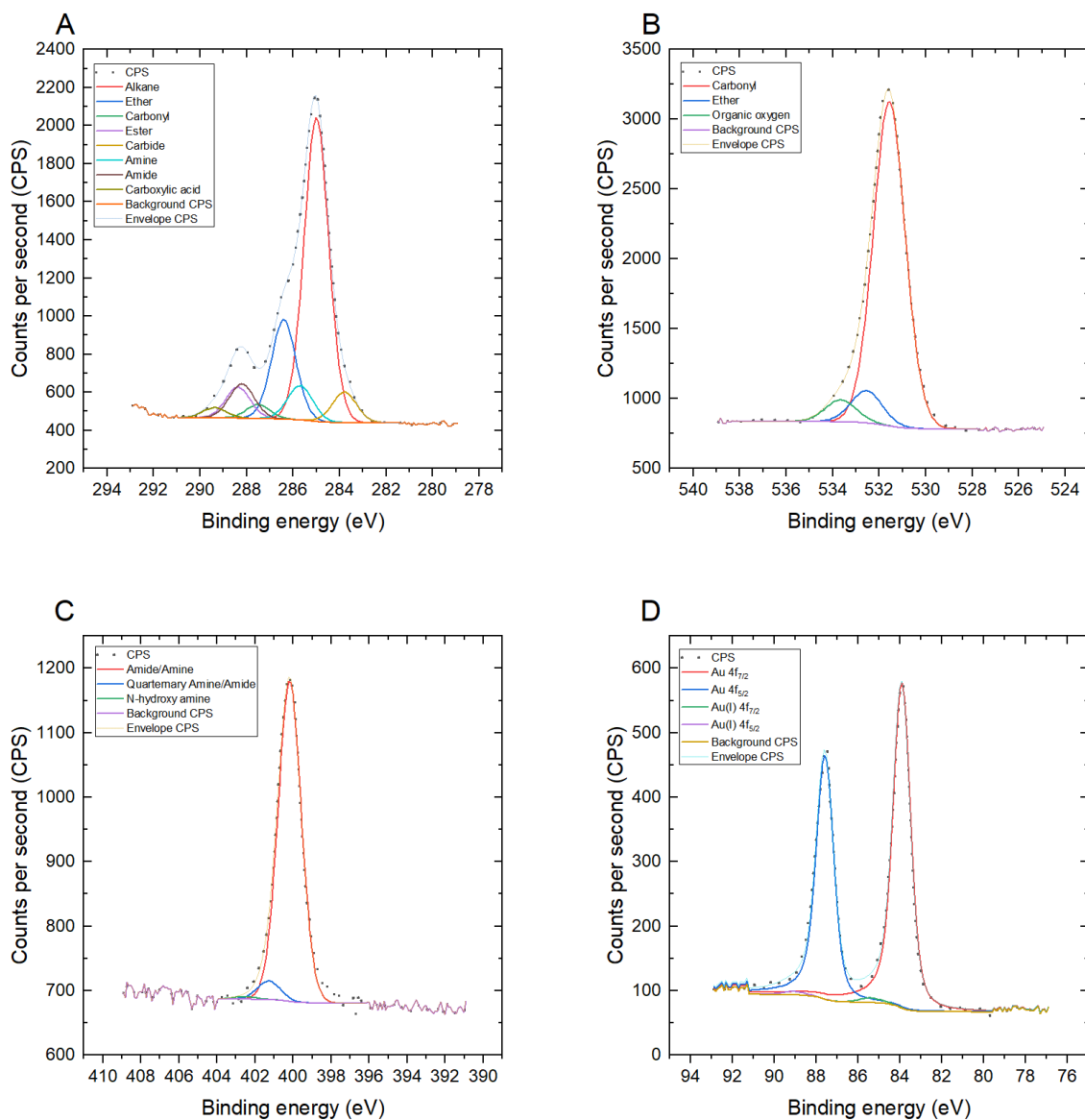


Figure S75. XPS of BSA-blocked neuraminic acid PHEA50@AuNP16 A) C 1s B) O 1s C) N 1s and D) Au 4f

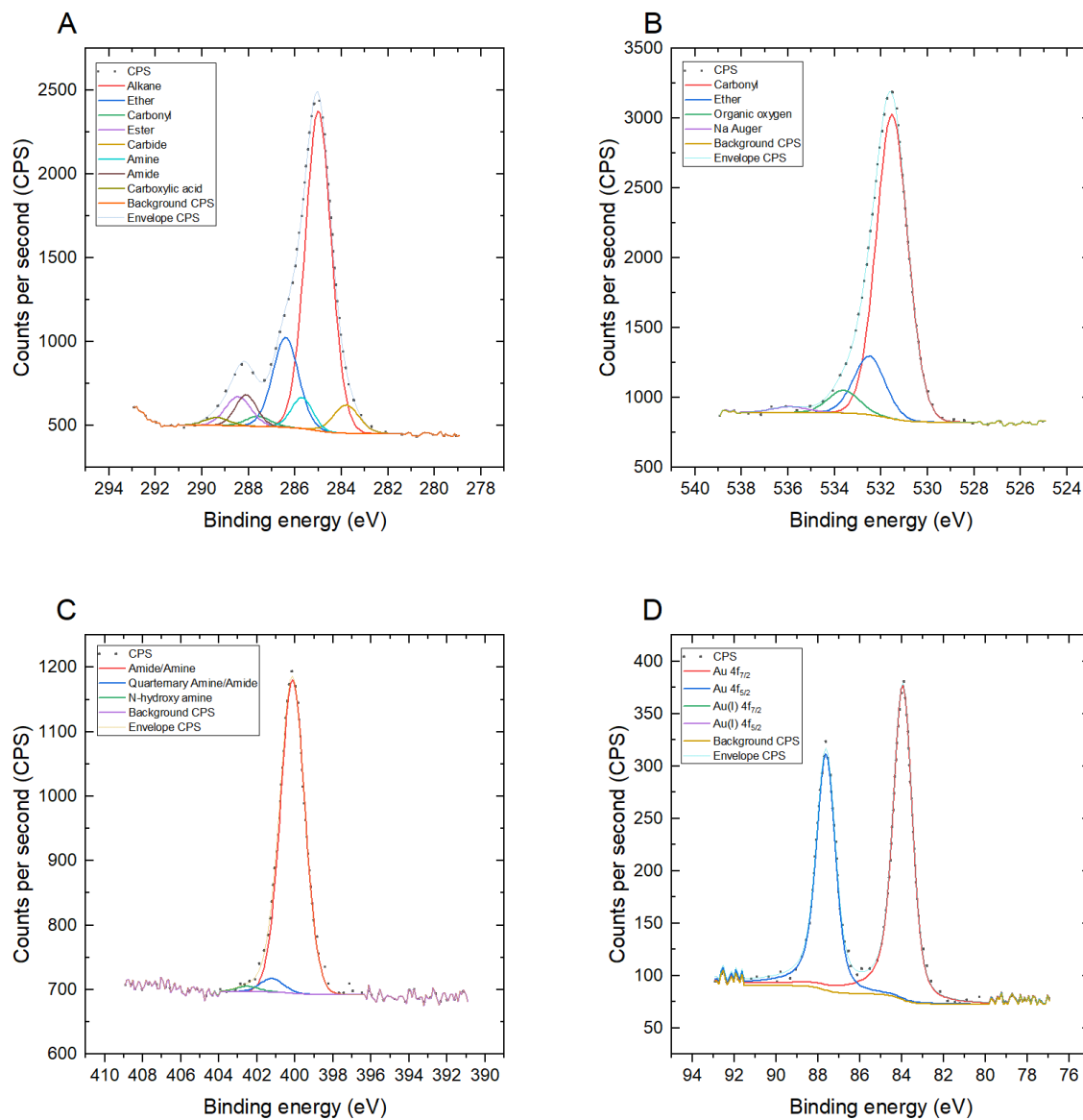


Figure S76. XPS of BSA-blocked neuraminic acid PHEA40@AuNP35 A) C 1s B) O 1s C) N 1s and D) Au 4f

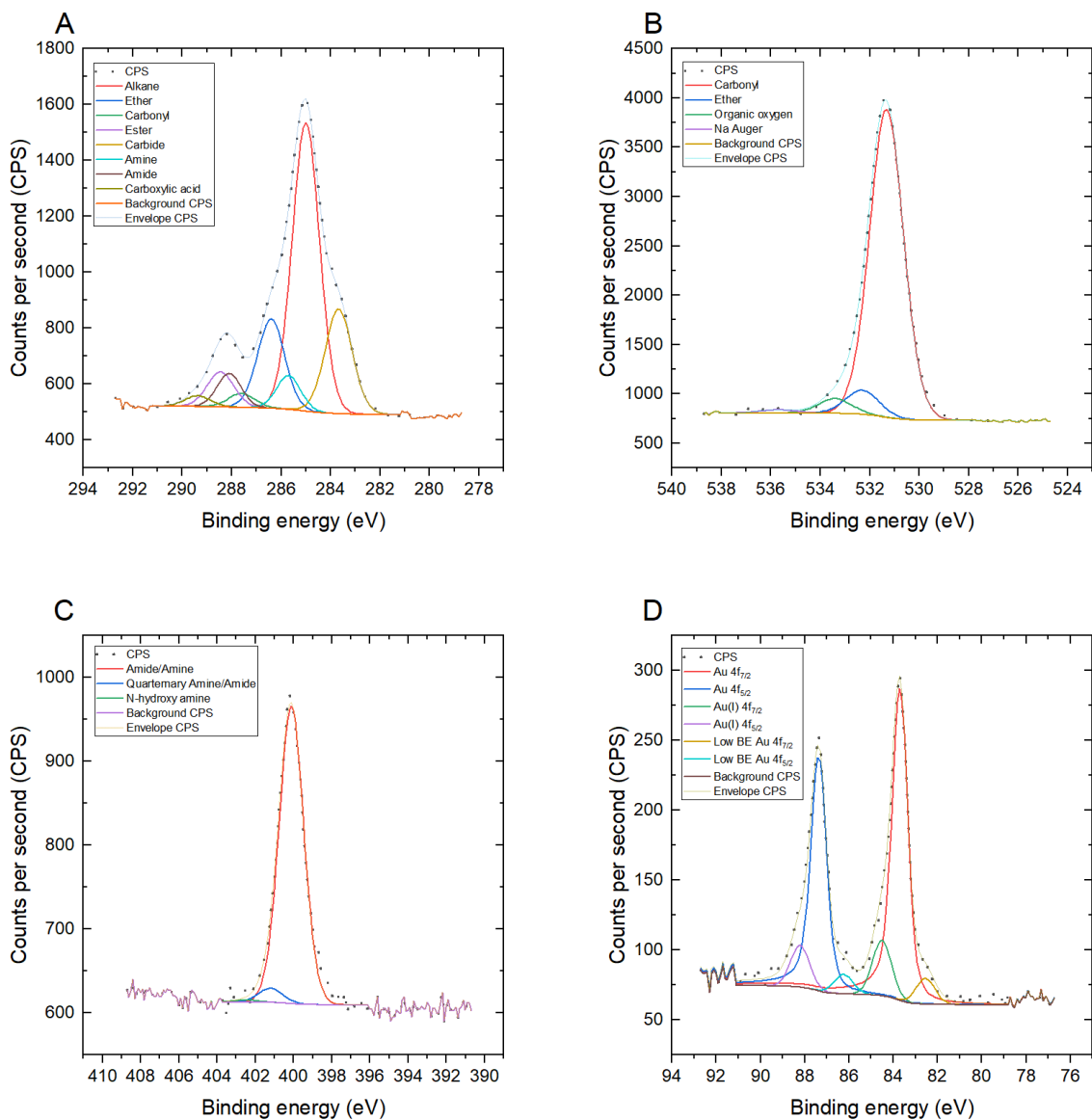


Figure S77. XPS of BSA-blocked neuraminic acid PHEA50@AuNP35 A) C 1s B) O 1s C) N 1s and D) Au 4f

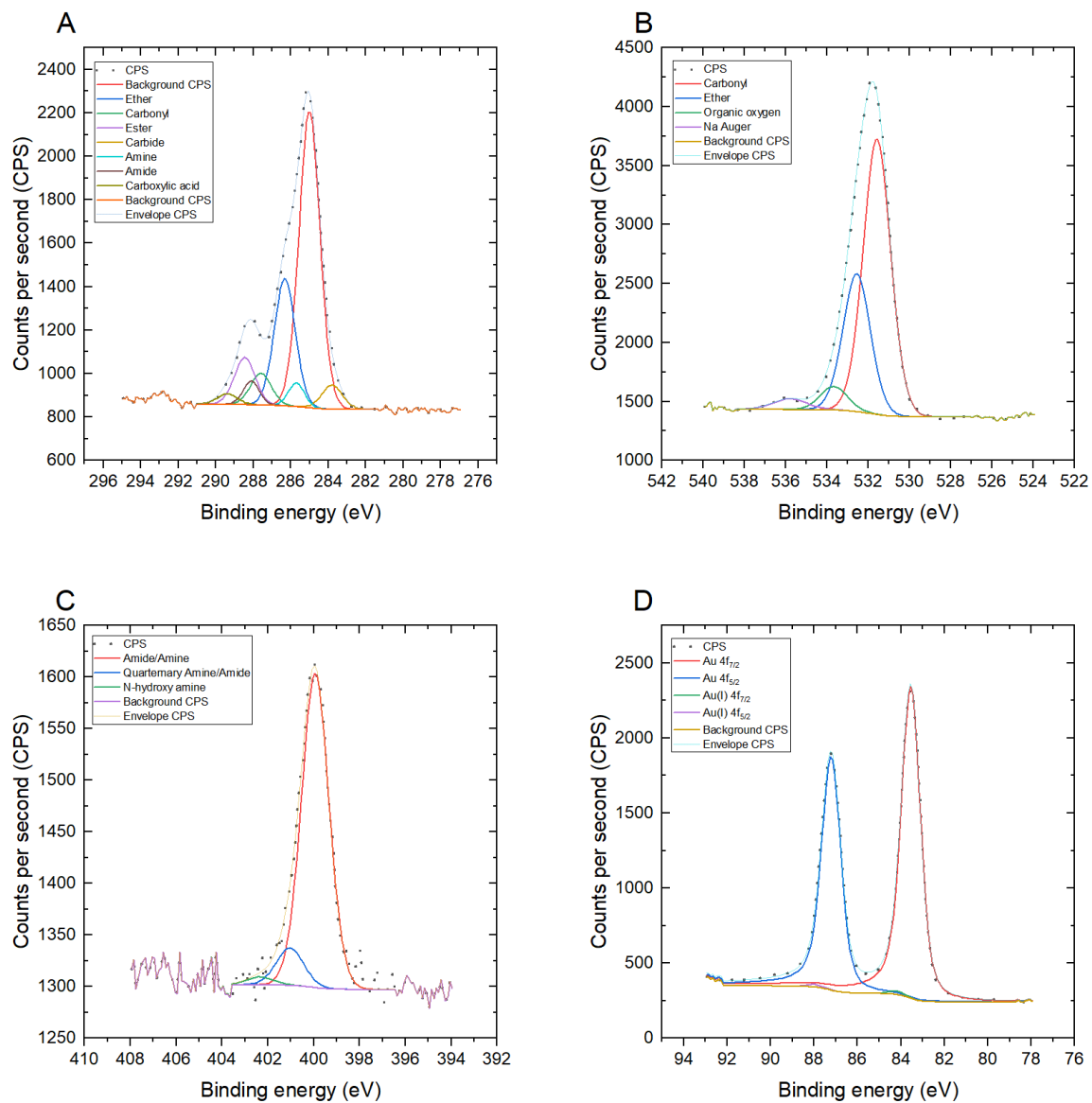


Figure S78. XPS of 1-deoxy-1-amino-glucose PHEA40@AuNP16 A) C 1s B) O 1s C) N 1s and D) Au 4f

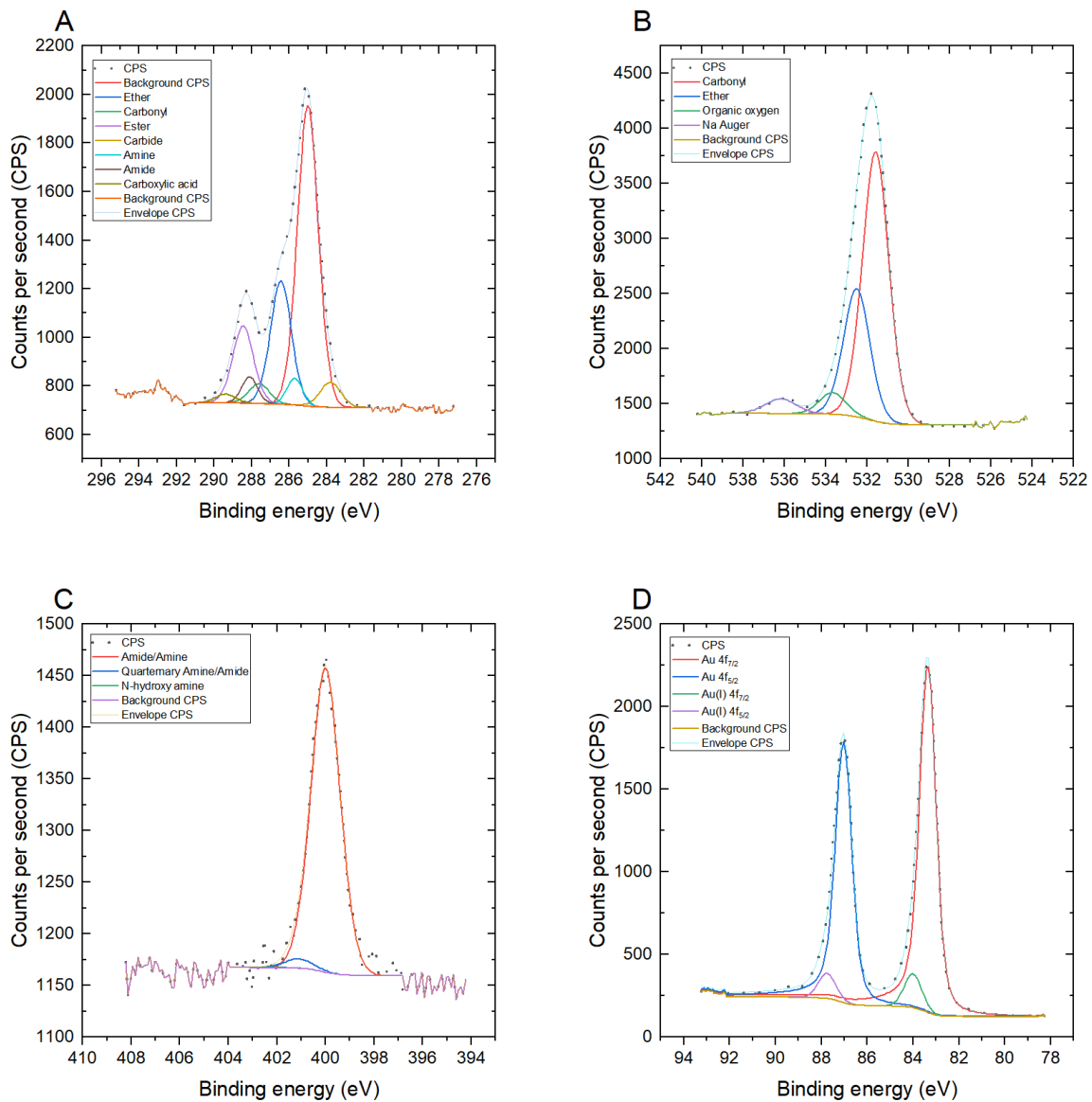


Figure S79. XPS of 1-deoxy-1-amino-glucose PHEA50@AuNP16 A) C 1s B) O 1s C) N 1s and D) Au 4f

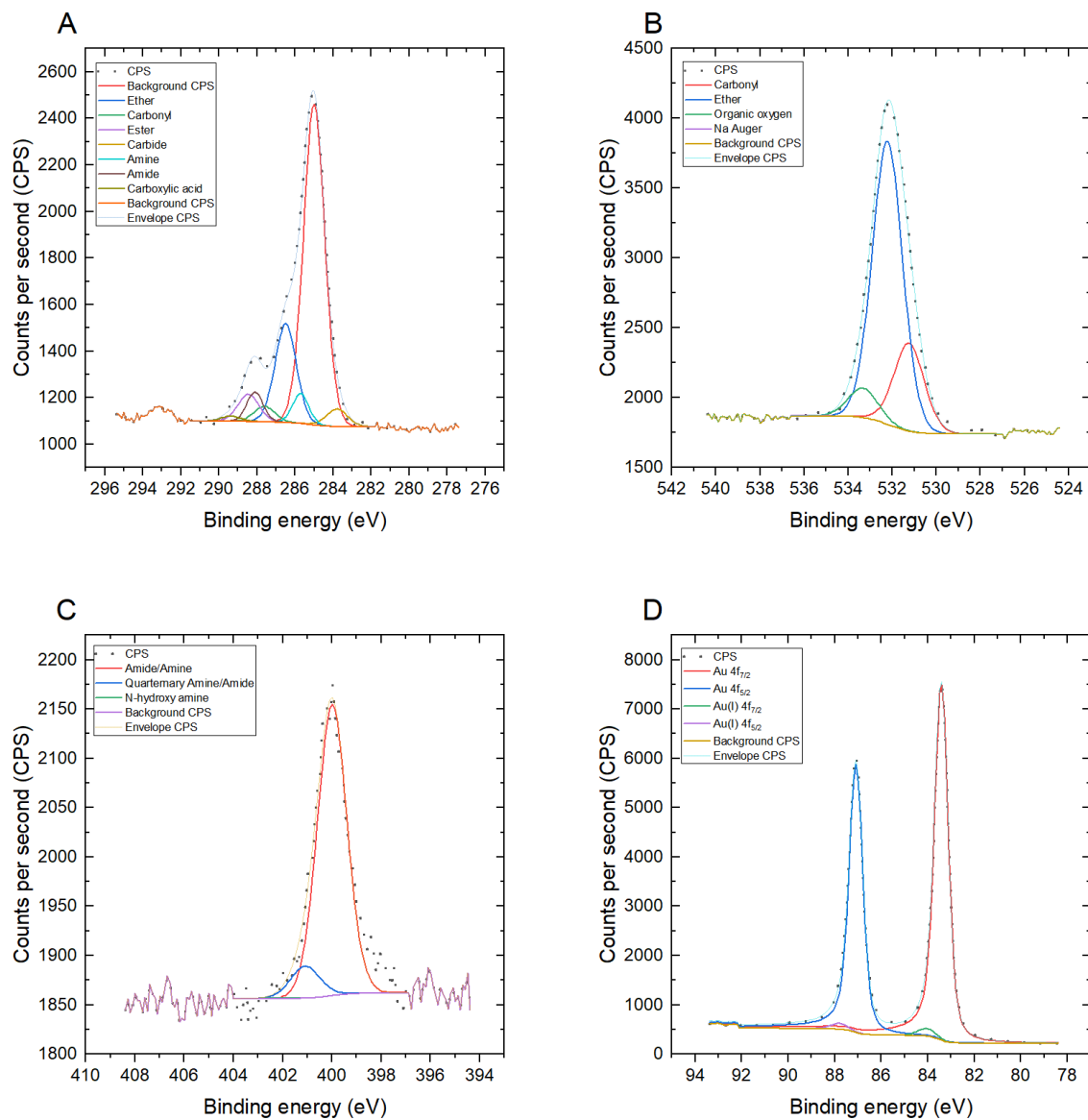


Figure S80. XPS of 1-deoxy-1-amino-glucose PHEA40@AuNP35 A) C 1s B) O 1s C) N 1s and D) Au 4f

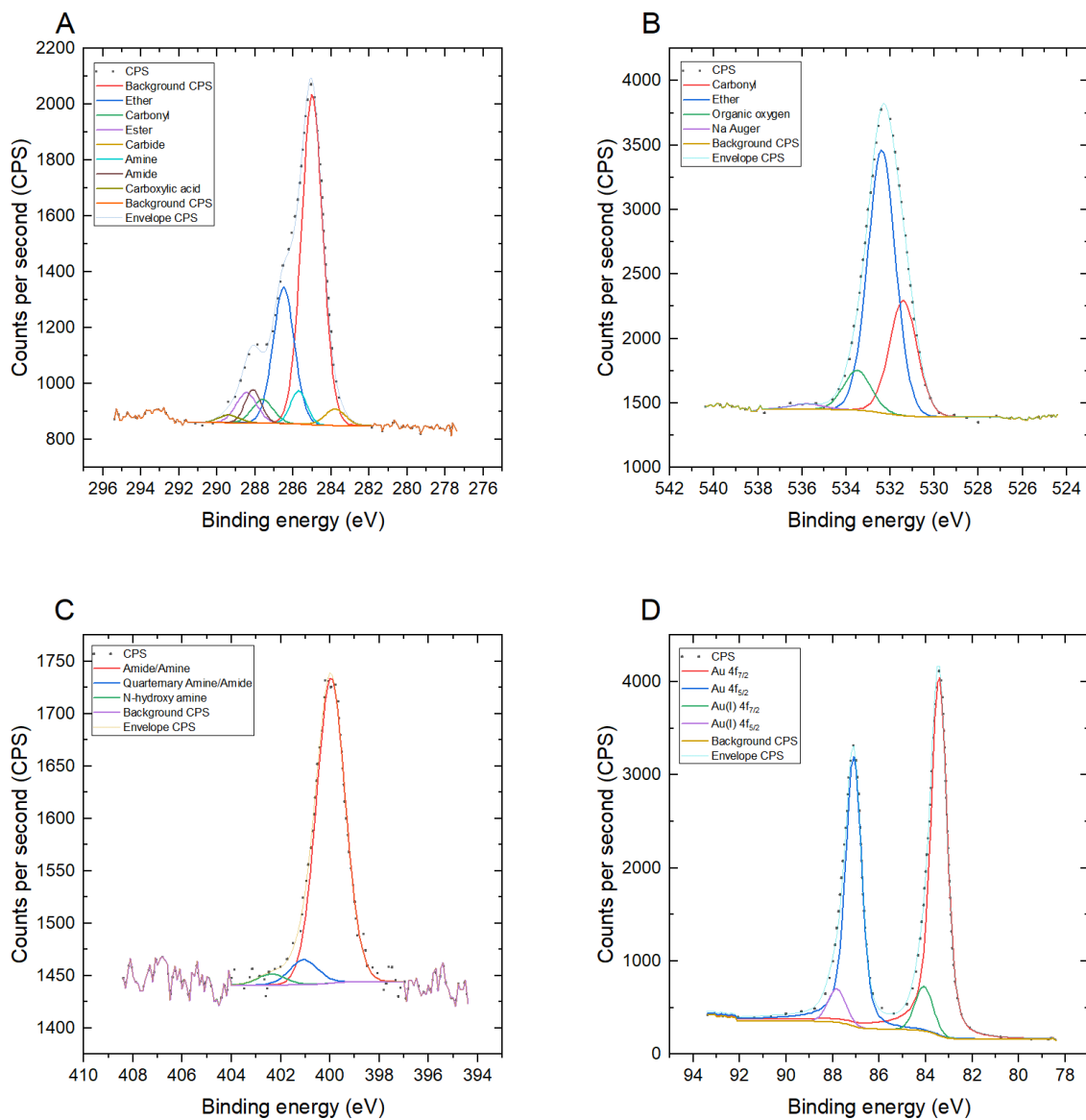


Figure S81. XPS of 1-deoxy-1-amino-glucose PHEA50@AuNP35 A) C 1s B) O 1s C) N 1s and D) Au 4f

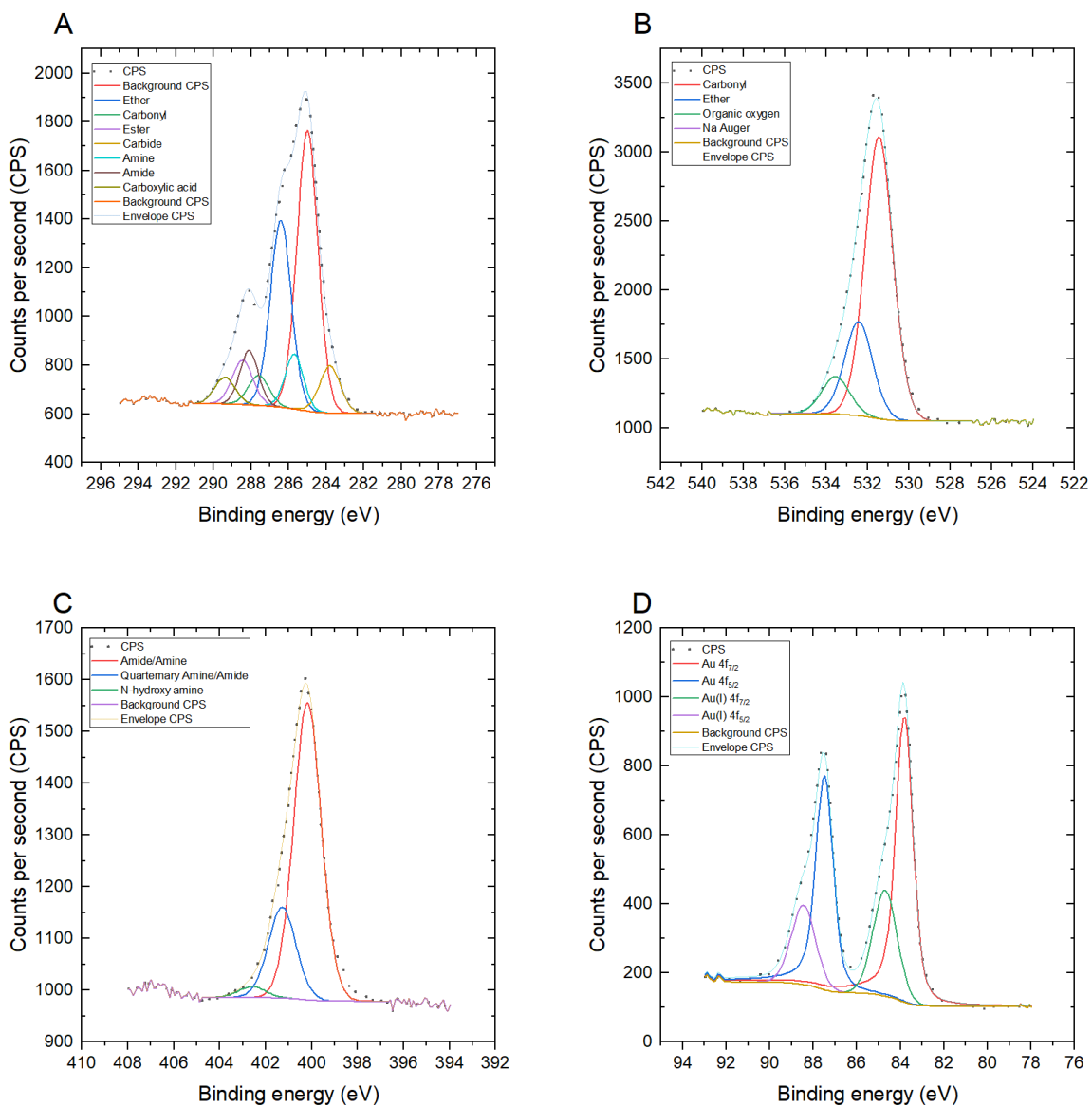


Figure S82. XPS of BSA-blocked 1-deoxy-1-amino-glucose PHEA40@AuNP16 A) C 1s B) O 1s C) N 1s and D) Au 4f

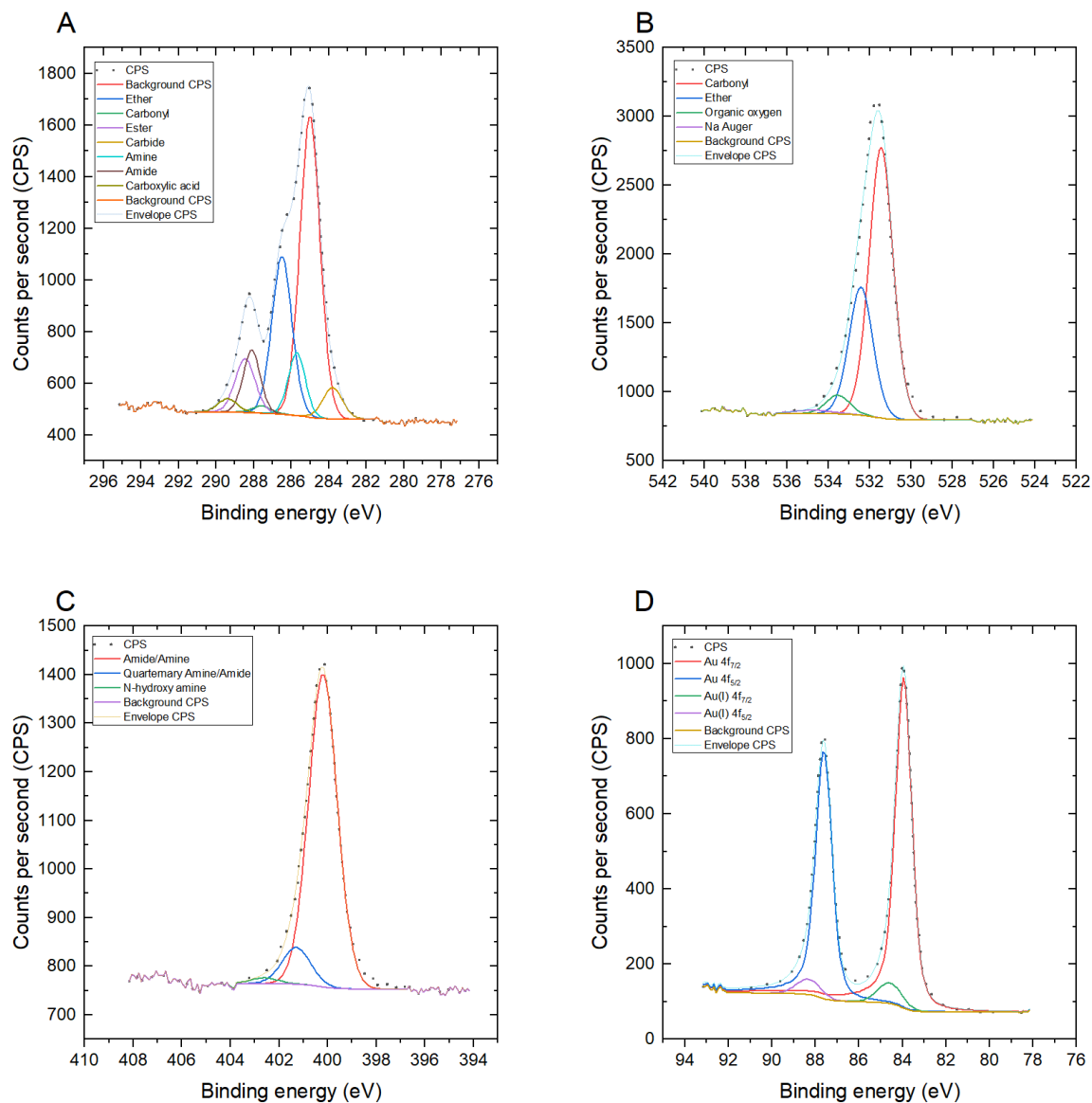


Figure S83. XPS of BSA-blocked 1-deoxy-1-amino-glucose PHEA50@AuNP16 A) C 1s B) O 1s C) N 1s and D) Au 4f

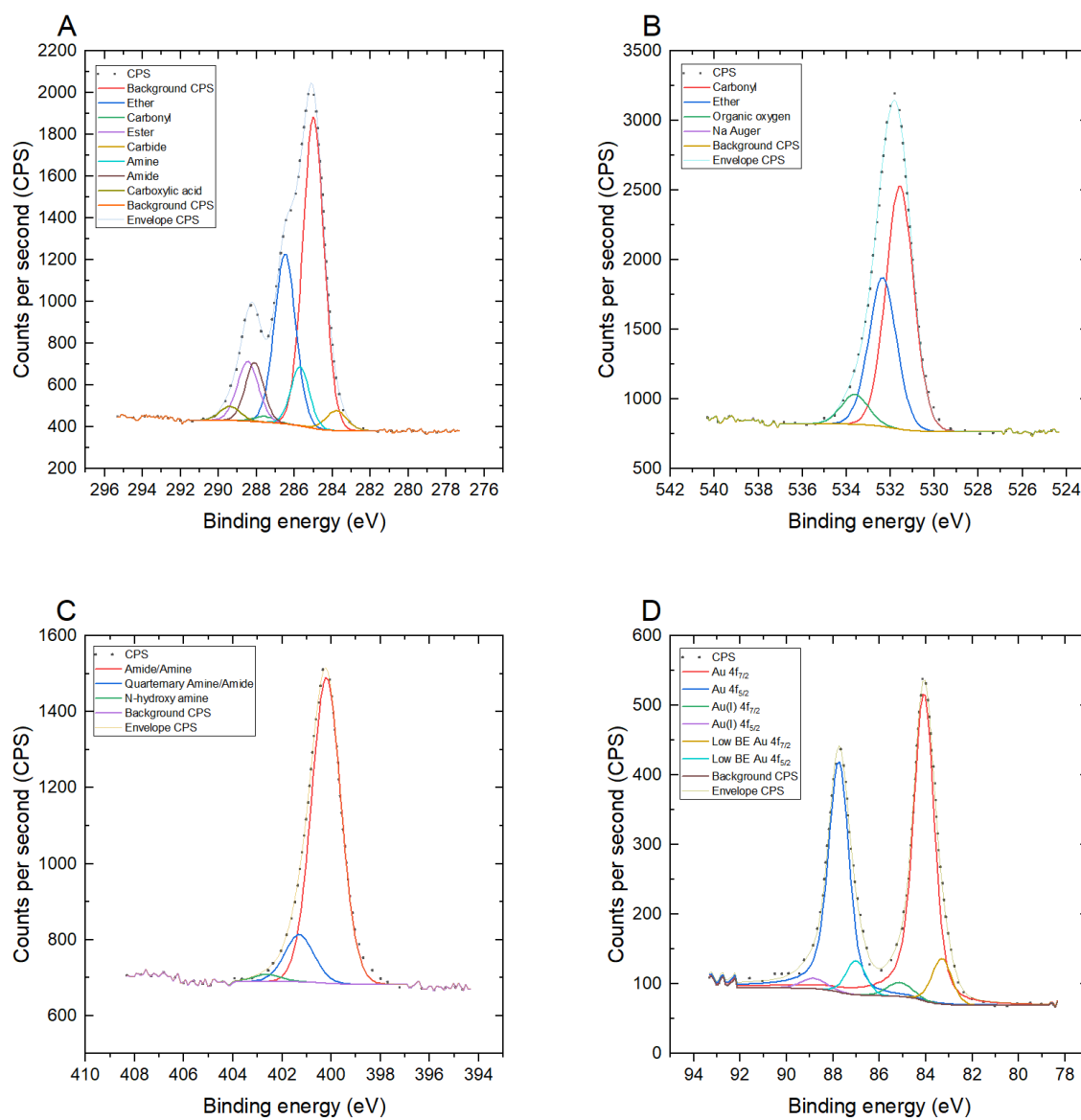


Figure S84. XPS of BSA-blocked 1-deoxy-1-amino-glucose PHEA40@AuNP35 A) C 1s B) O 1s C) N 1s and D) Au 4f

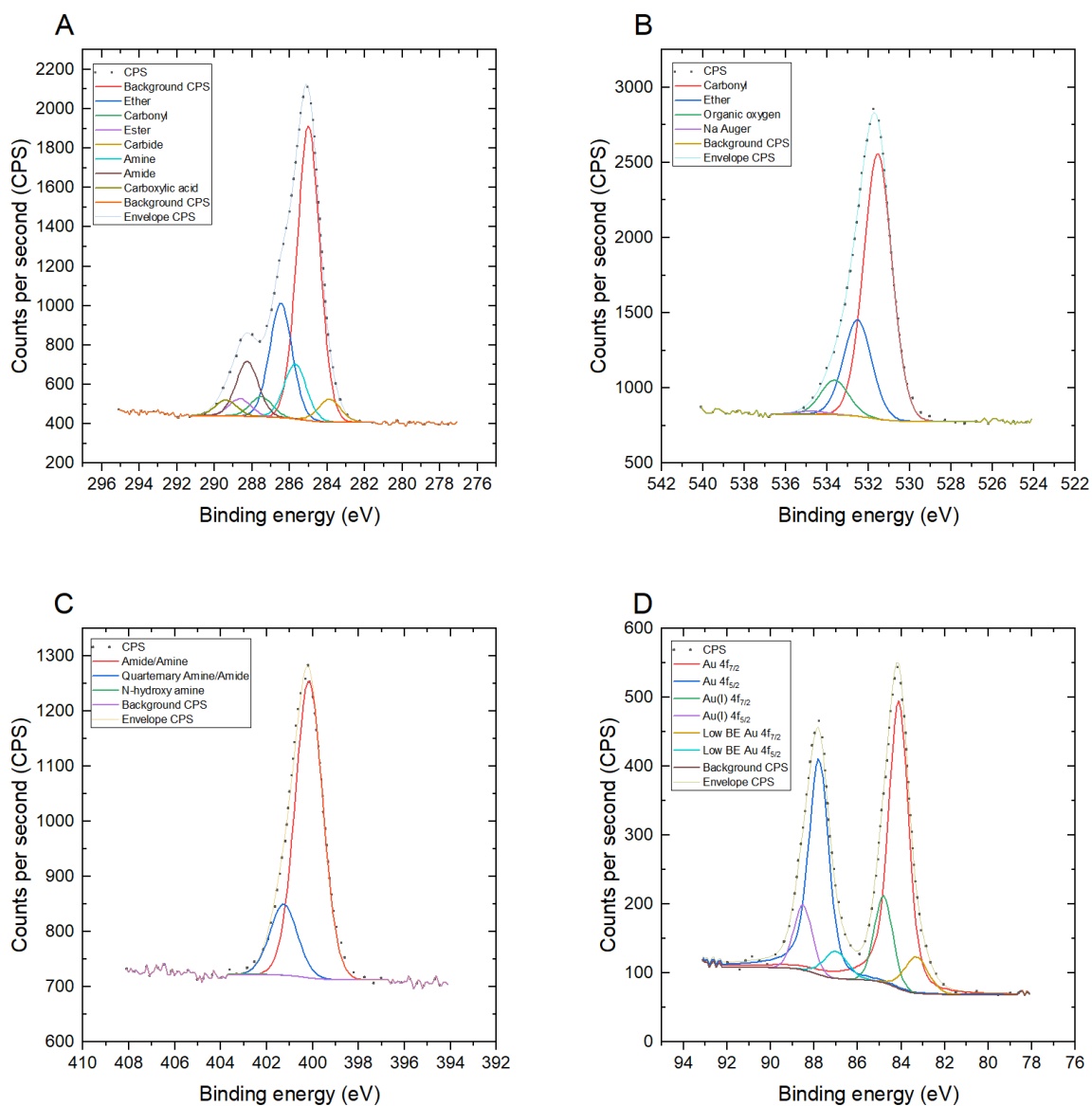


Figure S85. XPS of BSA-blocked 1-deoxy-1-amino-glucose PHEA50@AuNP35 A) C 1s B) O 1s C) N 1s and D) Au 4f

Particle Composition				Elemental Percentage Composition (%)				Elemental Ratios	
AuNP (nm)	PHEA DP	Sugar	Blocking agent	C 1s	O 1s	N 1s	Au 4f	N 1s/C 1s	N 1s/Au 4f
16	0	(citrate buffer)		55.21	43.91	0.64	0.24	0.012	2.67
16	40	NeuNAc		65.89	28.33	4.70	1.08	0.071	4.36
16	50	2,3SL		70.44	26.45	1.47	1.63	0.021	0.90
16	50	2,6SL		67.89	29.56	1.44	1.10	0.021	1.31
16	50	NeuNAc		61.36	32.00	5.19	1.45	0.085	3.58
35	0	(citrate buffer)		54.59	44.17	0.88	0.37	0.016	2.39
35	40	2,3SL		67.99	29.55	1.39	1.07	0.020	1.30
35	40	2,6SL		57.69	40.27	1.42	0.61	0.025	2.31
35	40	NeuNAc		60.69	31.49	5.70	2.12	0.094	2.68
35	50	2,3SL		68.45	28.75	1.50	1.29	0.022	1.17
35	50	2,6SL		68.08	30.04	1.12	0.76	0.017	1.48
35	50	NeuNAc		59.49	33.16	5.66	1.70	0.095	3.32
16	40	NeuNAc	BSA	68.01	22.65	8.40	0.94	0.124	8.96
16	50	NeuNAc	BSA	62.31	28.94	7.84	0.91	0.126	8.63
35	40	NeuNAc	BSA	65.26	26.89	7.32	0.53	0.112	13.83
35	50	NeuNAc	BSA	51.69	41.36	6.48	0.47	0.125	13.77

Table S22. Elemental composition of nanoparticles determined by XPS

Particle Composition				C 1s Bonding Percentage Composition (%)								Bond Ratios	
AuNP (nm)	PHEA DP	Sugar	Blocking agent	Alkane	Ether	Carbonyl	Ester	Carbide	Amine	Amide	Carboxylic Acid	Amide/Alkane	Amide/Ether
16	0	(citrate buffer)		58.16	15.44	4.09	15.22	0.74	0.54	0.54	5.26	0.0094	0.0352
16	40	NeuNAc		64.59	15.69	4.17	5.75	2.03	3.18	3.19	1.41	0.0493	0.2031
16	50	2,3SL		76.47	8.24	2.79	5.29	2.81	1.53	1.53	1.35	0.0200	0.1857
16	50	2,6SL		71.83	9.17	2.46	7.43	4.55	1.57	1.57	1.42	0.0219	0.1714
16	50	NeuNAc		58.86	17.57	4.15	6.05	3.24	4.08	4.09	1.95	0.0695	0.2327
35	0	(citrate buffer)		58.69	15.55	3.54	16.44	0.06	0.05	0.05	5.62	0.0009	0.0035
35	40	2,3SL		76.72	10.15	2.27	7.10	0.50	1.02	1.02	1.22	0.0133	0.1008
35	40	2,6SL		70.66	11.13	1.16	8.72	4.85	1.42	1.42	0.63	0.0201	0.1278
35	40	NeuNAc		59.84	19.51	2.60	7.15	1.86	4.17	4.18	0.70	0.0698	0.2141
35	50	2,3SL		76.94	9.75	3.53	6.07	0.37	1.03	1.03	1.29	0.0133	0.1052
35	50	2,6SL		75.44	8.46	2.74	5.32	3.81	0.82	0.82	2.60	0.0109	0.0969
35	50	NeuNAc		56.39	22.08	2.97	5.18	2.27	4.59	4.59	1.94	0.0815	0.2081
16	40	NeuNAc	BSA	58.08	17.47	2.05	5.99	2.81	5.95	5.95	1.70	0.1025	0.3408
16	50	NeuNAc	BSA	54.11	17.74	2.51	5.61	5.48	6.35	6.35	1.85	0.1174	0.3582
35	40	NeuNAc	BSA	59.39	16.71	1.90	5.51	5.27	4.85	4.86	1.51	0.0818	0.2908
35	50	NeuNAc	BSA	47.80	14.86	2.36	5.80	17.39	5.01	5.02	1.77	0.1049	0.3375

Table S23. C 1s bonding composition of nanoparticles determined by XPS

Particle Composition				Elemental Percentage Composition (%)					Elemental Ratios	
AuNP (nm)	PHEA DP	Sugar	Blocking agent	C 1s	O 1s	N 1s	Au 4f	F 1s	N 1s/C 1s	N 1s/Au 4f
16	40	1-Deoxy-1-amino-Glc		57.85	32.67	4.652	4.40	0.44	0.080	1.06
16	50	1-Deoxy-1-amino-Glc		56.38	34.3	4.261	4.16	0.90	0.076	1.03
35	40	1-Deoxy-1-amino-Glc		54.71	27.92	4.958	11.73	0.69	0.091	0.42
35	50	1-Deoxy-1-amino-Glc		54.82	31.25	5.002	8.32	0.60	0.091	0.60
16	40	1-Deoxy-1-amino-Glc	BSA	62.2	25.61	10.01	2.18		0.161	4.59
16	50	1-Deoxy-1-amino-Glc	BSA	61.18	26.05	10.83	1.94		0.177	5.59
35	40	1-Deoxy-1-amino-Glc	BSA	65.1	22.51	11.41	0.98		0.175	11.59
35	50	1-Deoxy-1-amino-Glc	BSA	67.74	22.63	8.463	1.16		0.125	7.28

Table S24. Elemental composition of nanoparticle controls determined by XPS

Particle Composition				C 1s Bonding Percentage Composition (%)								Bond Ratios	
AuNP (nm)	PHEA DP	Sugar	Blocking agent	Alkane	Ether	Carbonyl	Ester	Carbide	Amine	Amide	Carboxylic Acid	Amide/Alkane	Amide/Ether
16	40	1-Deoxy-1-amino-Glc		51.56	22.21	5.56	8.23	4.19	3.21	3.21	1.83	0.0623	0.1447
16	50	1-Deoxy-1-amino-Glc		50.32	20.70	3.38	12.94	4.25	3.46	3.46	1.49	0.0687	0.1670
35	40	1-Deoxy-1-amino-Glc		60.29	18.64	2.94	5.16	3.33	4.35	4.35	0.96	0.0721	0.2332
35	50	1-Deoxy-1-amino-Glc		55.31	22.87	4.00	5.08	2.76	4.32	4.32	1.34	0.0780	0.1887
16	40	1-Deoxy-1-amino-Glc	BSA	39.37	26.21	4.23	6.25	6.65	6.76	6.76	3.77	0.1717	0.2579
16	50	1-Deoxy-1-amino-Glc	BSA	44.80	23.46	1.08	8.06	4.68	7.95	7.95	2.01	0.1775	0.3390
35	40	1-Deoxy-1-amino-Glc	BSA	45.47	24.82	0.86	8.74	2.92	7.56	7.56	2.07	0.1663	0.3046
35	50	1-Deoxy-1-amino-Glc	BSA	49.45	19.25	3.41	2.97	3.86	9.21	9.21	2.64	0.1863	0.4785

Table S25. C 1s bonding composition of nanoparticle controls determined by XPS

¹H STD NMR Spectra

Preliminary STD spectra were obtained using the (mammalian cell expressed) spike protein with the ligands indicated at 5 mM. Clear STD signals were visible and for both NeuNAc and 2,3 sialylactose similar spectra were obtained confirming contact. A deeper analysis was not undertaken, and individual contacts were not assigned at this point.

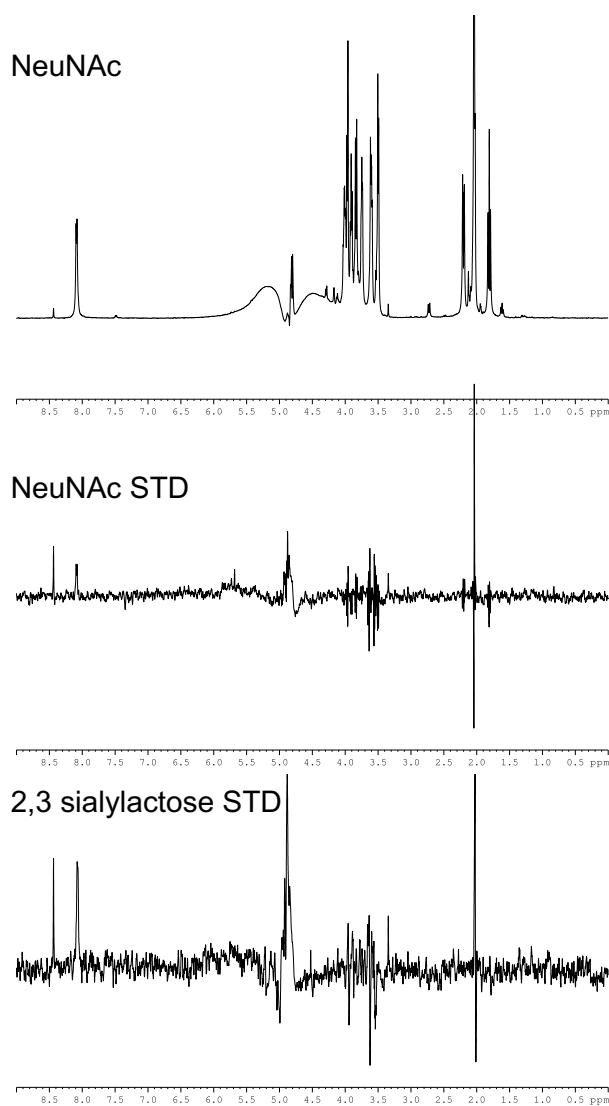


Figure S86. ¹H Saturation transfer difference NMR spectroscopy analysis of SARS-COV-2,S1 with NeuNAc and 2,3-sialylactose.

Spike (S1) Protein Thermal Shift Binding Analysis

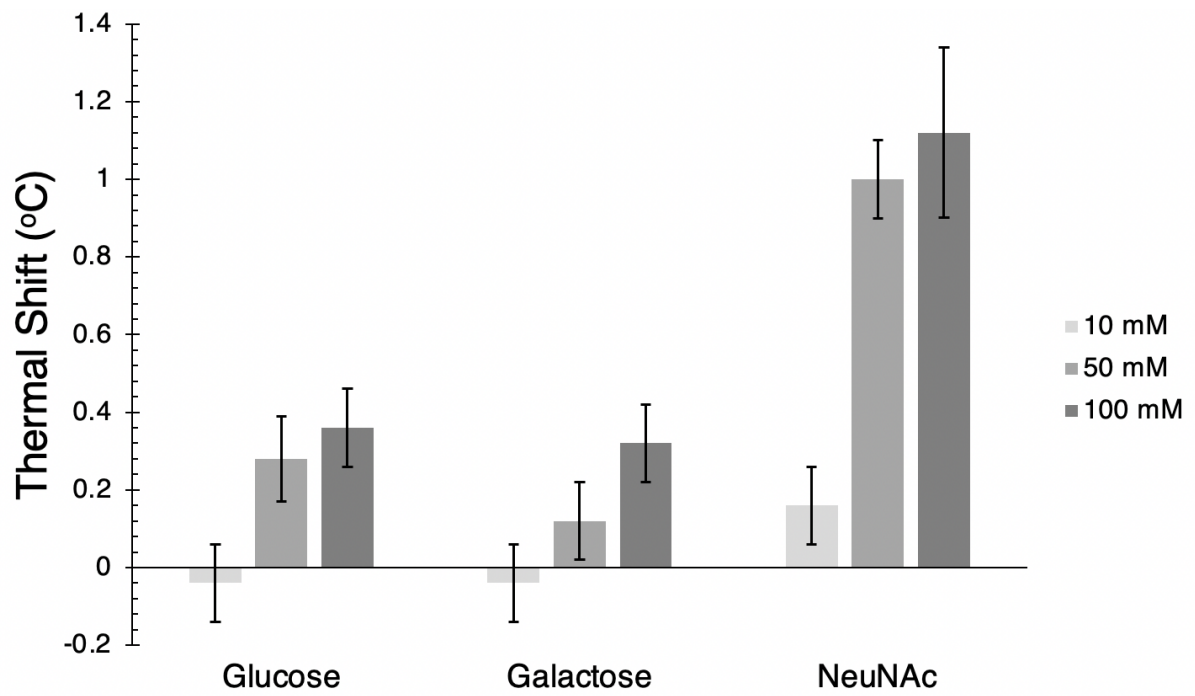


Figure S87. Protein thermal shift assay results plotted as total shift compared to SARS-COV-2,S1 protein alone. Errors bars are SD from a minimum of 5 runs.

References

- (1) Richards, S.-J.; Gibson, M. I. Optimization of the Polymer Coating for Glycosylated Gold Nanoparticle Biosensors to Ensure Stability and Rapid Optical Readouts. *ACS Macro Lett.* **2014**, *3* (10), 1004–1008.
- (2) Lim, D.; Brimble, M. A.; Kowalczyk, R.; Watson, A. J. A.; Fairbanks, A. J. Protecting-Group-Free One-Pot Synthesis of Glycoconjugates Directly from Reducing Sugars. *Angew. Chemie Int. Ed.* **2014**, *53* (44), 11907–11911.
- (3) Kuhn, R.; Lutz, P.; Macdonald, D. L. Synthese Anomerer Sialinsäure-methylketoside. *Chem. Ber.* **1966**, *99* (2), 611–617.
- (4) Orlova, A. V.; Shpirt, A. M.; Kulikova, N. Y.; Kononov, L. O. N,N-Diacetylsialyl Chloride—a Novel Readily Accessible Sialyl Donor in Reactions with Neutral and Charged Nucleophiles in the Absence of a Promoter. *Carbohydr. Res.* **2010**, *345* (6), 721–730.
- (5) François D. Tropper* , Fredrik O. Andersson, Stéphane Braun, R. R. Phase Transfer Catalysis as a General and Stereoselective Entry into Glycosyl Azides from Glycosyl Halides. *Synthesis (Stuttg.)*. **1992**, *7*, 618–620.
- (6) Jeong, N. S.; Brebis, K.; Daniel, L. E.; O'Reilly, R. K.; Gibson, M. I. The Critical Importance of Size on Thermoresponsive Nanoparticle Transition Temperatures: Gold and Micelle-Based Polymer Nanoparticles. *Chem. Commun.* **2011**, *47* (42), 11627–11629.
- (7) Bastús, N. G.; Comenge, J.; Puentes, V. Kinetically Controlled Seeded Growth Synthesis of Citrate-Stabilized Gold Nanoparticles of up to 200 Nm: Size Focusing versus Ostwald Ripening. *Langmuir* **2011**, *27* (17), 11098–11105.

- (8) Madeira, F.; Park, Y. M.; Lee, J.; Buso, N.; Gur, T.; Madhusoodanan, N.; Basutkar, P.; Tivey, A. R. N.; Potter, S. C.; Finn, R. D.; Lopez, R. The EMBL-EBI Search and Sequence Analysis Tools APIs in 2019. *Nucleic Acids Res.* **2019**, *47* (W1), W636–W641.
- (9) Haiss, W.; Thanh, N. T. K.; Aveyard, J.; Fernig, D. G. Determination of Size and Concentration of Gold Nanoparticles from UV - Vis Spectra. *Anal. Chem.* **2007**, *79* (11), 4215–4221.